HIGH TEMPERATURE MATERIAL PROPERTIES OF CALCIUM ALUMINATE CEMENT CONCRETE

by

Hammad Anis Khan

(NUST201260957MSCEE15212F)

Master of Science

in

Structural Engineering

NUST Institute of Civil Engineering (NICE)

School of Civil and Environmental Engineering (SCEE)

National University of Sciences and Technology (NUST)

Islamabad, Pakistan

(2015)

This is to certify that the

thesis titled

HIGH TEMPERATURE MATERIAL PROPERTIES OF CALCIUM ALUMINATE CEMENT CONCRETE

submitted by

Hammad Anis Khan

NUST201260957MSCEE15212F

has been accepted towards the partial fulfillment
of the requirements for the degree

of

MASTER OF SCIENCE

in

STRUCTURAL ENGINEERING

Dr. Wasim Khaliq
Associate Professor
NUST Institute of Civil Engineering (NICE)
School of Civil and Environmental Engineering (SCEE)
National University of Sciences and Technology (NUST),
Islamabad, Pakistan

DEDICATED

TO

MY PARENTS AND GRANDMOTHER

ACKNOWLEDGEMENTS

In the Name of Allah, the most Merciful, the Most Compassionate all praises be to Allah, the Lord of the worlds and prayers and peace be upon Muhammad His servant and messenger.

The completion of this project was only possible due to unlimited blessings of Almighty Allah and collaboration of many people, to whom I wish to express my gratitude.

First and foremost, I would like to thank my beloved parents and grandparent for their unconditional love and support throughout my life and for strengthening me to chase my dreams.

I would like to express my profound gratitude to my supervisor Dr. Wasim Khaliq, Associate Professor, NUST Institute of Civil Engineering, for his guidance and support throughout this project and especially for his confidence in me. I am grateful to him for motivating me along this arduous course. He inspired and encouraged me to be the best version of me. A special thanks for his countless hours of reflecting, reading, encouraging and most of all patience throughout the entire process.

There are number of people without whom this thesis might not have been written, and to whom I am gratefully indebted. I was fortunate to have an outstanding committee. I owe my sincere gratitude to Dr. Syed Ali Rizwan, Dr. Khaliq-ur-Rasheed Kiyani and Dr. Shaukat Ali Khan, who were more than generous with their expertise and precious time.

I am grateful to my colleagues especially Mr. Farrukh, Mr. Umaid and Mr. Waqas for their sincere help and guidance during this thesis work. I am also thankful to the laboratory staff of Structures lab, for their assistance and help during experimentation.

Hammad Anis Khan

ABSTRACT

Fire is one of the most dangerous hazards that can occur in any type of structure which result in the loss of life and property. Currently, the primary material used for construction of most structures is concrete. Material strength is one of the most important factor which define the performance of structure when exposed to fire. In recent years, researchers have been focusing on fire performance of both normal strength concrete (NSC) and high strength concrete (HSC) for structural members used in buildings.

When concrete is exposed to elevated temperatures rapidly, it results in additional stresses that are relieved by explosive spalling and cracks extending to the surface. This result in the decrease of strength and ultimately the capacity of the concrete in addition to that, it does not regain its original strength on cooling which makes concrete vulnerable to fire.

Calcium aluminate cement concrete (CACC) is a type of high performance concrete (HPC) which is much more durable and resistant to fire and can be used as a replacement of ordinary Portland cement concrete. A test program was designed to undertake high temperature tests on CACC and normal strength concrete (NSC) commonly used in buildings, domestic construction. Material properties include compressive and splitting tensile strength, elastic modulus, stress-strain response, toughness and mass loss of both CACC and NSC. These properties were investigated at various temperatures of 23, 200, 400, 600 and 800°C. Unstressed and residual test procedures were adopted to measure these properties.

The results obtained from high temperature tests of CACC revealed that the presence of alumina as a binding agent showed considerable enhancement in the mechanical performance compared to NSC. At elevated temperatures, the loss of compressive strength in NSC is much more prominent as compared to CACC. Reduction in the stress-strain response was observed in both CACC and NSC with the increase in temperature; however, an increase in axial strain was more in of CACC. Compressive toughness was higher in case of CACC as compared to NSC which increases up to 200°C, but decreases beyond this temperature. Scanning electron microscope (SEM) was also performed to differentiate the microstructural changes taking place in both types of concrete at elevated temperatures. Visual investigations after high temperature exposure revealed that CACC exhibits low cracking with less color changes as compared to NSC. Further, data generated from material property tests was utilized to develop simplified relations for expressing material properties of CACC as a function of temperature.

TABLE OF CONTENTS

CONTENT **Page No**

LIST OF FIGURES

LIST OF TABLES

CHAPTER 1

INTRODUCTION

1.1 General

Concrete out of all construction materials occupied an important place and is widely used in civil engineering structures, due to its versatility, ease of fabrication, strength and adaptability. Mostly concrete structures are subjected to different kinds of loads (dead, live, wind and impact etc) in addition to that, sometimes severe environmental threats like Earthquake, Fire etc. As a result the durability of concrete is given a prime importance as far as the concrete technology is concerned. However unlike other materials, the behavior of concrete is quite unpredictable and complex because it depends upon materials properties and proportions, chemical and physical characteristics of materials and curing conditions, etc. Under normal conditions, concrete structures are subjected to a range of temperatures no more harsh than that imposed by ambient environmental settings. However, these structures are always under threat to fire, which results in an extreme thermal gradient.

The temperature induced variation in the properties of concrete which are more complex than for most materials because not only is the concrete a composite material whose constituents have different properties, but it also depends on moisture and porosity (Mehta and Monteiro, 2006). Exposure of concrete to elevated temperatures affects its thermal, mechanical, deformation and physical properties. When it is exposed to the elevated temperatures there is deterioration of concrete in which of particular importance is the loss in compressive strength, cracking and spalling of concrete, destruction of bond between the cement paste and the aggregates, and the gradual deterioration of hardened cement paste (Georgali and Tsakiridis, 2005). This exposure to high temperature rapidly results in additional stresses that are relieved by spalling and cracks extending to the surface. This result in the decrease of strength and ultimately the loss in capacity of the concrete; in addition to that, it does not regain its strength on cooling which makes concrete vulnerable to fire. Hence, proper fire safety provisions as per the building codes should be provided to ensure safe performance of structures against fire (ACI 216.1, 2007; ACI 318-11, 2008). To evaluate the performance of concrete against fire, the characteristics of concrete play a fundamental role. The performance of concrete is determined in terms of its properties which includes mechanical properties, thermal properties, deformation properties and material specific characteristics such as spalling in concrete. The thermal properties consisting of specific heat, thermal conductivity, thermal diffusivity, and

thermal expansion are important material properties that effect the development of thermal response of concrete structural members. The mechanical properties, which include extent of strength loss and stiffness deterioration, are given the prime importance and significantly influence fire response of structural system (Khaliq, 2012).

Calcium aluminate cement (CAC) is one of the most important non-Portland cement used in the construction because of special properties they possess. High performance concrete (HPC) have emerged with the use of CAC, having excellent performance in terms of strength and durability, surpassing average performance of conventional Normal Strength Concrete (NSC). They are utilized where resistance to chemical corrosion, mechanical abrasion and impact like in industrial floors is required. In addition, they have been employed in the sewer lines, where resistance to biogenic corrosion is of primary importance and where concrete made with ordinary portland cement (OPC) fails to sustain. Its rapid hardening property and resistance to abrasion has led it to be increasingly used for repairs of hydraulic dams in areas susceptible to abrasion e.g. spillways, sluice gates etc (Scrivener et al., 1999).

It has been established that the performance of concrete made with CAC against fire resistance is better to that of Portland cement concrete. It is very popular for its use as a refractory material e.g. in the lining of the kilns, steel industry etc (Karadeniz et al., 2007; Katsavou et al., 2012). With the increase in the use of this material in building construction, it has to satisfy the appropriate fire safety requirements specified in the building codes (ACI 216.1, 2007; ACI 318-11, 2008). The performance of concrete made with CAC when exposed to elevated temperatures has not been established i.e. at present there is very limited information on high temperature material properties of calcium aluminate cement concrete (CACC).

In this research, an experimental investigation on characterizing high temperature performance of CACC at material level is made, in which CAC was used as a replacement of OPC in NSC made of traditional limestone aggregate. A test program was designed at the National University of Sciences and Technology (NUST), Pakistan, to investigate material properties of both CACC and NSC when exposed to various elevated temperatures of 23, 200, 400, 600 and 800°C. Material properties namely compressive and splitting tensile strength, elastic modulus, stress-strain response, compressive toughness and mass loss were observed under unstressed and residual test procedures for both CACC and NSC.

1.2 Calcium Aluminate Cement (CAC)

Calcium aluminate cement is also known as high alumina cement (HAC), which was introduced as a type of cement containing 32-45% Al_2O_3 in UK after World War I. These are prepared by fusing and grinding the aluminous and calcareous materials in suitable proportions. CAC is an expensive binder, since the production of this cement requires relatively pure raw materials (bauxite and limestone) to meet the need of high alumina content. This type of cement is different from Portland cement which usually contains very small amount of alumina as shown in Figure 1.1. This shows the proportioning of chemical composition of different types of cementitious materials. Afterwards, different types of aluminous cements are developed having alumina content ranging from 50 to 90 percent. Common trait of all these cements is that the hydrates produced are predominantly calcium aluminates due to which they are best known as CAC (Scrivener and Capmas, 1998). The mineralogy of CAC shows that calcium oxide (CaO) and alumina (Al_2O_3) are the principal oxides. Depending upon their percentage within CAC, they combine to give monocalcium aluminate (CA) as major active phase. This active phase reacts with water under hydration reaction to give calcium aluminate hydrates.

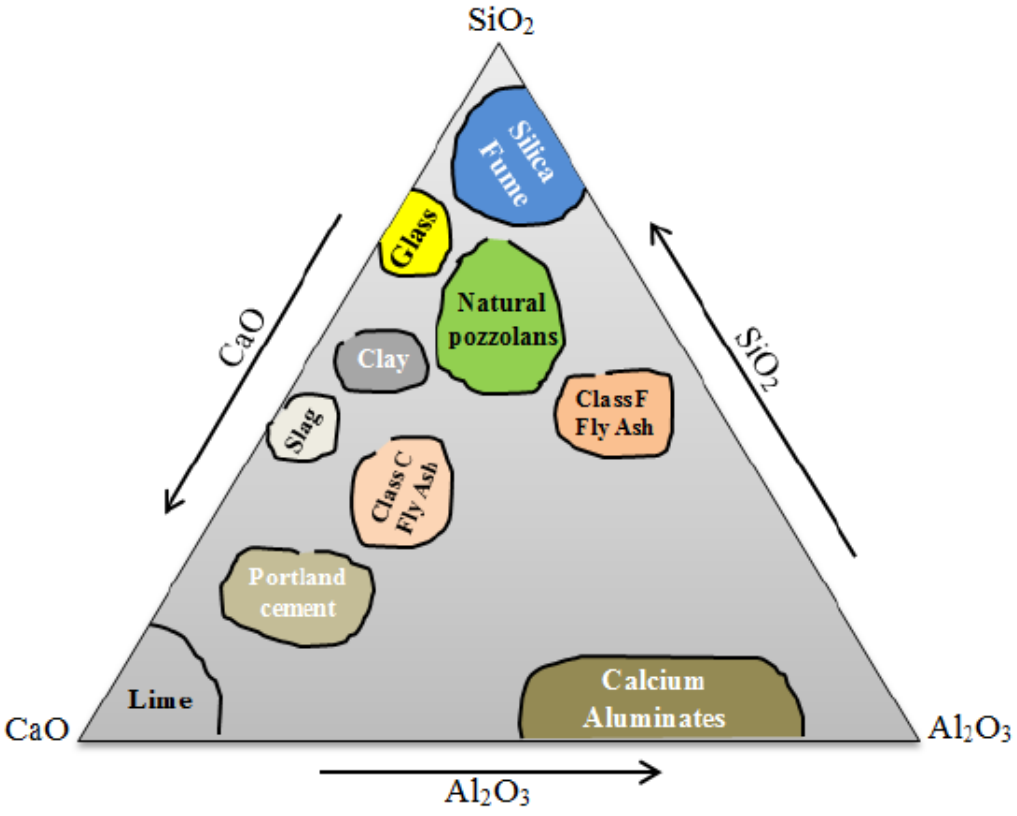

Figure 1.1 – Ternary phase diagram of the CaO–Al_2O_3–SiO_2 system. Navy (2004).

The high-performance concrete (HPC) prepared from CAC is used where unique properties are required which enable them to be used in severe environments. Such type of concrete extends the range of applications for cementitious materials. Some of the additional properties achieved by the use of CAC are as follows:

- Resistance to chemical attacks, particularly acids.
- Abrasion resistance in hydraulic structures e.g. Dam flushing gates.
- Resistance to chemical and mechanical wear e.g. Industrial floors.
- Resistance to thermal shock e.g. fire training building.

In addition to all this, due to the rapid hardening and strength gaining property, CAC is used as a repair material. If we compare it with OPC, it can even give us 28 days strength of OPC just within 5 to 6 hours (Ideker et al., 2013). Roads which are repaired with these materials can be operational within few hours after casting and traffic delays can be minimized. Scrivener et al. (1999), found that CAC simulates the biogenic corrosion on Portland and CAC mortars using the simulation chambers, which accelerates the degradation process 20 times i.e. exposure to 250 days is equivalent to 16 years of field exposure. Figure 1.2, shows the results of this test in which we can see the performance of Portland cement mortar, CAC mortar and CAC mortar with synthetic aggregate. The degradation against biogenic corrosion is evaluated in term of weight. The influence of substrate can be seen against which the Portland cement mortar is completely degraded as compared to CAC mortar.

The ability of CACC structures to perform better against high temperatures makes it an indispensable construction material. Such concrete is suitable for structures where there is cyclic firing at temperatures around 1000°C. Portland cement based concrete will fail in such conditions due to the repeated dehydration and rehydration of $Ca(OH)_2$ and CaO which will seriously affect the structural integrity. For such cases, the use of CACC will increase the service life of the structure.

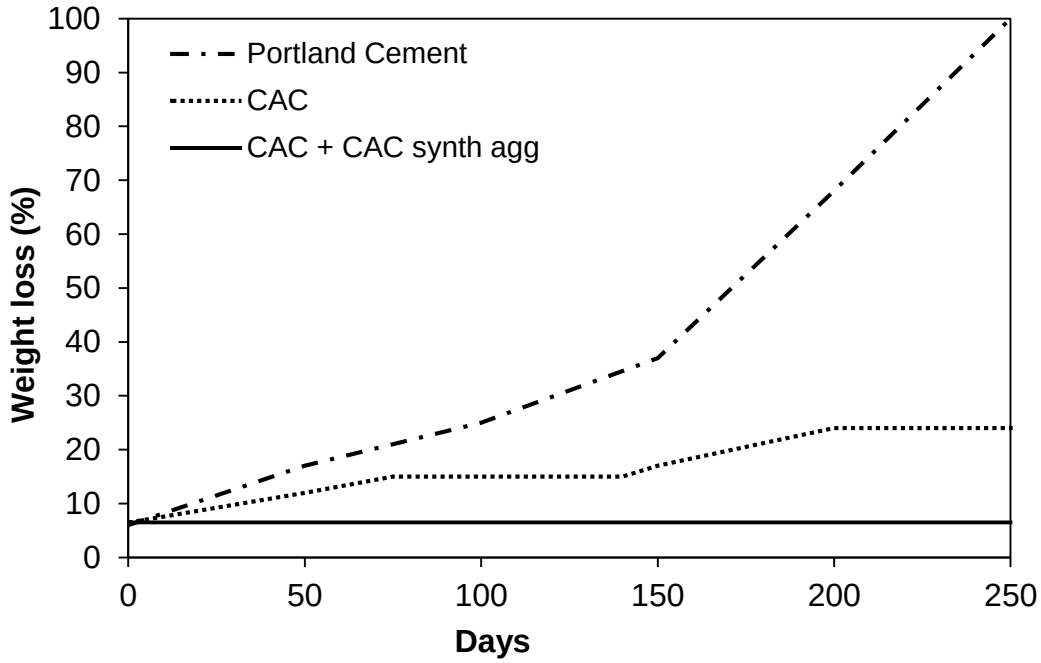

Figure 1.2 – Weight loss in simulation chamber against biogenic corrosion. Scrivener et al. (1999).

1.3 Behavior of Concrete against Fire

Concrete generally exhibits good fire resistance properties and that is why it finds wide applications in building and infrastructure works. When concrete is subjected to elevated temperatures the relevant criteria for performance are its mechanical properties (load carrying capacity, tensile strength, elastic modulus, stress strain response and toughness), thermal properties, deformation properties and material specific characteristics such as spalling in concrete. Similar to the other materials, these properties change substantially with the change in temperature. These properties vary as a function of temperature and depend on the composition and characteristics of concrete.

When we consider the fire resistance design the primary importance is given to the compressive strength of concrete (f'_c) at an elevated temperature. This property of concrete depends upon interface transition zone, water-cement ratio, types of admixtures, type of stress, aggregate type and size, etc (Mehta and Monteiro, 2006). The compressive strength of concrete at elevated temperatures is well researched. The major factors on which the high temperatures compressive strength depends are also identified which include binders in the batch, room temperature strength, type of aggregate used, rate of heating and type of test setup. Figure 1.3 shows us the variation of compressive strength ratio of NSC at elevated temperature with upper and lower

bounds showing the limit of variation in reported test data. It can be seen that there is very little loss in strength of concrete up to 400°C (Khaliq, 2012).

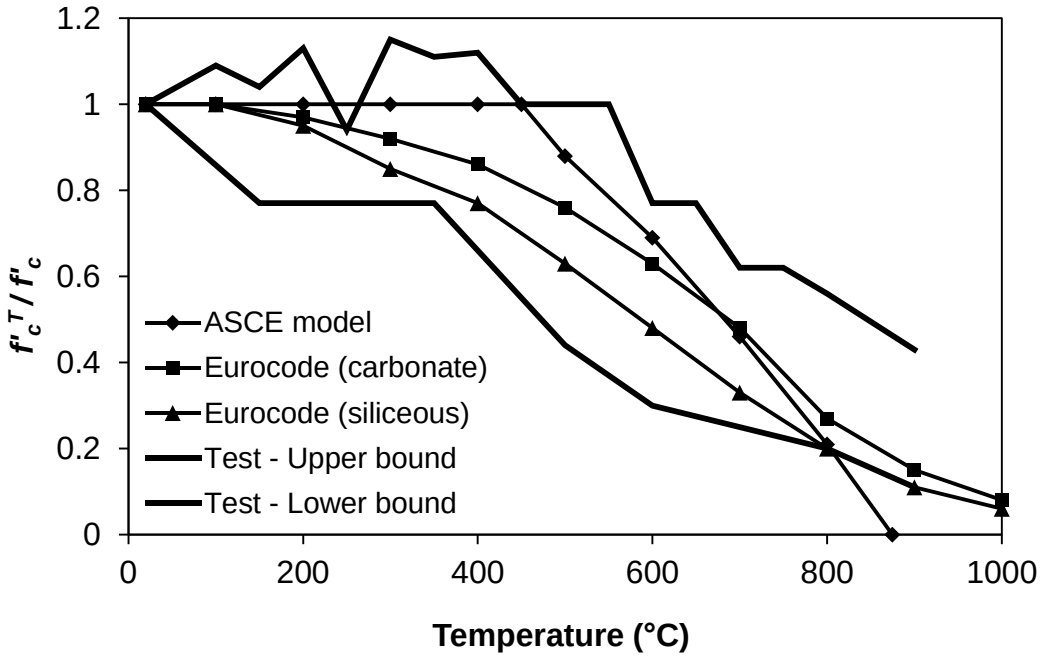

Figure 1.3 – Variation in relative compressive strength of NSC as a function of temperature. Khaliq (2012)

Another property which is given due importance is modulus of elasticity of concrete (E_c) which is closely related with its stiffness and is defined as the ratio of stress to strain when deformation remains elastic. This elastic modulus is strongly affected with the change in temperature and decreases with the increase in temperature. This reduction is due to the cracking in the microstructure starting from the interface transition zone, disintegration of hydrated cement products and increase in porosity, which leads to the loss of stiffness of concrete. Figure 1.4 illustrates the ratio of elastic modulus at elevated temperatures to that at room temperature. It can be seen that there is a general decrease in elastic modulus found in all types of concrete irrespective of the type of aggregate (ACI 216R-89, 2001).

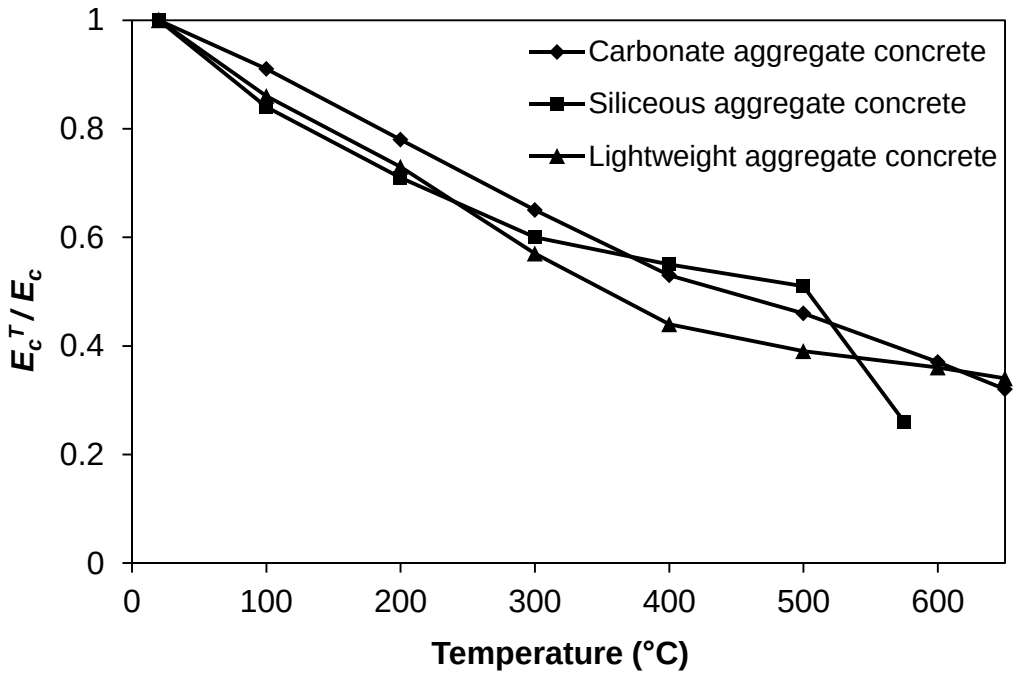

Figure 1.4 – Relative modulus of elasticity of concrete as a function of elevated temperature. ACI 216.1 (2007)

The stress-strain curve of concrete becomes nonlinear and inelastic because of the generation of the micro cracks with the increase in the load. This property is also affected with the change in temperature i.e. with the increase in temperature the initial slope starts decreasing and the ultimate value of deformation keep on increasing. This is due to the reason that as the temperature increases and reaches around 250°C there is the loss of the non-evaporable water. Above 400°C, calcium hydroxide $Ca(OH)_2$ which forms a major portion in the hydrated products of concrete starts to disintegrate (Li et al., 2004). Further, at 600°C the calcium-silicate hydrate (C-S-H) gel, which binds the ingredients of concrete as cement paste and gives the strength to the concrete, starts to crumble, resulting in critical loss of compressive strength and severely affects the stress-strain response of concrete (Georgali and Tsakiridis, 2005).

Tensile strength (f'_t) which define the concrete's ability to withstand cracking and the propagation of microcracks as a result of tensile stresses. Concrete being vulnerable to tensile cracking increases the importance of this property to be understood (Chan et al., 1999). Almost similar factors affect the tensile strength of the concrete on which the compressive strength of concrete depends upon, with prime importance given to aggregate-paste interface transition zone and microstructure of concrete. Tensile strength of concrete is very low as compared to its compressive strength. As the compressive strength is vulnerable to elevated temperatures so is the case in tensile strength. Under fire conditions, this property is even more critical

because of fire induced spalling (Khaliq and Kodur, 2011). It also depends on factors similar to those which effect compressive strength of concrete.

Density is an important property of concrete, which is the mass of a unit volume of the concrete, comprising of solid material and the air-filled pores. Durability and strength of concrete greatly depends upon this property. With the increase in temperature, concrete due to high amount of moisture will experience loss of mass which ultimately results in the increase in the porosity of the concrete due to evaporation. This increase in mass loss with the increase in temperature will ultimately affect the stiffness and durability of concrete.

Another property which is given due importance is compressive toughness (T_c). It is actually a derived property which is obtained from the stress-strain curve of the concrete when tested in compression. This actually represents the amount of energy absorbed per volume of the material before rupturing. As the fire severely affects the stress-strain response of the concrete so it ultimately affects the toughness of the material.

1.4 Research Objectives

For evaluating the high temperature performance of concrete in terms of fire resistance, knowledge on the material properties of concrete at elevated temperatures is very important. These properties include compressive strength, tensile strength, elastic modulus, stress-strain response, toughness, stiffness, mass loss, and extent of spalling. The primary objective of this research study is to evaluate the performance of CACC in terms of these material properties when exposed to elevated temperatures as high as 800°C. The main objectives are stated below:

- To quantify the performance of CACC made of traditional limestone aggregates in terms of its material properties at elevated temperatures and to compare it with NSC prepared from OPC when exposed to same conditions.
- To compare the performance of CACC in terms of different test scenarios i.e. unstressed and residual test conditions.
- To perform the visual assessment of fire-damaged concrete which includes the study of color changes, cracking and spalling of the surface.
- To study the effect of elevated temperatures on the physical properties of both CACC and NSC like mass loss.
- To develop the simplified mathematical relations for expressing material properties (compressive and tensile strength, elastic modulus, toughness and mass loss) of CACC as a function of temperature.

- To study the microstructural changes in CACC and NSC specimens using Scanning Electron Microscope (SEM) imagery after the exposure to elevated temperatures.

1.5 Research Tasks

To accomplish the above mentioned objectives following tasks were performed:

- Conduct literature review.
- Develop the test setup for both types of test (compression test and split tensile test) on samples at high temperature.
- Perform the mix design which is applicable on both types of concrete.
- Preparation of NSC cylinders from OPC and CAC which can be easily tested at high temperature.
- Conduct compression and split tensile tests on concrete samples under unstressed (hot) test setup and residual test setup to measure the mechanical properties of CACC.
- Process the test data to develop stress-strain curves for CACC and NSC.
- Evaluate the experimental results.
- Analyze the results to establish the high temperature material properties of both concretes with respect to time and to develop mathematical relationships for these properties as a function of temperature.
- Conclusions and recommendations

1.6 Research Significance

The effect of elevated temperatures on the material properties of NSC especially compressive strength is well established. However, the performance of CACC at elevated temperatures is relatively less studied with lack of data on the material properties namely tensile strength, stress-strain response, mass loss and compressive toughness. While, some information on residual compressive strength of CACC is available, there is hardly any study on the high temperature behavior of CACC. In the present study, not only the material properties of CACC are determined at different elevated temperatures on unstressed specimens but its trend is also compared with the residual conditions. In addition, microscopic analysis is also performed using scanning electron microscope (SEM) to understand the performance of CACC in terms of its material properties at elevated temperatures based on its microstructure and to study the morphological changes due to conversion reactions. The data acquired from this study will be used to propose simplified mathematical relationships for different structural properties of

CACC as a function of temperature. These relationships can be used as input parameters in computer programs for evaluating the fire resistance performance of concrete structural members. The study on residual concrete properties will help to evaluate the post-fire strength of concrete structures for retrofitting of structures.

1.7 Thesis Outline

Chapter 1 is a preliminary chapter about the significance of CAC, the behavior of concrete when it is exposed to fire, objectives and research significance of the study, and thesis overview.

Chapter 2 describes the literature review in details. A brief literature review includes the performance of NSC at elevated temperatures. In addition to that, properties and behavior of CAC are also discussed in chapter 2.

Chapter 3 represents the procedure and materials of test setup, the testing facility and specimens used to evaluate the structural properties of NSC from CAC. The testing apparatus and data acquisition system is also elaborated in Chapter 3.

Chapter 4 discusses the tests carried out, observations, test results and evaluation of test results.

The conclusions based on findings of this research and recommendations for further studies are presented in Chapter 5.

CHAPTER 2

LITERATURE REVIEW

2.1 General

The performance of concrete against fire is well known and it exhibits good fire resistance properties which have been employed as a structural material in buildings and infrastructure works. With the advancement in the field of material engineering, the studies on improving the properties of concrete have increased which leads to the evolution of new types of concretes like High Strength Concrete (HSC), Self-Consolidating Concrete (SCC), Calcium Aluminate Cement Concrete (CACC) and Fly Ash Concrete (FAC). The CAC also known as high alumina cement is recognized for its high temperature resistance/refractory performance. CAC is used in variety of combinations with other minerals and admixtures to achieve wide range of properties. Although it is well known for its refractory properties very limited information is available on performance of CACC when exposed to elevated temperatures. This makes knowledge on properties and behavior of CACC very significant to be studied.

The fire resistance of concrete structural member is very crucial as it has to satisfy the fire safety requirements which are specified in the building codes (ACI 216.1, 2007; ACI 318-11, 2008). This fire resistance of concrete structural members is governed by high temperature thermal and mechanical properties of constituent concrete. For predicting the fire resistance of structural concrete, knowledge on high temperature material properties is very important which includes thermal, mechanical and deformation properties. These properties depend upon the characteristic and composition of concrete and vary with the change in temperature.

The thermal properties exhibit the extent up to which the heat transfer can takes within the concrete structural member, whereas the mechanical properties determine the extent of strength loss. The deformation properties display the deformation within the concrete structural member as a result of elevated temperatures. The mechanical properties that determine the fire performance of RC members are compressive and tensile strength, modulus of elasticity and stress-strain response of constituent material at elevated temperatures.

In this chapter behavior and properties of CAC are highlighted. Moreover, previous studies on the effect of high temperature on the material properties of concrete are also reviewed.

2.2 Material properties of concrete at elevated temperature

2.2.1 General

The mechanical properties that determine the fire performance of RC members are compressive and tensile strength, elastic modulus and stress-strain response of constituent material at elevated temperatures. There has been a lot of research on the mechanical properties of concrete when it is exposed to elevated temperatures. High temperature mechanical properties are evaluated on small samples of concrete usually cylinders and cubes. Due to the lack of test standards on high temperatures unlike room temperature property measurements, these tests are performed on wide range of specimen sizes. The cylinder specimens of size 75x150, 100x200, and 150x300 mm whereas cube specimens of size 100x100, 150x150 and prism specimens of size 100x300 are usually used for high temperature.

The compressive strength (f'_c) influences the load-carrying capacity of a structure. Compressive strength of concrete is generally considered to be its most valuable property. Compressive strength of concrete at elevated temperatures is of primary interest in fire resistance design. Unlike other properties this property of concrete is well researched. Compressive strength of concrete at ambient temperature depend upon water-cement ratio, aggregate-paste interface transition zone, curing conditions, aggregate type and size, admixture types and type of stress (Mehta and Monteiro, 2006). At high temperatures, this property is highly influenced with the room temperature strength, rate of heating and binders such as (Silica fume, fly ash and slag). The tensile strength of concrete (f'_t) is another essential property of concrete. It is much lower than its compressive strength due to the ease with which cracks can propagate under tensile loads-unlike compressive loads, when cracks tend to close. It is an important property because cracking in concrete is due tensile stresses and the failure in tension is often governed by microcracking (Mindess et al., 2003). Under the fire conditions, this property becomes more crucial especially in the cases where fire induced spalling occurs in a concrete structural member (Khaliq and Kodur, 2011).

Concrete's elastic modulus (E_c) is a measure of its stiffness or resistance to deformation. The behavior of a structure is often dependent on the elastic modulus of concrete and this modulus is strongly affected by temperature. At higher temperature, disintegration of hydrated cement products and breakage of bonds in microstructure of cement paste reduce elastic modulus and the extent of reduction depends upon the loss of moisture, high temperature creep and type of aggregate (Kodur, 2014).

The high temperature compressive stress-strain behavior of concrete is of significant importance in the fire resistance analysis of RC structural members. These high temperature stress-strain curves are helpful in understanding the response of structural RC member under fire conditions. The stress-strain relationships at elevated temperature may be derived from the room-temperature relationships if the variation of maximum stress and corresponding strain with temperature are known (Baldwin and North, 1973). The high temperature stress-strain response is dependent on factors such as aggregate-paste interface transition zone, curing conditions, aggregate type and size. Compression toughness (T_c) is another material property, which is the energy absorbed during the compressive strength test until failure. This property is evaluated as the area under the stress-strain curve of the concrete material (Marar et al., 2001). This is actually the ability of the material to absorb energy due to compression before failure which makes this property very important. As this property depends upon the stress-strain response of the material, so at elevated temperature with the change in stress-strain curve this property also changes.

Another material property which is given due importance is the loss of mass (M) of concrete with the increase in temperature. This property comes under the thermal property of concrete. Mass is a property that enables concrete to absorb and store significant amounts of heat. Higher mass in concrete acts as heat sink, by absorbing and holding heat for longer time. This delays the heat transfer through material in an RC member, thus mass loss influences thermal properties of the concrete as well as strength and stiffness properties of RC members. Mass loss of conventional NSC and HSC has been investigated earlier with most of the information pertaining to NSC (Khaliq, 2012).

2.2.2 Testing Methods for High Temperature Material Properties

Various investigators used various methods to evaluate the material properties of concrete at elevated temperatures which indicates that, generally, the tests can be categorized according to cold or hot testing. In cold testing, specimens are gradually heated to a specified temperature, permitted to thermally stabilize at that temperature for a given period of time, allowed to slowly cool to ambient room temperature, and then tested to determine residual material properties. In hot testing, specimens are gradually heated to a specified temperature, permitted to thermally stabilize at the temperature for a prescribed period of time, and then tested at temperature to determine material properties. During heating and cooling, the specimens may be either loaded or unloaded. Phan and Carino (2002), describes these tests under three test methods for

determining the high temperature strength properties namely stressed, unstressed and residual test methods.

Figure 2.1, 2.2 and 2.3 shows the main difference between the three types of testing methods to evaluate the high temperature mechanical properties of concrete. In case of stressed method, the specimen is preloaded to a certain load usually 30-60% of the room temperature ultimate compressive strength of concrete. Specimens are then exposed to the required temperature and further loaded to failure. In case of unstressed test method, specimens are first heated to the required temperature without the preload. Once the equilibrium is reached i.e. the required temperature is reached the specimens are subjected to loading till failure. Whereas in case of residual test method, test specimens is heated to the target temperature and it is maintain till steady state is reached, and then it is allowed to cool down to room temperature. Specimen is loaded to failure at ambient temperature to obtain the residual strength of concrete. Mostly, unstressed test method is used which depicts the performance of concrete at specified elevated temperatures.

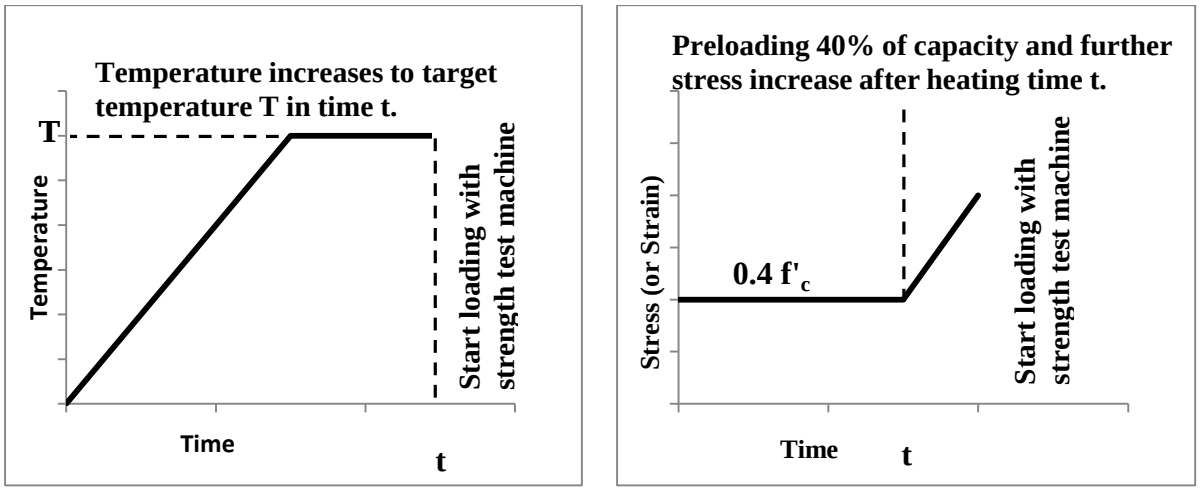

(a) Heating scheme, (b) Loading Scheme

Figure 2.1 – Stressed test method under preload. Khaliq (2012)

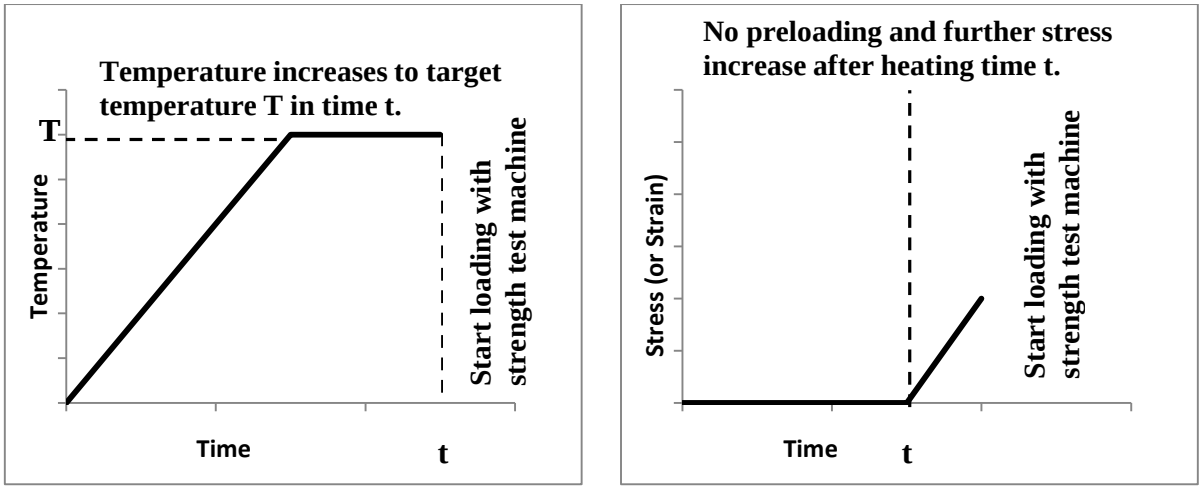

(a) Heating scheme, (b) Loading Scheme

Figure 2.2 – Unstressed test method without preload. Khaliq (2012)

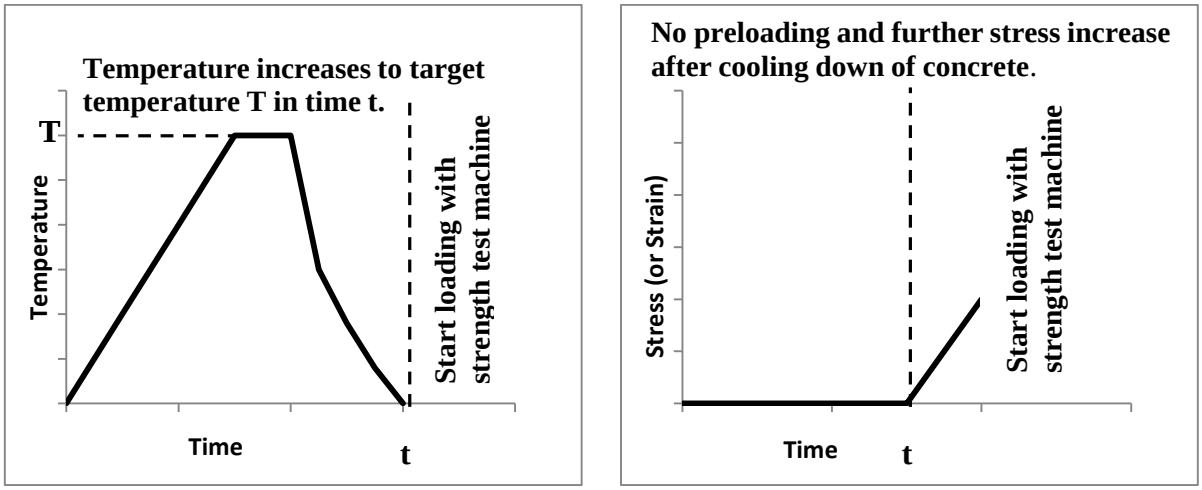

(a) Heating scheme, (b) Loading Scheme

Figure 2.3 – Residual strength measurements. Khaliq (2012)

2.2.3 Previous Studies on High Temperature Material Properties of Concrete

There have been a lot of previous researches on evaluating the high temperature material properties of concrete. In evaluating these properties, the samples are either stressed or unstressed at the specified temperature. Few of the researchers have employed these techniques to measure the response of concrete (Abrams, 1971; Furumura et al., 1995; Harada et al., 1972; Lankard, 1971; Lie and Kodur, 1996; Roux, 1974).

On the other hand, many researchers have adopted the residual strength measuring technique i.e. they have measured the response after the sample cools down to room temperature

(Abrams, 1971; Campbell-Allen, 1965; Malhotra, 1956; Morita, 1992; Phan et al., 2001; Zoldners, 1960).

2.2.3.1 Compressive Strength

Compressive strength is considered to be one of the most important characteristic of concrete. Good amount of data is available on compressive strength of concrete at elevated temperatures for NSC and HSC. Few of the notable studies are presented here to generate information on the high temperature compressive strength of concrete.

Abrams (1971), investigated the effect of high temperature on normal strength concrete with siliceous, limestone and expanded shale aggregates. He reported that, at temperatures above 430°C siliceous aggregate concrete loses greater proportion of its strength than concrete made with limestone or lightweight aggregate but once the temperature reaches 800°C, the difference disappears. This trend can be seen in Figure 2.4.

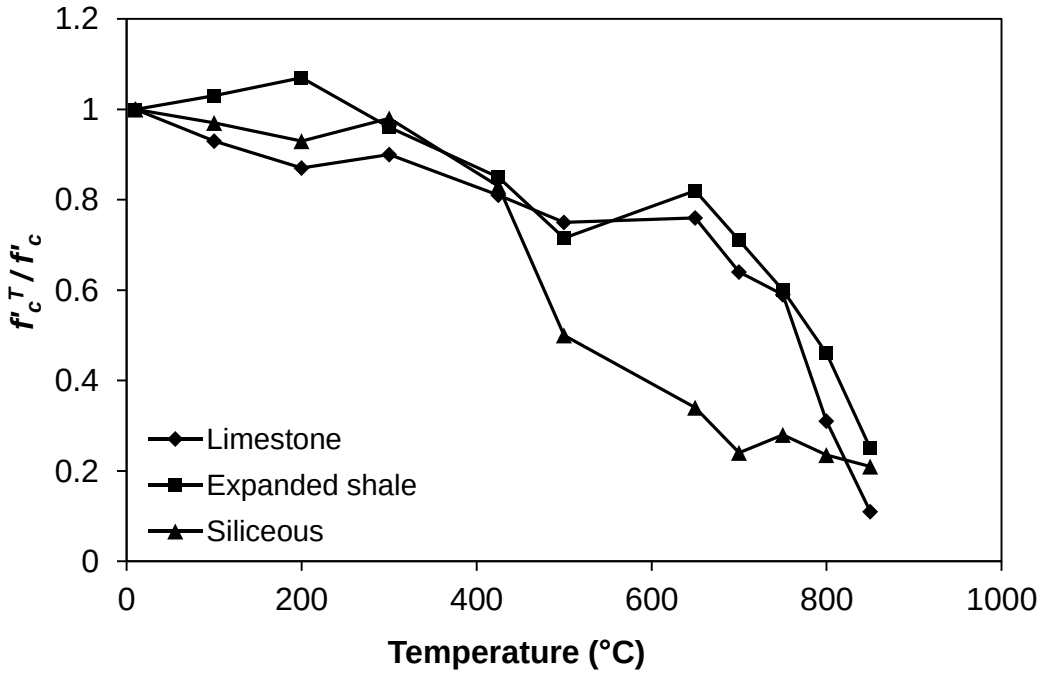

Figure 2.4 – Reduction in compressive strength of concrete using different types of aggregates. Abrams (1971)

In addition to that, Abrams (1971) also evaluated the reduction in strength when concrete is made with limestone aggregate using three test methods of high temperature i.e. unstressed test method, stressed test method and residual strength test method. The reduction in strength in all the three cases can be seen in Figure 2.5. It can be seen that samples which are stressed during heating performs much better than the other two cases, whereas heating unloaded specimens leads to the lowest strength if the subsequently cooled concrete.

Morita (1992), evaluated the residual compressive strength of both NSC and HSC. He selected different range of concrete having compressive strength ranging from 19.6 to 74 MPa. He reported that HSC has a higher rate of reduction in residual compressive strength (and modulus) than a NSC. This reduction in compressive strength can be seen in Figure 2.6.

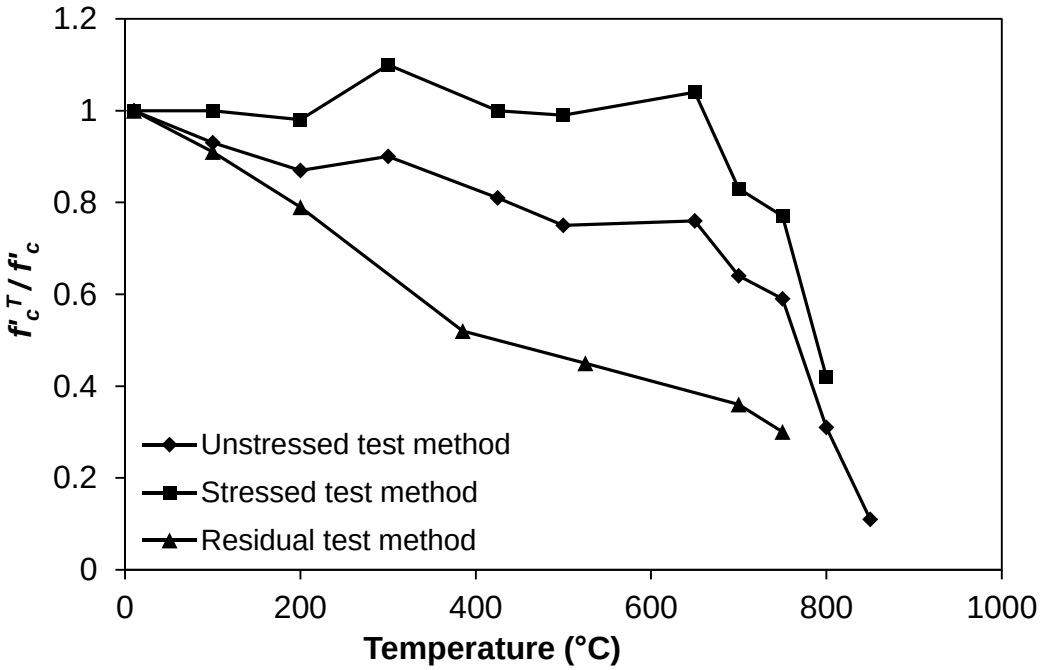

Figure 2.5 – Reduction in Strength of concrete when using different type of test method. Abrams (1971)

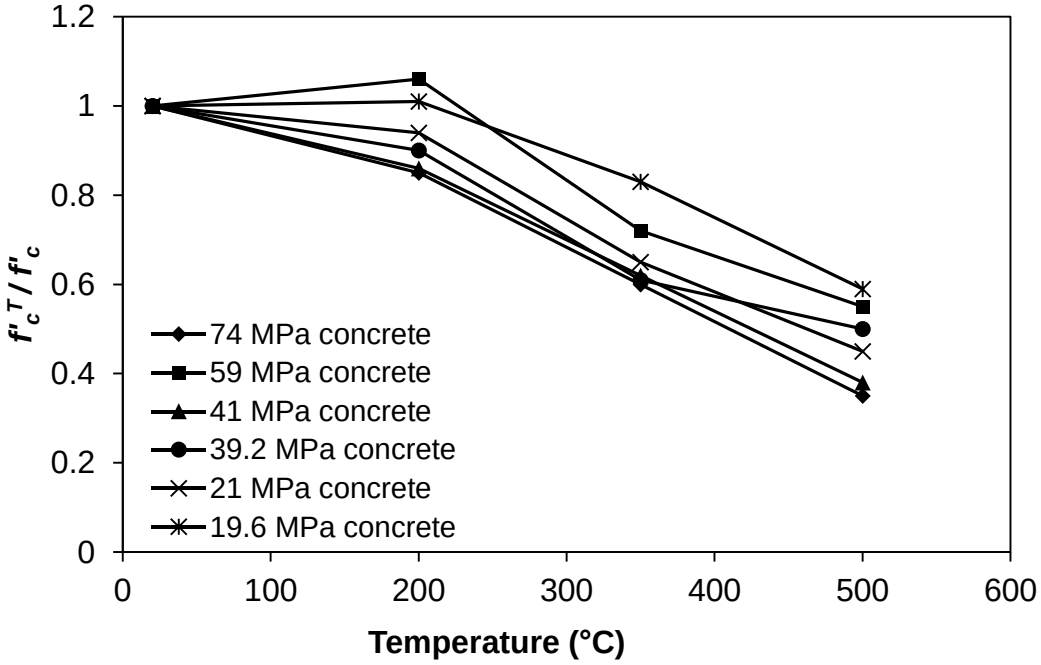

Figure 2.6 – Residual normalized strength vs temperature.

Furumura et al. (1995), performed the high temperature test on ordinary Portland cement concrete using unstressed test method. He obtained the results of three types of concrete i.e. 21, 42 and 60 MPa as presented in Figure 2.7. Results obtained for each of the concretes were similar in that the compressive strength decreased at 100°C, recovered to the room temperature strength at 200°C, and then decreased monotonically with increasing temperature beyond 200°C.

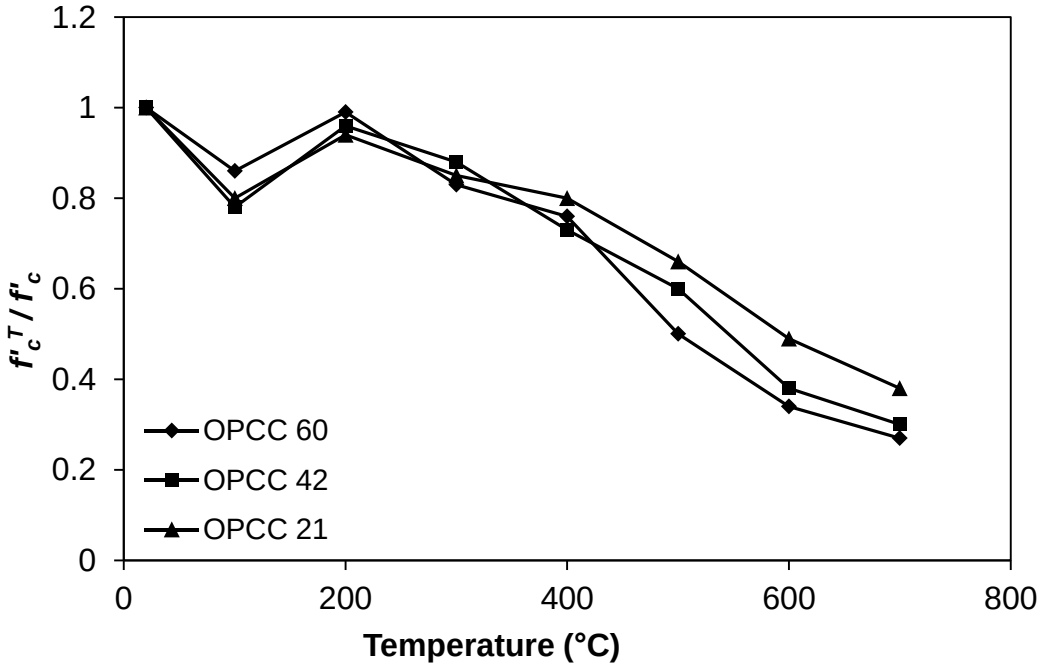

Figure 2.7 – Unstressed normalized strength vs temperature of ordinary portland cement concrete.

Carette et al. (1982), performed the experiments to investigate the use of pozzolans in NSC at elevated temperatures. He found out that there was no difference between the relative loss of strength between concrete made with Portland cement only and concrete containing fly ash or ground granulated blast furnace slag. Similarly, he also evaluated the relative loss in compressive strength which is slightly smaller for water/cement ratio of 0.6 than at the water/cement ratio of 0.45. Even the change in water/cement ratio of NSC with the addition of pozzolans did not show any effect on high temperature material properties of concrete. Figure 2.8 shows the loss of strength observed by him in NSC made with ordinary Portland cement with water to cement ratio of 0.45.

Lie and Kodur (1996), investigated the high temperature strength properties of NSC with and without steel fibers. They reported that the compressive strength of concrete with steel fibers degrade much faster as compared to similar concrete without steel fibers at elevated

temperatures. They also concluded that the effect of aggregate type on the compressive strength is not significant.

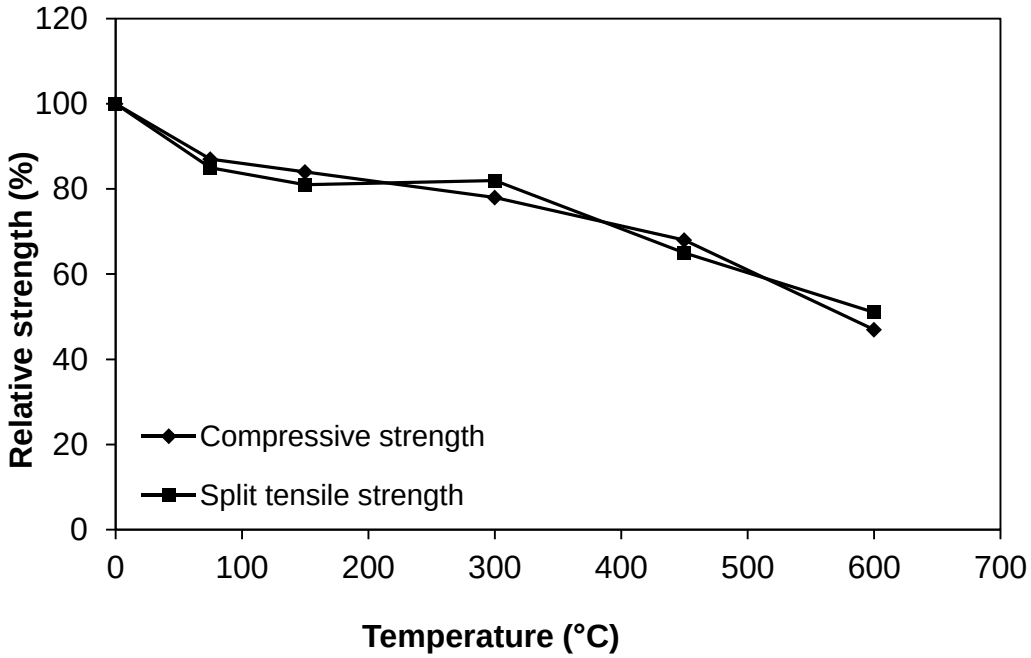

Figure 2.8 – Influence of high temperature on compressive and split tensile strength of NSC.

Zoldners (1960), observed the effect on the compressive strength of four types of concrete having different types of aggregates, after being exposed to elevated temperatures. Figure 2.9 show us the trend of concrete with different types of aggregate. It can be seen that the major loss of strength in concrete take place after 500°C, whereas before this temperature they all retained 70 to 80 % of their strength.

Chan et al. (1999), investigated the residual compressive strength of both NSC and HSC after exposure to elevated temperatures. He recognized three distinct temperature ranges having an effect on loss of compressive strength of concrete namely, 20-400°C, 400-800°C, and 800-1200°C. He observed that only small part of strength was lost in 20-400°C (1-10% for HSC and 15% for NSC), however severe loss occurred in 400-800°C range. This severe loss in 400-800°C was attributed to deterioration of calcium silicate hydrate (C-S-H) gel and cementing ability due to dehydration of concrete. They suggested the temperature range of 400-800°C be regarded as critical strength-loss range for concrete. Above 800°C the residual strength was reported as only the small portion of the original strength.

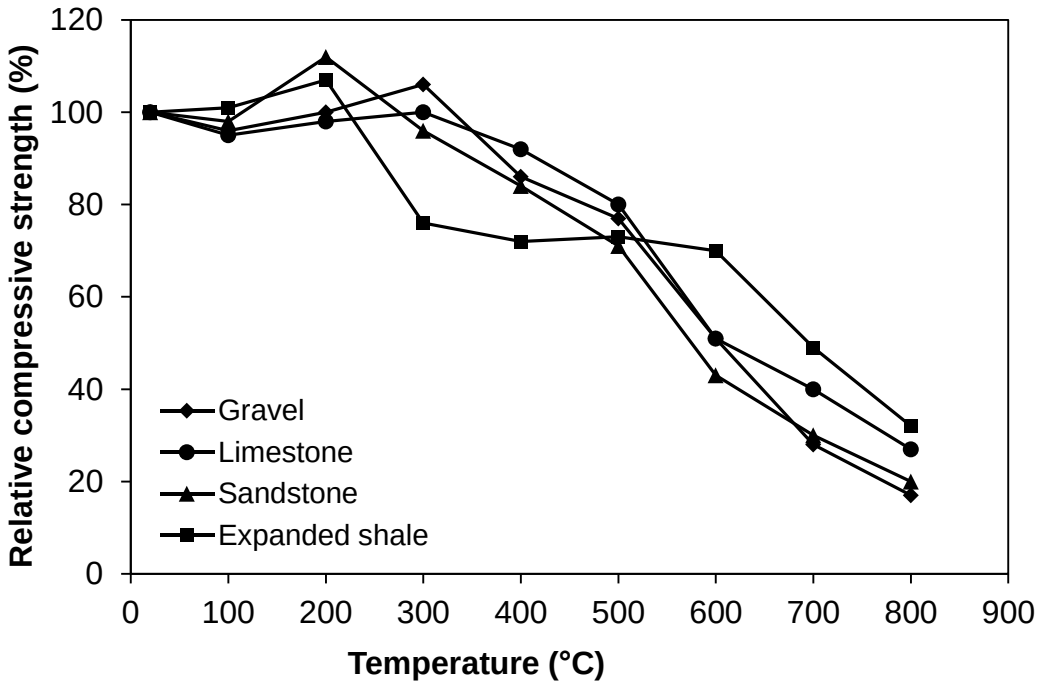

Figure 2.9 – Loss of compressive strength with increasing temperature: Portland-cement concretes.

Li et al. (2004), investigated the residual material properties of NSC and HSC at elevated temperatures. They investigated the influence of temperature, water content, specimen size, strength grade and temperature profiles on material properties. Authors reported that the compressive strength of HSC drops with temperature after 200°C. The strength loss in HSC was higher (36.8%) in 20-400°C as compared to NSC (28.8%), and this higher loss was attributed to dense microstructure and impermeability of HSC. It was also reported that water content had minimum effect on high temperature strength loss of concrete. As for specimen size, it was concluded that compressive strength loss of larger concrete specimens was lower than that in smaller size specimens.

The review of the above mentioned compressive strength properties showed that a lot of research has taken place in evaluating the high temperature behavior of NSC and even HSC. In addition, it can be seen that there is a lot of variations in the results presented by various investigators. Moreover, there is very little data available on high temperature strength properties of CACC. Therefore, data on this type of concrete as a function of temperature is needed for evaluating the fire response of structural members made with CACC.

2.2.3.2 Tensile Strength

Tensile strength of concrete at room temperatures can be evaluated through three methods namely, flexural tensile, direct tension, and splitting tensile strength tests. Flexure tensile strength is obtained through subjecting a concrete beam to third-point flexural loading ASTM C78 (2009). The direct tensile strength is measured by testing cylinder or prism specimens by applying axial tensile load in a suitable test machine until specimen breaks in direct tension ASTM C1583 (2004). This method is unreliable because the holding devices (grips) introduce secondary stresses in the specimens resulting into unreliable data. The splitting-tension test is an indirect test for tensile strength of concrete in which a horizontal concrete cylinder is loaded in compression through bearing strips placed along two axial lines that are diametrically opposite on the specimen ASTM C496 (2004). The load is increased till the failure occurs by splitting the sample along the vertical diameter (Khaliq and Kodur, 2011).

Tensile strength of concrete is dependent on compressive strength of concrete, water/cement ratio, aggregate-paste interface transition zone, presence of any flaw and microstructure of concrete (Neville, 2004). A review on the literature indicates that there has been very limited information available on the tensile property of concrete at elevated temperatures. In addition, it is worth mentioning that all the previous studies on high temperature tensile strength of concrete are based on the residual test method. In this method the sample is allowed to cool down after the exposure to the desired temperature which cannot represent the tensile strength of hot concrete which is required to predict the spalling of the concrete. Some of the noteworthy studies are presented here, which will help us to generate the information on the behavior of concrete at high temperature.

Noumowe et al. (1996), performed the residual tests on normal-strength (38.1 MPa) and high-strength (61.1 MPa) calcareous aggregate concrete to evaluate the effect of elevated temperature on the direct-tensile and splitting tensile strengths. The experimental results are shown in Figure 2.10. It can be seen that the residual tensile strengths for both NSC and HSC decreased similarly and almost linearly with increasing temperature. Also, tensile strengths measured by the splitting tensile test were consistently higher than those obtained by the direct tension test.

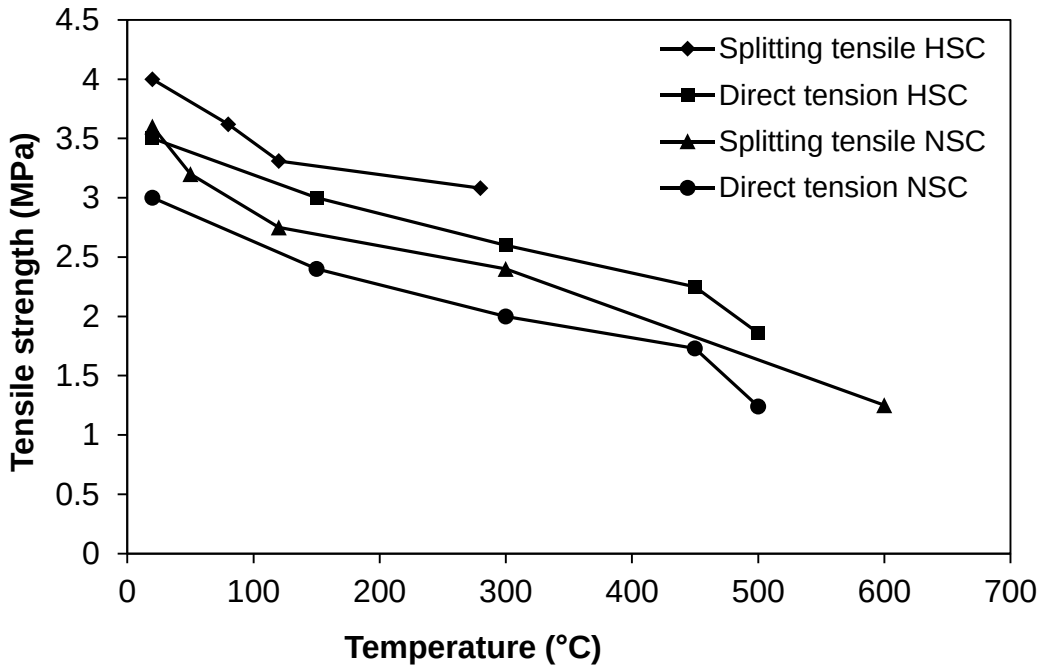

Figure 2.10– Residual tensile strengths of HSC and NSC.

As the tensile strength of concrete, depends upon aggregate-paste interface transition zone, presence of any flaw and microstructure. So with the increase in temperature, the thermal damages in the form of microcracks increases which ultimately affects the tensile strength of the concrete.

Carette et al. (1982), investigated the temperature effect on the tensile strength of NSC. He exposed that concrete cylinders to 600°C and investigated their tensile strength using residual test method. He reported that 65-70% reduction of strength takes place at 600°C. This effect on the tensile strength of NSC can be seen in Figure 2.8. He also concluded that water/cement ratio and type of aggregate have a significant influence on the splitting tensile strength of NSC.

Eurocode 2 (2004), fire provisions recommend accounting for tensile strength properties of concrete in fire resistance calculations. It treats both NSC and HSC alike for temperature dependent tensile strength of concrete by provision of a simple relationship for representation of tensile strength of concrete with temperature. On the other hand, ACI 216.1 (2007) does not provide any guideline or relationship for tensile strength of concretes.

2.2.3.3 Elastic Modulus

Elastic modulus is another important material property of concrete, as it is a measure of its stiffness and resistance to deformation. It is also influenced with the rise in temperature. It degrades with the increase in temperature thus influencing the fire resistance property of concrete structural members. This decrease in the elastic modulus with the increase in temperature is due to the disintegration of hydrated cement paste and breakage of bond in microstructure at interfacial transition zone. The extent of loss depends upon the moisture loss, high temperature creep and type of aggregate (Bažant and Kaplan, 1996).

Marechal (1972), evaluated the change in the elastic modulus of NSC within wide range of temperatures both above and below room temperature. He studied that the modulus of elasticity of NSC keeps on reducing at a much faster rate after 100°C due to increase in the porous volume of concrete in addition to the cracking in the microstructure of the concrete. The influence of temperature on the modulus of elasticity can be seen in Figure 2.11.

Castillo and Duranni (1990), investigated the effect of temperature experimentally on elastic modulus of both NSC and HSC in 23-800°C temperature range. The authors measured the elastic modulus at elevated temperature using closed-loop servo-controlled hydraulic testing machine integrated with an electric furnace. They reported that both NSC and HSC have similar loss of elastic modulus under elevated temperature. The rate of loss of modulus was not very sharp till 400°C but a much faster loss was observed between 400-600°C. The higher loss above 400°C is due to the progressive dehydration and loss of bond between the materials. This change in modulus of elasticity with increase in temperature is shown in Figure 2.11. The degradation in the NSC can be attributed to excessive thermal stresses and physical and chemical changes in the concrete microstructure.

Xiao and König (2004), reviewed the studies performed in china on the evaluation on the high temperature properties of concrete. Figure 2.12 shows the variation in elastic modulus on NSC and HSC from researcher of china. It can be seen that the elastic modulus after high-temperature exposure (residual) was lower than that obtained at high temperature.

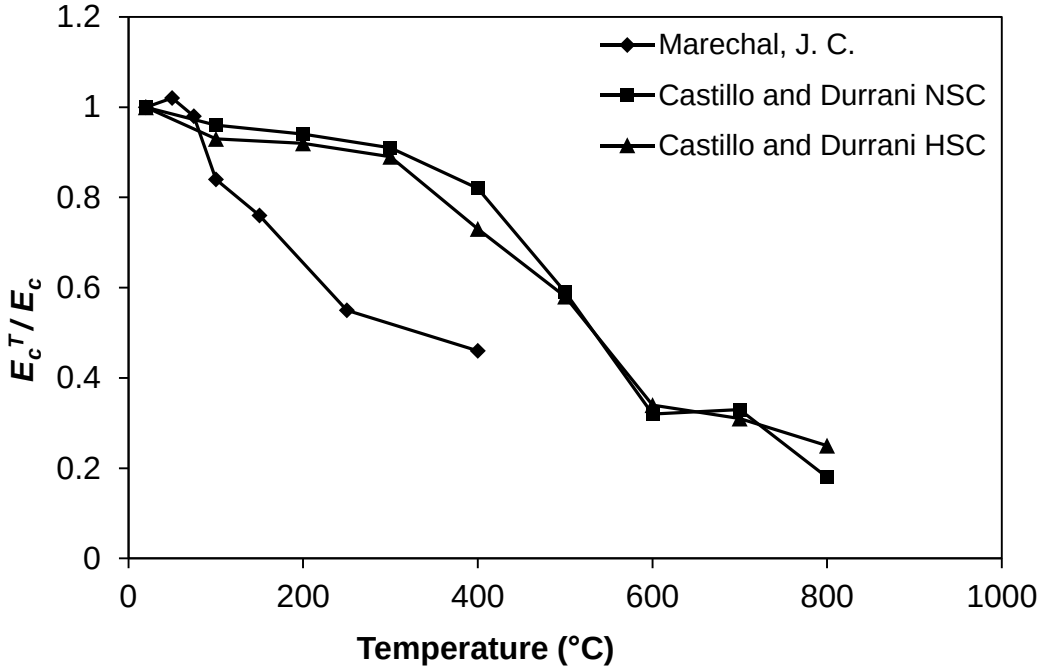

Figure 2.11– Influence of temperature on elastic modulus of concrete.

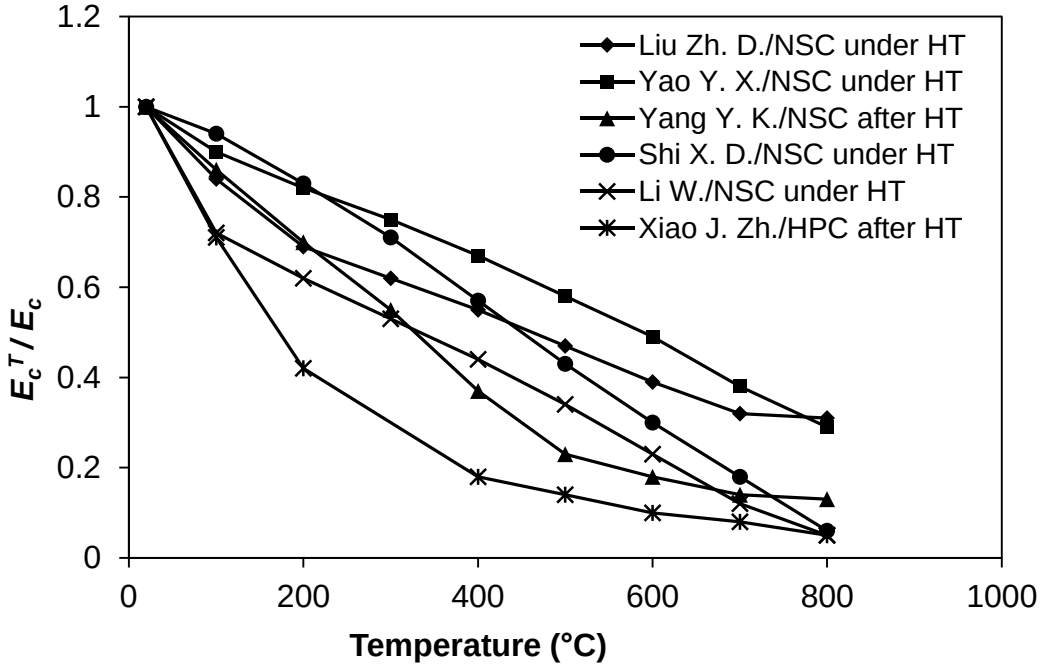

Figure 2.12 – Temperature dependence of the concrete's elastic modulus (normalized).

2.2.3.4 Stress-Strain Response

The mechanical response of concrete is usually expressed in the form of stress-strain relationship, which is frequently used as the input data in the mathematical models for evaluating the response of the concrete structural members against fire. Generally, because of decrease in compressive strength and increase in ductility of concrete, the slope of the stress-

strain curve decrease with the increase in temperature. The strength has a significant influence on the stress-strain response both at room and elevated temperatures (Kodur, 2014). Limited data is available on the stress-strain behavior of concrete at elevated temperatures because of the complexity of the stress-strain curve of concrete. However, few of the researchers have carried out the experimentations to investigate the stress-strain curve of concrete under all three test conditions (stressed, unstressed and residual).

Castillo and Duranni (1990), studied the effect of transient high temperature on stress-strain response of HSC and NSC under both stressed and unstressed test conditions in 23-800°C range. It was found in this study that there was no difference in the response of stress strain curve of both types of concrete. In case of NSC, there was no significant variation in the value of strain at peak stress between 100-200°C. There was slight increment in the value of strain at peak stress between 300-400°C. However, there was a significant increase in strain at peak stress in 500-800°C range. At 800°C, the value of the strain at peak stress was recorded four times the value at room temperature. This change in variation of stress-strain curve at different temperature is shown in Figure 2.13.

Furumura et al. (1995), studied the stress strain response of NSC and HSC by testing the concrete cylinders of both types of concrete. He reported that the response of both types of concrete is very different which is due to the strength of the concrete. It was observed that both types of concrete showed brittle behavior at lower temperatures i.e. below 500°C. However beyond 500°C, the stress-strain curve showed much more ductile response. This trend is attributed to the reason that at higher temperature thermal stresses are developed which causes internal microcracking as a result the slope of the stress-strain curve was decreased i.e. ultimately the modulus of elasticity of the concrete is affected.

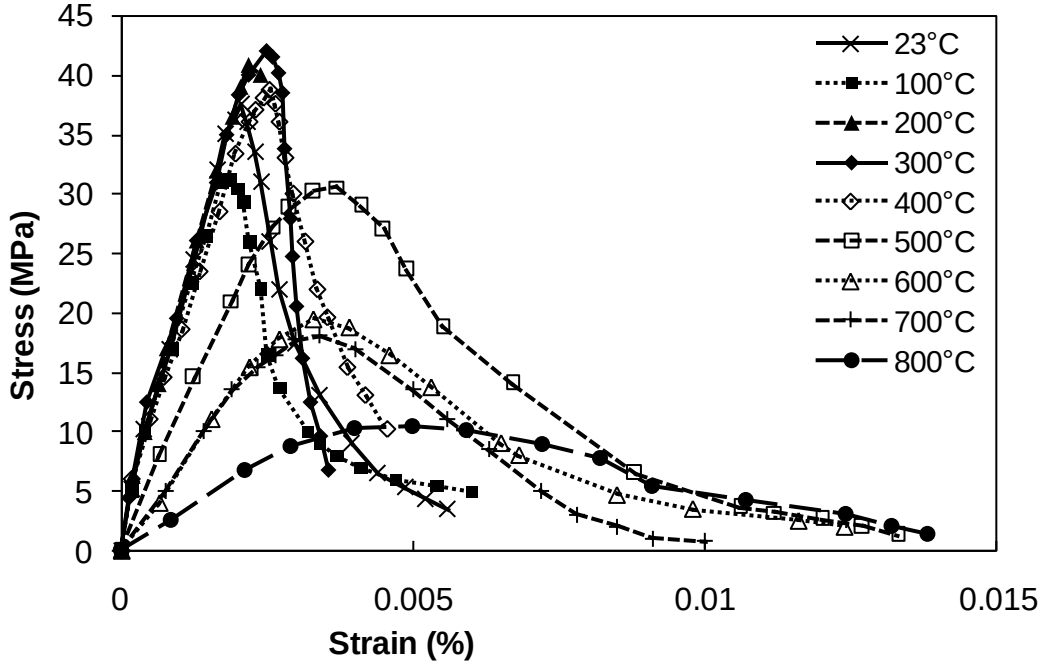

Figure 2.13 – Stress-strain response of NSC at elevated temperature.

2.2.3.5 Toughness

When the performance of the concrete is to be mentioned another material property which is given due importance is compressive toughness (T_c), which is used to determine the energy absorbed by each cylindrical specimen of concrete during the compressive strength test. This property is a derived property and is evaluated as the area under the stress-strain curve of the concrete material. This property tells us about the fracture, post-peak ductility and the energy absorbing capacity of the concrete when it is subjected to compressive load which makes this property very important (Marar et al., 2001). Toughness or energy absorption capacity can be determined from the area under the stress–strain curve in compression, which is the total energy absorbed prior to complete rupturing of the specimen.

Few of the researchers have given importance to this property and measured the energy absorption capacity of different types of concrete (Campione and Mindess, 1999; Campione et al., 1999; Marar et al., 2001; Marar et al., 2011; Prabha et al., 2010). JSCE SF-5 (1984), is usually followed by the researchers to evaluate compressive toughness of concrete which describes the energy absorbed during compression.

As toughness is a measure of the energy absorption capacity and ductility of the concrete, so it is actually used to characterize the concrete's ability to resist fracture and sustain inelastic deformations without substantial decreases in the load carrying capacity (Marar et al., 2011). With the increase in temperature in case of fire, there is a decrease in the stiffness of the

concrete and ultimately the load carrying capacity of the concrete structure which makes it vulnerable. As energy absorption capacity and ductility of concrete tells us about the ability of concrete to sustain fracture and inelastic deformation, so they should be evaluated in terms of toughness of concrete at elevated temperatures. As this property depends upon the stress-strain response of the material which makes it a derived property (Marar et al., 2001), so we can investigate this property of material by studying its stress-strain curve at elevated temperatures for both types of concrete. At present there is very little data available on toughness of concrete and its response at elevated temperatures, which makes this property to be explored.

2.2.3.6 Mass loss

The mass loss with temperature is usually measured by means of thermogravimetric analyzer technique (ASTM C1868, 2010). In this technique, a specimen of known mass is heated at a constant temperature while its mass is continuously monitored as a function of time. At the end of a pre-determined time interval or temperature, the loss in mass of specimen is calculated as a percent of the original mass.

Hu et al. (1993), investigated the thermal properties of construction material available in China. In this study, mass loss is recorded as a function of temperature up to 1000°C. In this study, they evaluated mass loss for carbonate and siliceous aggregate concrete. It was found in this study that mass loss in siliceous aggregate concrete was not high and it dropped only 97% at 1000°C. On the other hand, it was reported that mass loss in carbonate aggregate concrete was 97% for temperature up to 650°C, but there was a rapid mass loss in 650-900°C as it dropped to 75% in this range.

Lie and Kodur (1996), evaluated the mass loss of steel fiber reinforced NSC made with siliceous and carbonate aggregate at elevated temperature. Mass loss was investigated using thermogravimetry technique up to 1000°C. It was found out in this study that mass loss in concrete was not more than 3% up to 600°C for both types of concrete. However, there was a considerable loss in mass up to about 30% for carbonate aggregate concrete in range of 600 to 800°C, which was attributed to dissociation of dolomite in carbonate aggregate. However, in case of siliceous aggregate concrete only 3-4% mass was lost in the entire temperature range of 20-1000°C. It was also found out that mass loss of concrete is not significantly affected by the presence of steel fiber reinforcement in concrete in entire temperature range.

Kodur and Sultan (2003), investigated the mass loss in plain and steel fiber reinforced HSC in temperature range of 0-1000°C. Mass loss was measured using thermogravimetric analyzer

(TGA) up to 1000°C. It was observed that loss in mass was just 3% up to 600°C for both siliceous and carbonate concrete. Between 600 to 700°C there was a considerable drop in mass for carbonate aggregate concrete.

Mass loss of concrete at elevated temperatures is highly influenced with the type of aggregate (Hu et al., 1993; Kodur and Sultan, 2003; Lie and Kodur, 1996). The mass loss is minimal for both carbonate and siliceous aggregate concretes up to about 600°C. However, beyond 600°C, carbonate aggregate concrete experiences larger percentage of mass loss as compared to siliceous aggregate concrete. This higher percentage of mass loss in carbonate aggregate concrete is attributed to dissociation of dolomite in carbonate aggregate around 700°C. Figure 2.14 illustrates the variation of mass loss of concrete as a function of temperature for concrete made with carbonate and siliceous aggregate.

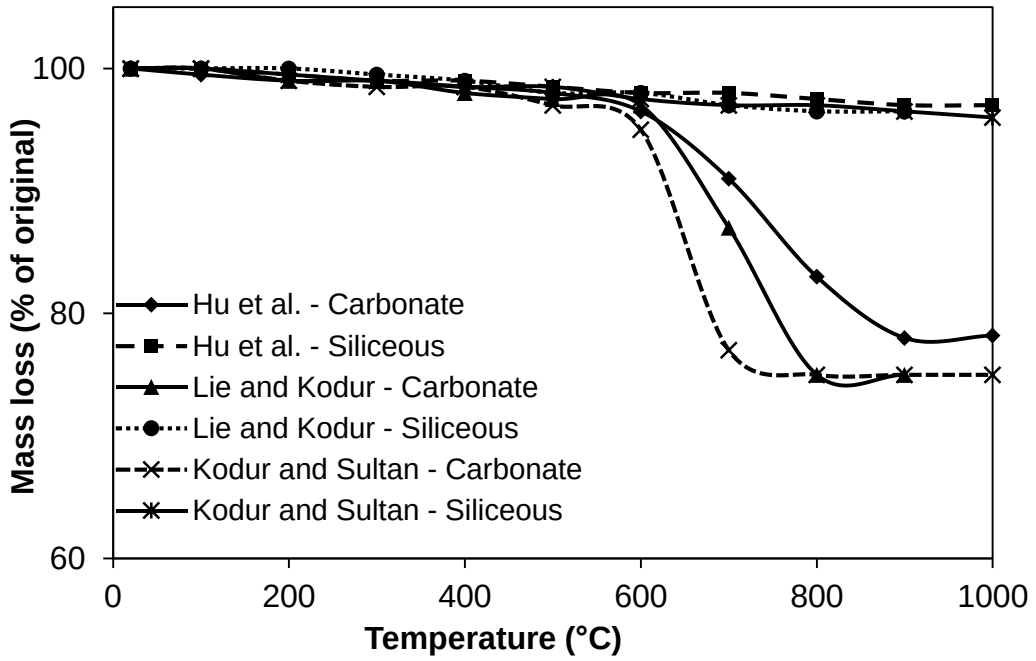

Figure 2.14 – Variation in mass loss as a function of temperature with different aggregates.

Khaliq (2012), evaluated the variation of mass loss as a function of temperature for plain HSC, SCC, FAC and NSC. It was observed that there was no significant loss in mass till 600°C in all types of concrete, however, moderate mass loss up to 10% takes place in 600-800°C in case of SCC and FAC. Higher mass loss up to 20% was observed in HSC in 600-800°C. All of these concretes were made up of carbonate aggregate. The variation in mass loss as a function of temperature can be seen in Figure 2.15 for all types of concrete.

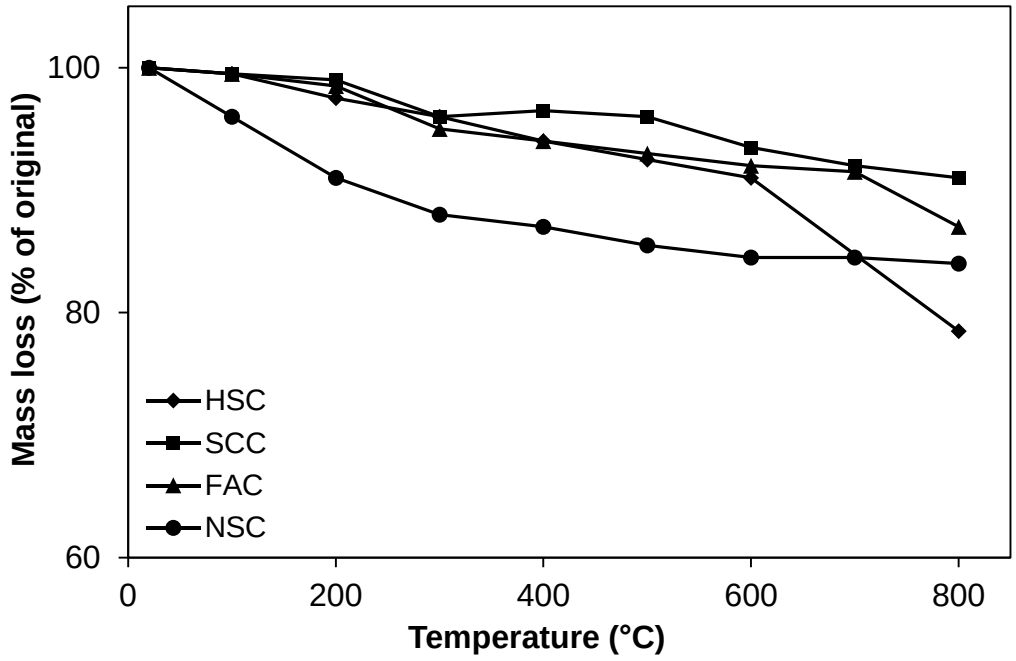

Figure 2.15 – Mass loss as a function of temperature for HSC, SCC, FAC and NSC. Khaliq (2012)

2.3 Calcium aluminate cement (CAC)

2.3.1 General

CAC is versatile special non-Portland cement that is used in high performance applications such as those requiring: resistance to chemical attack, high early strength, refractory, resistance to abrasion, and/or low ambient temperature placement (Ideker et al., 2013; Scrivener et al., 1999). In this section, general behavior of CACC and previous studies on the material properties of CACC when it is exposed to elevated temperatures are presented.

2.3.2 Hydration of CAC

The mineralogy of CAC shows that calcium oxide (CaO) and alumina (Al_2O_3) are the principal oxides. Depending upon their percentage within CAC, they combine to give monocalcium aluminates ($CaAl_2O_4$ or CA) as a major active phase and dodecacalcium heptaaluminate ($C_{12}A_7$). They react very rapidly with water, resulting in the rapid formation of calcium aluminate hydrates. However, unlike portland cement, the formation of CAC hydrates depends upon the availability of moisture and environmental temperature (Scrivener and Capmas, 1998). Hydration products of CAC are subdivided into two categories: metastable hydrates and stable hydrates. Difference in the solubility and density of those hydrates affect the process of conversion from metastable to stable hydrates.

2.3.3 Conversion Process in CAC

Calcium aluminate decahydrate (CAH_{10}) is usually formed below 15°C, which convert to dicalcium aluminate octahydrate (C_2AH_8) and gibbsite (AH_3) with the increase in temperature. However, CAH_{10} and C_2AH_8 are metastable in nature having low density, less porosity and almost occupy all the available space, converts to stable tricalcium aluminate hexahydrate (C_3AH_6) and AH_3 with the liberation of water at temperatures above 27°C. This process is known as conversion reaction and is described in Equations 1 and 2 below. This reaction is inevitable and its rate depends upon temperature and availability of moisture (Scrivener et al., 1999).

$$2CAH_{10} \rightarrow C_2AH_8 + AH_3 + 9H \quad (1)$$

$$2C_2AH_8 \rightarrow C_3AH_6 + AH_3 + 9H \quad (2)$$

2.3.4 Behavior of CAC as a Refractory Concrete

CAC was originally developed for its excellent cementing and sulfate resistant property but later it was observed that this cement not only have the desired property of sulfate resistance, but it perform very well against high temperature. It is their heat resistant property, which has become one of the most important today. The high lime and silica contents of Portland cement render it unsuitable to produce refractory concrete for use at elevated temperatures, due to the formation of hydrates having low melting point. The refractoriness of CAC increases with the increase in proportions to alumina/lime ratio, thus higher the alumina content better will be its capacity to resist high temperature. (Scrivener and Capmas, 1998).

The capacity of an element to resist fire is determined by three major factors: thermal properties, mechanical properties and its capacity to withstand heat and water pressure without cracking and spalling and losing strength. ACI 216.1 (2007), provide guide for determining the fire endurance of concrete elements.

2.3.5 Previous studies on CAC at Elevated Temperature

Few of the research programs carried out in determining the basic physical and material properties of refractory concrete prepared from CAC are presented here.

2.3.5.1 Porosity

Porosity is actually the volume occupied by the air pockets in the total volume of the concrete. These air pockets greatly affect the mechanical (strength etc) and thermal properties (thermal conductivity etc) of concrete. An important function of these pores is that they release the steam

pressure build up from the heated water in the concrete. Without this release in pressure, there is a danger of explosive spalling in the concrete, a problem encountered in high performance concretes, which are extremely dense and are of low porosity (Ali, 2002; Kodur, 2000).

Gibbels (1970), evaluated the porosity of refractory concretes when fired to different elevated temperatures. It was observed that the porosity in an aluminous cement concrete when fired at 950°C results in an increase in porosity from 27% to 31%. During heating this increase is immediately followed by decrease in porosity due to the closing of pores caused by smelted material in concrete as shown in Figure 2.16. It can be seen from the figure that the lightweight refractory concrete possess more porosity which explains their low densities.

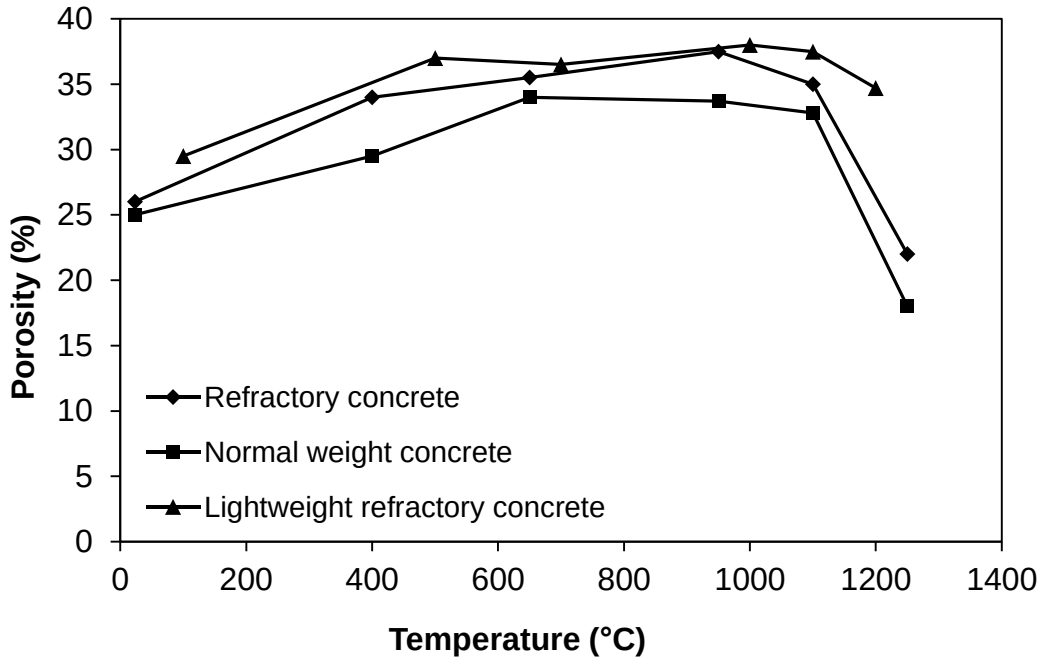

Figure 2.16 – Variation of Porosity in refractory concretes with Preheat temperature.

2.3.5.2 Density

Density of the material is closely related to the porosity, specific gravity and individual densities of the constituent materials. Most refractory concretes tend to have the density less than 130 pcf, compares to 140-160 pcf of normal weight structural concrete. Lightweight refractory concretes have densities ranging from 20 pcf to 100 pcf (Onodera, 2002).

Maslennikova (1970), evaluated the cold compressive strength of refractory concretes having different densities. Figure 2.17 shows the relationship of ceramsite refractory concrete, its density and pre heat temperature. It can be seen that the maximum strength is achieved by concrete having 1400 g/cm^2 which is around 22 MPa as compared to 1300 g/cm^2 which is just

14 MPa. It can be seen that these strengths are highly dependent upon the temperature and it starts decreasing as the temperature increases.

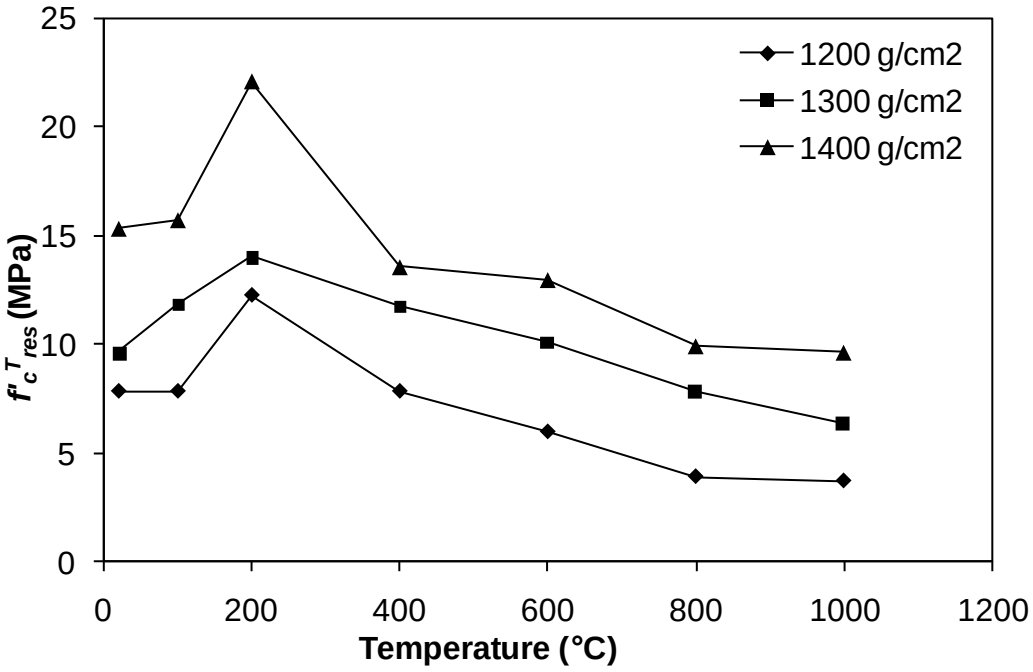

Figure 2.17– Relationship between cold compressive strength of ceramsite refractory concretes and its density and temperature of Pre-heat.

2.3.5.3 Strength

Most of the tests on concrete exceeding 1000°C are conducted to evaluate only the cold compressive strength because of the logistics involved. The cold compressive strength is simply the compressive strength of concrete after it has been heated to a specified temperature and then allowed to cool down to room temperature. A drawback of this method is that it may not accurately measure the concrete's real compressive strength at service temperature.

Mitusch (1970), performed the experiments on aluminous cement concrete having different aggregates types and content and observed the variation of strength with the increase in temperature. Figure 2.18 shows that with the increase in the aggregate content the performance of the concrete is improved. In addition, it can be seen that after 1000°C there is an increase in the cold compressive strength. This gain in strength is due to the development of the ceramic bond. This bond is established by the solid reaction between the cements and the fine aggregates with the increase in temperature resulting in an increase in bond strength (Neville, 2004).

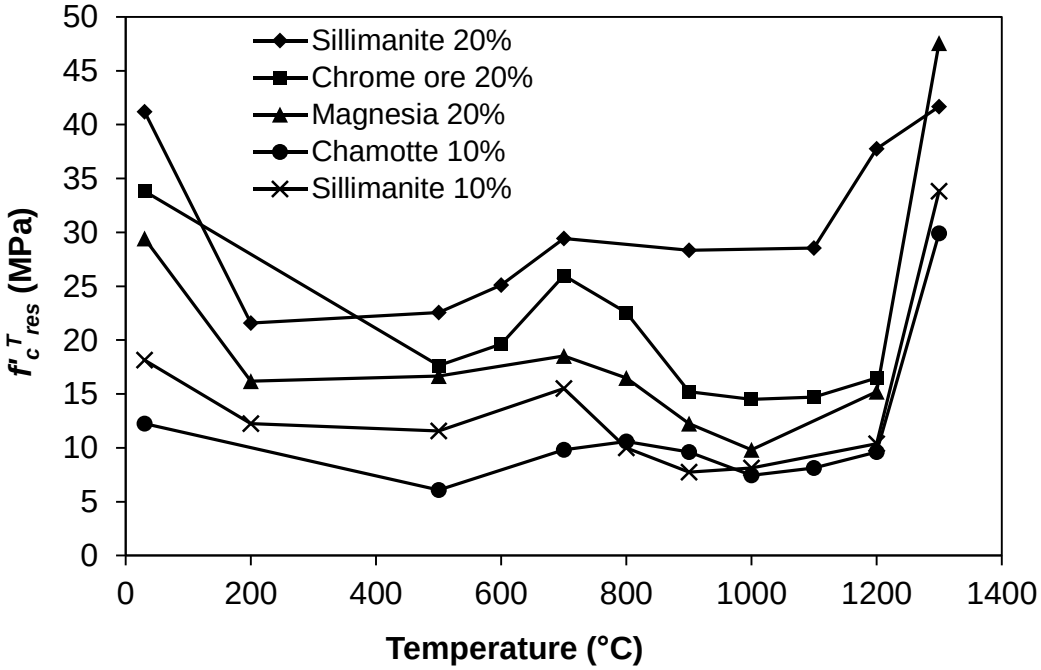

Figure 2.18 – Intermediate maxima of the cold compressive strength of Pre-heated aluminous cement concretes.

Mitusch. et al. (1970), performed the hot compressive test on the aluminous cement concrete as it represents the concrete's real strength under load and temperature. Figure 2.19 show the variation in hot compressive strength at specified temperatures.

By comparing Figure 2.18 and 2.19 it can be seen that the cold compressive strength is about one third time higher than the hot compressive strength. The hot compressive strength also experiences the similar reduction in compressive strength with the increase in temperature up to approximately 1000°C, after that there is no data available to show the gain in strength with the formation of ceramic bond. The effect of this ceramic bond will be different on the bonding when the specimen is exposed to service load and temperature concurrently, as opposed to just a loading following the firing.

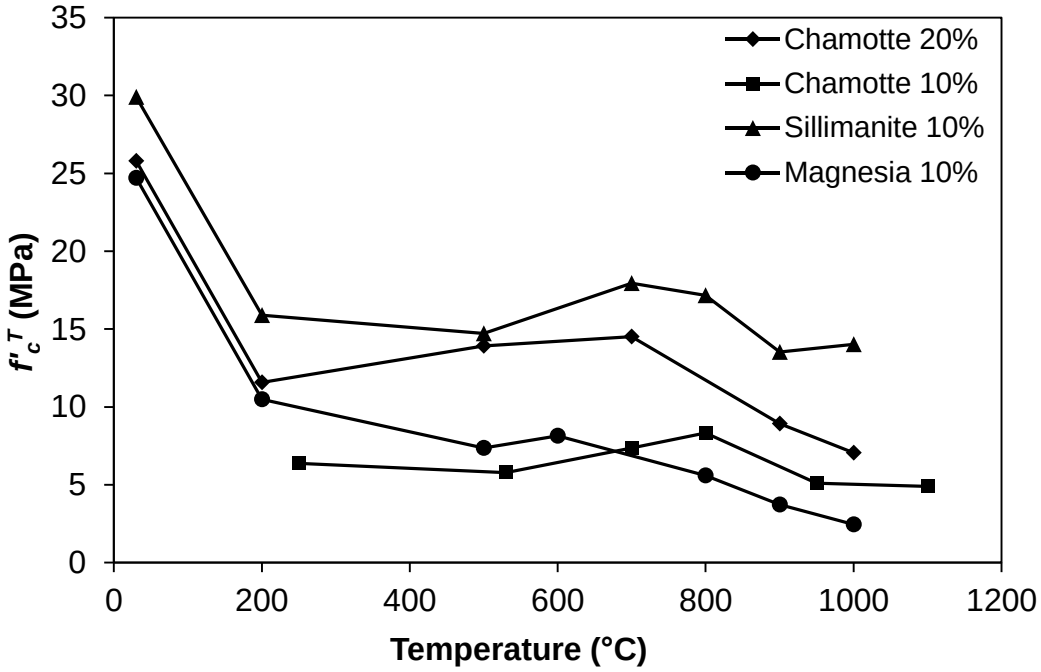

Figure 2.19 – Hot compressive strength of aluminous cement concretes.

Zoldners et al. (1963), conducted a study to investigate the performance of aluminous concrete with different types of refractory aggregate at elevated temperatures. It can be seen in Figure 2.20 that with the increase in temperature there is a loss in strength. This behavior of high alumina concrete is comparable with that of Portland cement concrete as in both types of concrete there is an appreciable loss in strength. Sudden drop in strength was observed up to 400°C which is linked to the conversion reaction within the microstructure of CACC. However, the loss of strength was reduced and remains gradual from 400°C till 800°C. It can be seen that the minimum value of strength vary between 5 % and 26 % of the original value at room temperature. Further a slight increase in strength was observed beyond 800°C and 1000°C in phonolite and anorthosite aggregate concrete respectively, due to the development of ceramic bond. As a result high alumina cement can withstand very high temperatures. This increase in strength after firing to temperature as high as 1000°C is not observed in Portland cement concrete which makes this concrete vulnerable to fires.

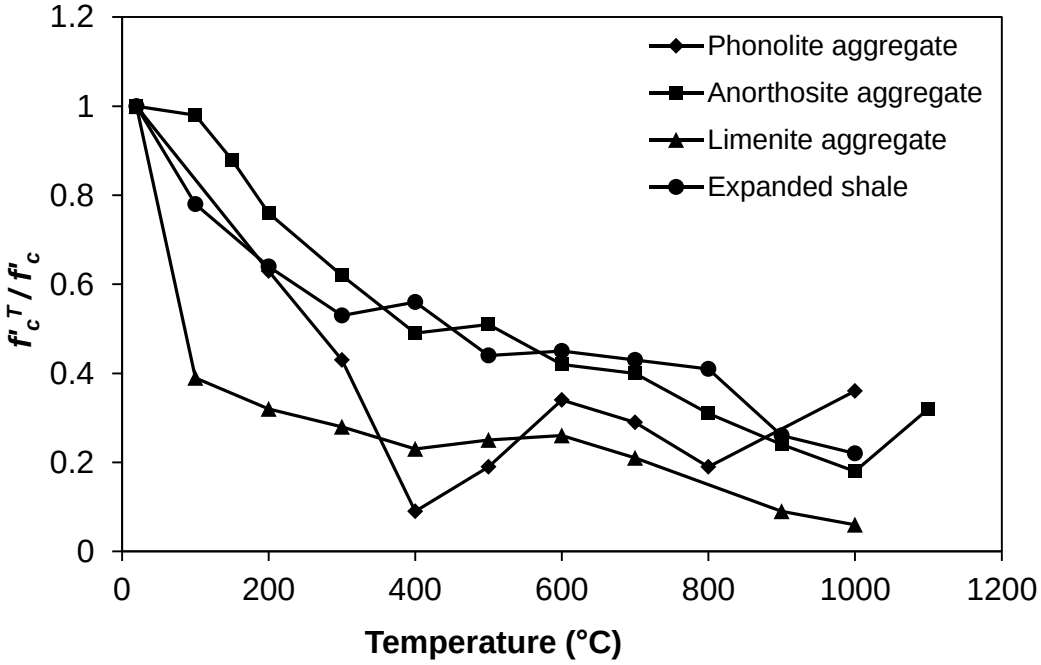

Figure 2.20 – Strength of high alumina cement concretes made with different aggregate as a function of temperature.

2.4 Summary

Based on state-of-the-art literature review, it is concluded that the fire performance of the concrete whether it is NSC or CACC mainly depends upon the material properties which includes compressive strength, tensile strength, elastic modulus, stress-strain response, mass loss and toughness. The above review shows that good amount of data is available on the material properties of NSC at elevated temperatures. But this data is not available for CACC which is desirable if we want to use it in building construction. Thus the primary objective of this research is to evaluate the high temperature material properties for CACC. Further, the generated test data can be used to develop mathematical relations for various properties as a function of temperature.

CHAPTER 3

EXPERIMENTAL PROGRAM

3.1 General

For evaluating the performance of concrete at elevated temperatures, material properties of calcium aluminate cement concrete (CACC) is required. The material properties include compressive and tensile strength, elastic modulus, mass loss, compressive toughness and stress-strain response of constituent material at elevated temperatures. As discussed earlier in the literature review, there is a lack of data available on the mechanical and material properties of CACC at high temperature. Availability of high temperature material property relations for CACC is critical for evaluating the strength degradation of structural members made with such concrete types.

In order to evaluate the effect of elevated temperatures on these material properties of CACC, high temperature property tests were carried out which includes, compressive strength test, splitting tensile strength test, stress-strain behavior and elastic modulus. The generated property data was utilized to develop the relations for various material properties as a function of temperature in 23-800°C. Details of experimental design, test equipment and test procedures are discussed in this chapter.

3.2 Design of Material Property Experiments

The test program was designed to undertake high temperature material property tests on both CACC and NSC. Numbers of cylindrical specimens were fabricated from each batch of concrete mixes. These cylinder specimens were tested at various temperatures of 23, 200, 400, 600 and 800°C to evaluate the high temperature material properties.

Due to lack standardized test methods for the high temperature strength tests on concrete in ASTM standards, RILEM (1995; 2000) were mostly followed to evaluate the mechanical and material properties of concrete. In addition to that, special handling techniques were used as a part of this study to transfer the heated cylinders from furnace to strength test machine. For this purpose thermal jacket was used to transfer the specimen for performing the compressive strength tests and stress-strain tests. In addition, insulated steel bracket frame was used to transfer specimens for splitting tensile strength tests (Khaliq, 2012).

For evaluating the material properties of concrete two test methods were used namely, unstressed test method and residual test method which are discussed in the literature review

chapter. The material properties of both types of concretes (NSC, CACC) were evaluated using these methods but special handling techniques were used only in unstressed test method.

3.3 Preparation of Specimen

3.3.1 Material

The following material were used in this study, which are described as follows.

3.3.1.1 Cement

Ordinary Portland cement (CEM-I 43.5 R) and calcium aluminate cement (CA-50) shown in Figure 3.1 were used in the experimental program as binders for making NSC and CACC, respectively. Physical and chemical properties of binders are shown in Table 3.1.

(a) CAC (CA-50) (b) OPC (CEM-I)

Figure 3.1 – Binders used in concrete.

3.3.1.2 Fine Aggregate

Natural sand in saturated surface dry (SSD) condition was used as a fine aggregate having a fineness modulus of 2.22 and water absorption of 1.5% obtained from lawrencpur region. It was clean, free of any organic, deleterious materials and relatively free from clay. The results of aggregate gradation on fine aggregate performed are shown in Table 3.2. The results were compared with the upper and lower limits specified by ASTM C33 (2003). The physical properties of sand obtained by performing laboratory tests are shown in Table 3.3.

Table 3. 1 – Physical and chemical properties of powders

Sr. No.	Properties	Material	
		OPC CEM1 (%)	CAC CA-50 (%)
1.	SiO_2	22	7.6
2.	Al_2O_3	5.25	54.5
3.	CaO	63.5	33.4
4.	Fe_2O_3	3.25	2.6
5.	MgO	2.56	0.7
6.	SO_3	1.51	0.2
7.	$Na_2O + K_2O$	1.2	0.4
8.	Specific Gravity	3.15	3.34

Table 3. 2 – Gradation of Fine Aggregate

Sieve No	Sieve size (mm or µm)	Weight Retained (gms)	Percent Retained (%)	Cumulative Percentage Retained (%)	Cumulative Percentage Passing (%)	ASTM C 33 – 03
#4	4.75 mm	5	0.5	0.5	99.5	95 – 100
#8	2.36 mm	56	5.6	6.1	93.9	80 – 100
#16	1.18 mm	45	4.5	10.6	89.4	50 – 85
#30	600 µm	191	19.1	29.7	60.3	25 – 60
#50	300µm	491	49.1	78.8	21.2	5 – 30
#100	150µm	182	18.2	97	3	0 – 10
Pan		30	3	---	0	
Total		1000		222.7		

Table 3. 3 – Laboratory test results

Sr. No.	Properties	Results
1.	Max. Aggregate Size	19 mm
2.	Fineness modulus	2.22
3.	Specific gravity of fine aggregates	2.66 (SSD)
4.	Water absorption of fine aggregate	1.5 %
5.	Specific gravity of coarse aggregate	2.63 (SSD)
6.	Impact value of coarse aggregate (%)	11.4
7.	Water absorption of coarse aggregate	0.65 %

3.3.1.3 Coarse Aggregate

The coarse aggregate used in this study consists of a mixture of crushed and few round gravels obtained from margalla crush. All the aggregates used were in SSD condition having specific gravity of 2.63 and 19 mm maximum size. The physical properties obtained by performing laboratory tests are shown in Table 3.3. Gradation of coarse aggregate is shown in Table 3.4. The results were compared with the upper and lower limits specified by ASTM C33 (2003).

3.3.1.4 Water

Drinking tap water was used for mixing and curing of concrete.

3.3.2 Mix Proportion

Before preparing the cylinders for the mechanical property test, different material property tests were performed to carry on with the mix design of NSC as per ACI 211.1-91 (2002) mix design procedure. Two mixes of concrete were prepared having different binders but same mix design. Water to cement ratio of 0.5 was used with a target compressive strength of 20 MPa at 28 days. No admixture or additive is added in the concrete. The slump cone test was performed to check the workability of concrete. The details of the laboratory test results, mix proportions and laboratory conditions are given in Table 3.3 and 3.5.

Table 3. 4 – Gradation of coarse aggregate

Sieve No	Sieve size (mm or µm)	Weight Retained (gms)	Percent Retained (%)	Cumulative Percentage Retained (%)	Cumulative Percentage Passing (%)	ASTM C 33 – 03
¾”	19 mm	0	0	0	100	100
½”	12.5 mm	250	8.33	8.33	91.667	90 – 100
3/8”	9.5 mm	1470	49	57.33	42.67	40 – 70
#4	4.75 mm	1160	38.67	96	4	0 – 15
#8	2.36 mm	115	3.83	99.83	0.167	0 – 5
Pan		5	0.167	100	0	
Total		3000				

Table 3. 5 – Mix proportions for NSC and CACC

Components	NSC	CACC
Ordinary Portland cement (CEM-I), Kg/m^3	410	-
Calcium Aluminate cement (CA-50), Kg/m^3	-	410
Fine Aggregate ASTM C-33, Kg/m^3	657	657
Coarse Aggregate ASTM C-33, Kg/m^3	1055	1055
Water, Kg/m^3	205	205
Water to cement ratio (w/c)	0.5	0.5
Slump (mm)	110	125
Humidity at casting (%)	44	44
Ambient temperature at casting (°C)	23	23

3.3.3 Mixing of concrete

A motor operated drum mixer having maximum capacity of 2.5 cft (0.07 m^3) is used for mixing of concrete. Conventional method of mixing was used for both types of concrete mixes as per ASTM C192 (2002).

3.3.4 Sample preparation

Concrete cylinders were cast at the same time under similar conditions confirming ASTM C192 (2002). A total of 40 cylinder specimens each, 100x200 mm (100mm dia by 200mm long) were fabricated for undertaking the unstressed and residual material property tests. Concrete mixes are placed in layers inside the mould. After filling the mould, trowel was used to plane the surfaces of the specimens. All the specimens were removed from moulds after the required time i.e. 24 hours and placed for curing at a controlled environment of 95% humidity and 23°C temperature for 28 days. Figure 3.2 shows the sample ready for testing. Room temperature compressive strengths were also obtained at 3, 14 and 28 days for both types of mixes i.e. NSC and CACC. The details of compressive strength are given in Table 3.6.

(a) NSC samples (b) CACC samples

Figure 3.2 – Samples ready for testing.

Table 3. 6 – Compressive strength of NSC and CACC mixtures

Age of Concrete (Days)	Compressive Strength (MPa)	
	NSC	CACC
3	8.79	10.934
14	16.58	19.12
28	23.06	26.00

3.4 Material Property Tests

Mechanical property tests, namely compressive strength, splitting tensile strength, elastic modulus and stress-strain curves were carried out on NSC and CACC after exposure to elevated temperatures. In addition to that, mass loss and toughness were also evaluated for both types of mixes at different levels of temperatures. The detail of test matrix is shown in Table 3.7. Details on specimen fabrication, test equipment, and test procedure are presented in this section.

3.4.1 Test Specimens

A total of 40 specimens each, 100x200 mm were fabricated for undertaking the unstressed and residual material property tests. This size is selected due to the limitation of the heating chamber of the electric furnace. The heating chamber is of 200 x 250 x 275 mm size and specimens smaller than the furnace chamber can fit inside easily for exposure to elevated temperatures. Before the testing of concrete cylinders, they were removed from the curing pond

and the ends were ground as per ASTM C39 (2009) requirements for perpendicularity and planeness. The detail on size and number of cylinders for high temperature material properties is given in Table 3.8 after considering both types of test methods which are used. For both compressive and splitting tensile strength tests one sample was tested at each target temperature. However, if some ambiguity and uncertain results were observed then additional tests were performed to confirm the results. Two K type thermocouples were also instrumented on the surface of the cylinder to measure the temperature rise on the surface of cylinder during heating and stabilization times. Figure 3.3 shows the location of these thermocouples on a cylinder and the test setup of the furnace.

Table 3. 7 – Test Matrix for evaluation of high temperature mechanical properties

Sr. No.	Test Method	Property	Temperature Range (°C)	Test Equipment	Concrete Types (Mixes)	No. of cylinders (100x200)
1.	**Unstressed Test Method**	Compressive strength	23-800°C @ 200°C interval	Electric Furnace, thermal jacket, strength machine	NSC, CACC	10
2.		Tensile strength	23-800°C @ 200°C interval	Electric Furnace, Steel bracket, strength machine	NSC, CACC	10
3.		Elastic Modulus	23-800°C @ 200°C interval	Electric Furnace, thermal jacket, strength machine	NSC, CACC	10
4.		Stress-strain curves	23-800°C @ 200°C interval	Electric Furnace, thermal jacket, strength machine	NSC, CACC	10
5.	**Residual Test Method**	Compressive strength	23-800°C @ 200°C interval	Electric Furnace, strength machine	NSC, CACC	10
6.		Tensile strength	23-800°C @ 200°C interval	Electric Furnace, Steel bracket, strength machine	NSC, CACC	10
7.		Elastic Modulus	23-800°C @ 200°C interval	Electric Furnace, strength machine	NSC, CACC	10
8.		Stress-strain curves	23-800°C @ 200°C interval	Electric Furnace, Control strength test machine	NSC, CACC	10

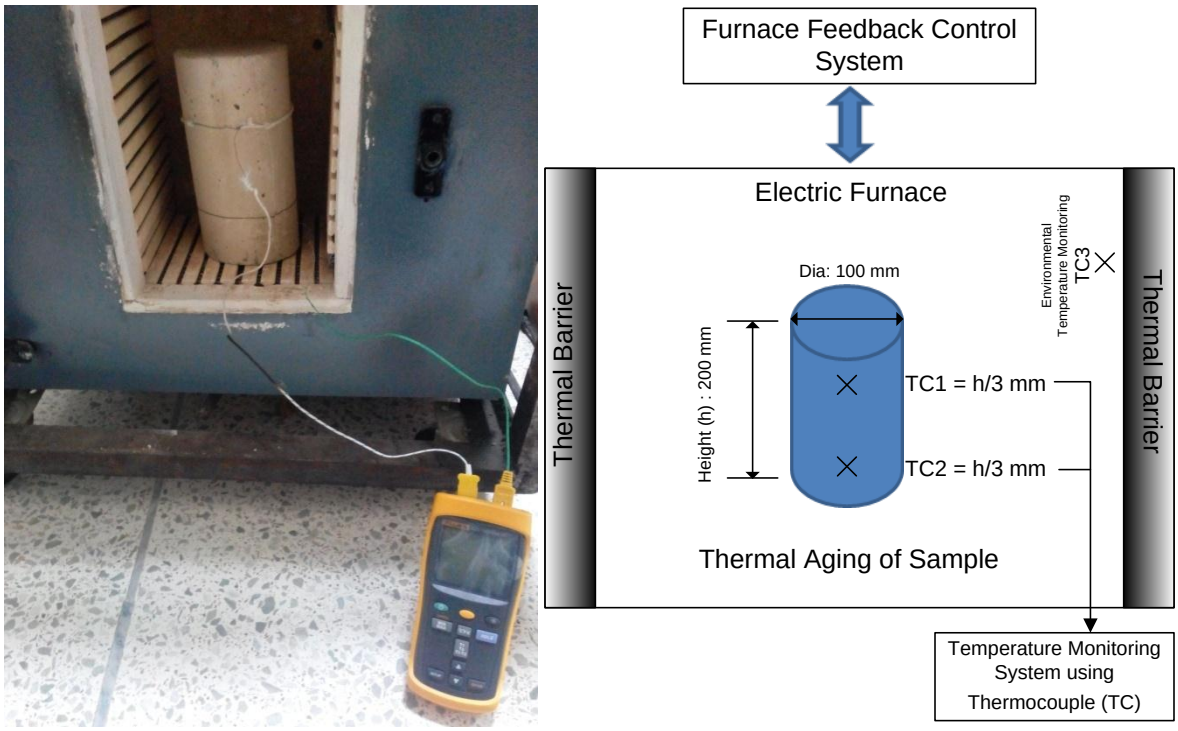

(a) Cylinder inside furnace (b) Experimental setup of furnace

Figure 3.3 – Arrangement of thermocouples and experimental setup of furnace.

Table 3. 8 – Details of cylinders at different levels of Temperatures

Sr. No.	Mix Type	Temperature Level Exposed (°C)	Compressive Strength Test	Elastic Modulus	Stress-Strain Curve	Splitting Tensile Test	Remarks
Cylinder Size (100x200 mm)							
1.	**Normal Strength Concrete (NSC)**	23°C		4		4	**For both Unstressed and Residual tests**
2.		200°C	2	2	2	2	
3.		400°C	2	2	2	2	
4.		600°C	2	2	2	2	
5.		800°C	2	2	2	2	
6.	**Calcium Aluminate Cement Concrete (CACC)**	23°C		4		4	**For both Unstressed and Residual tests**
7.		200°C	2	2	2	2	
8.		400°C	2	2	2	2	
9.		600°C	2	2	2	2	
10.		800°C	2	2	2	2	

3.4.2 Test Apparatus

The test setup for measuring the material properties consisted of strength test machine to carry out the compressive strength test (including elastic modulus, compressive toughness and stress-strain curve tests) and splitting tensile strength test, an electric furnace to heat up the concrete cylindrical specimens, an insulated jacket and a steel bracket frame to handle heated specimens. In order to evaluate these properties at elevated temperature appropriate heating conditions have to be simulated. The electric furnace shown in Figure 3.4, was used to expose the concrete specimens to different elevated temperatures and was specially designed for simulating high temperature conditions as high as 950°C temperatures. It is equipped with an internal thermocouple for monitoring the furnace temperature, a timer to control heating and a hold temperature controller to stabilize the temperature at different levels. The furnace has chamber dimension as 200 x 250 x 275 mm size and samples larger than this size can't be adjusted inside.

Figure 3.4 – Electric Furnace used to heat the concrete cylinders.

Strength test machine was used to determine the high temperature compressive and splitting tensile strength as shown in Figure 3.5. This is a load controlled strength test machine capable of loading the concrete cylinders up to 5000 KN with an automatic loading rate controller during testing. This was manufactured by 'CONTROLS'. For elastic modulus and stress-strain response tests, modifications were done to the strength test machine by introducing a 600 KN load cell and linear variable displacement transducer (LVDT). These instruments were connected to a data acquisition system (CONTROLS data logger) for recording the load-

displacement response. This data logger equipment is based on ‘Data soft’ measurement software, which helps in recording multiple readings automatically at a frequency of five readings per second and was averaged out to one reading/sec as a final result.

Special arrangements were made for handling, transporting and loading the heated samples in compression and splitting tensile strength tests in case of unstressed test method. Thermal jacket and safety equipment (gloves and forceps) were used for moving the heated samples from electric furnace to the strength test machine for compressive strength tests as shown in Figure 3.6. This thermal jacket is composed of ‘fiberfrax’ high temperature insulation blanket sheet material and was design to wrap tightly around heated cylinder. Use of this thermal jacket allow safe and easy transfer of cylinders for carrying out compressive and stress-strain curve tests for temperatures up to 800°C. This pre-heating technique used to heat the specimens and to keep them hot during the tests is generally adopted in investigating the mechanical properties of concrete at elevated temperatures (Bamonte and Gambarova, 2009; Bamonte and Gambarova, 2012; Khaliq, 2012). In addition to that, this thermal jacket also helped to minimize the heat loss in the cylinders during testing. However, no thermal jacket was used for evaluating the residual compressive strength.

Figure 3.5 – Controls strength test machine used for mechanical properties.

Figure 3.6 – Thermal jacket and safety equipment for handling the heated cylinders.

Splitting tensile strength test is more complicated test as it requires placing of the cylinder in a precise manner under test machine to apply a diametrical compressive force as per ASTM C496 (2004). This activity becomes more challenging when we try to perform this test on cylinders under elevated temperatures after exposing them to 800°C temperature. To overcome this problem, a specially designed and insulated steel bracket frame was introduced by Khaliq (2012), to transfer the heated cylinder from furnace and to tensile strength test machine. This assembly was modified to carry the 100x200 mm heated cylinder specimens which is shown in Figure 3.7. This frame was modified to have an opening of 50x210 mm at the bottom and was designed in such a manner that the cylinder could be placed on sides extending out of this opening. Also two 40 mm wide and 30 mm deep rectangular notches were made on both vertical side of this assembly to incorporate steel loading strip of 38x25 mm cross-section. In this way, steel loading strip will be align on top of diametrical side of cylinder, whereas, the opposite side will be exposed through the bottom opening in frame as shown in Figure 3.7. To preserve the temperature in the cylinder, this frame was insulated with fiberfrax material. Thus, this frame not only helped carrying out splitting tensile strength test at elevated temperatures, but also allowed safe transfer and precise positioning of cylinders specimens, as shown in Figure 3.8. However, no insulation was used for evaluating the residual splitting tensile strength.

Before evaluating the tensile strength of cylindrical samples of NSC and CACC using this specially designed steel bracket frame at elevated temperatures, these samples were tested at room temperature using the assembly according to the ASTM C496 (2004) and this specially designed steel bracket frame. Figure 3.9 shows the sample ready to take the splitting tensile

strength test as per ASTM C496 (2004) and this assembly introduced by Khaliq (2012). Table 3.9 compares the splitting tensile strength of both types of test assemblies for NSC and CACC.

Table 3. 9 – Comparison of Splitting Tensile strength of NSC and CACC

Sr. No.	Sample Mix	Sample No.	ASTM C 496 (MPa)	Steel Bracket Assembly (MPa)
1.	NSC	Specimen 1	2.698	2.364
2.		Specimen 2	2.681	2.783
3.		**Average**	**2.69**	**2.57**
4.	CACC	Specimen 1	2.932	3.10
5.		Specimen 2	3.133	3.93
6.		**Average**	**3.032**	**3.51**

The test equipment for mass loss calculations consisted of an electrical furnace and weight balance. The mass loss measurements, both at room and high temperatures, were carried out by utilizing a highly sensitive balance that has accuracy up to 1 gram. The concrete specimens were exposed to target temperatures of 200, 400, 600, and 800°C in an electric furnace and were kept in it for two hours and 30 minutes till steady state condition were attained. Heated specimens were then quickly taken out (without much heat loss in case of unstressed test method) and weighed as shown in Figure 3.10. Mass loss was then evaluated using room temperature and high temperature weight measurements of cylinder.

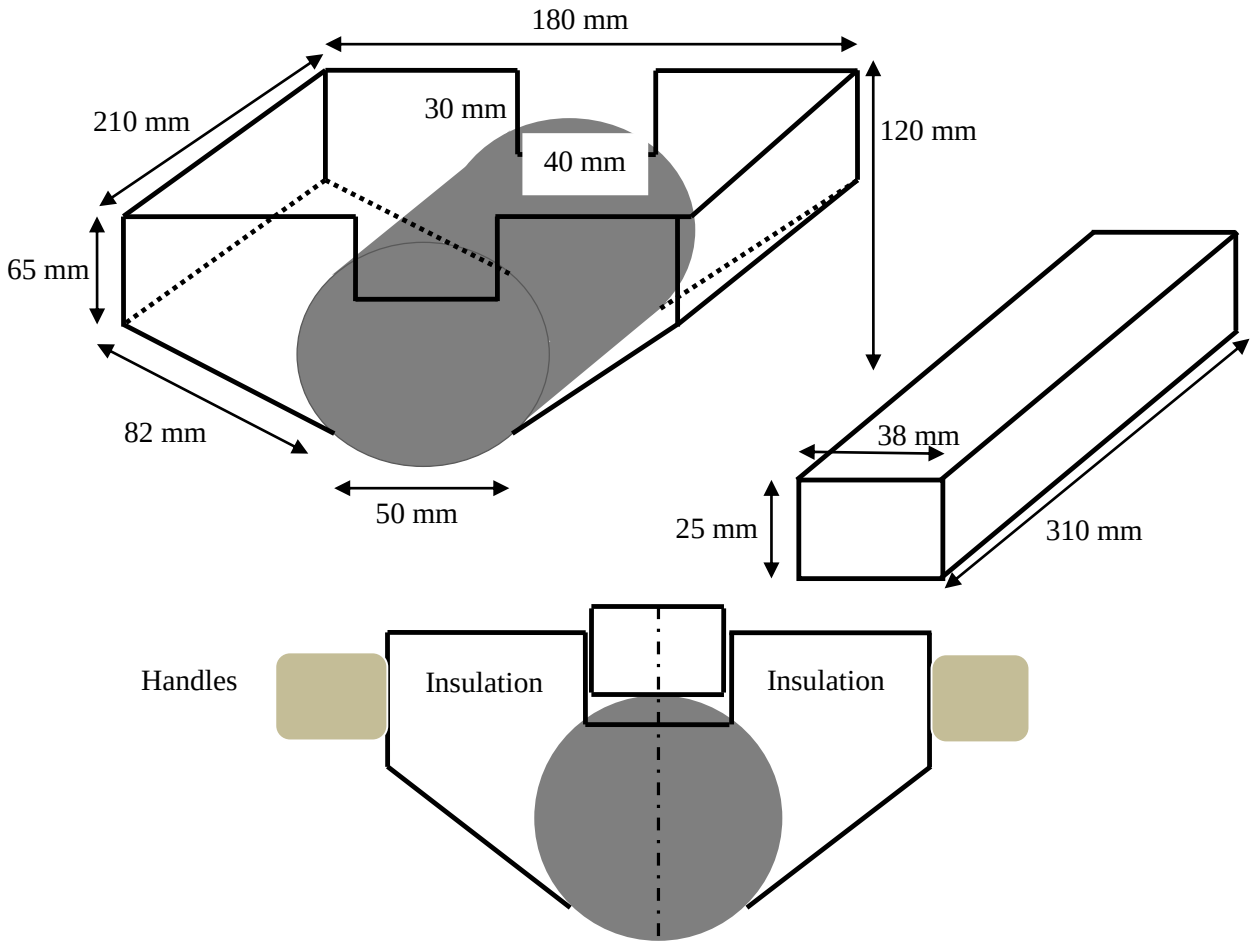

Figure 3.7 – Design details of steel bracket frame assembly.

Figure 3.8 – Insulated steel bracket frame for handling and preserve the heat in cylinders during splitting tensile strength tests.

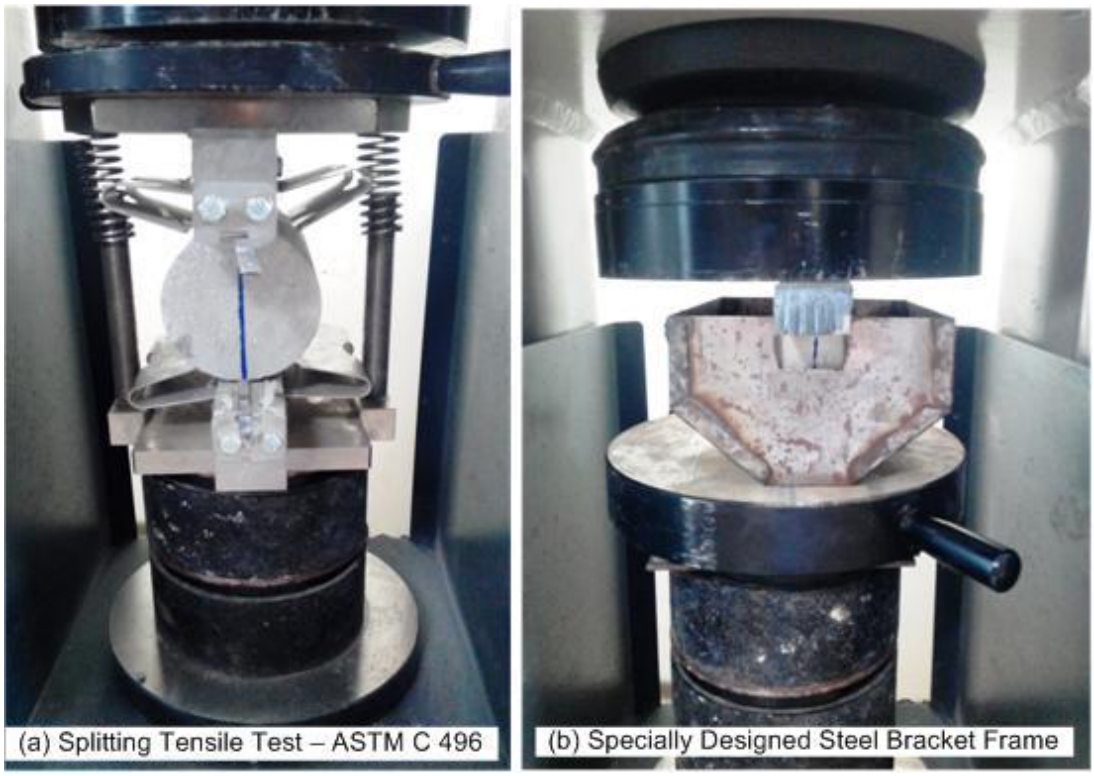

Figure 3.9 – Samples ready for split tensile strength test at room temperature.

Figure 3.10 – Cylinder being weighed after exposure to elevated temperature.

3.4.2.1 Scanning Electron Microscopy (SEM)

Scanning electron microscopy was done using the JEOL JSM 6390 LV instrument with secondary electron imaging microscope available at School of chemical and material engineering (SCME), NUST. The SEM samples were taken from the fractured cylinders according to ASTM C1723 (2010), since the microstructure details are accentuated and favorable for viewing within the fractured surface. The specimens of both NSC and CACC were studied at specified ages after being exposed to elevated temperature. The purpose was to study the changes in microstructure and morphology of the hydration products after the exposure of samples to elevated temperatures. Figure 3.11 shows the scanning electron microscope used for obtaining SEM images.

Figure 3.11 – Scanning Electron Microscope.

3.4.3 Test Procedure

3.4.3.1 General Procedure

The material property tests were carried out at different temperature levels using two types of test methods, namely unstressed test method and residual test method which are explained in Section 2.2.2. Figure 3.12 shows the two stages of testing when unstressed test method was adopted. First the cylinders are heated without any preload till the target temperature, and after the hold time at this target temperature the cylinders are moved to the strength test machine for loading without any loss of heat. Figure 3.13 shows the two stages of testing when residual test method is adopted. In this case, first the cylinders are heated without any preload till the target

temperature and it is maintained till the steady state is reached. Once the equilibrium is reached the samples are allowed to cool down to the room temperature normally. After that cylinder are loaded in the strength test machine till the failure to obtain the residual strength of concrete.

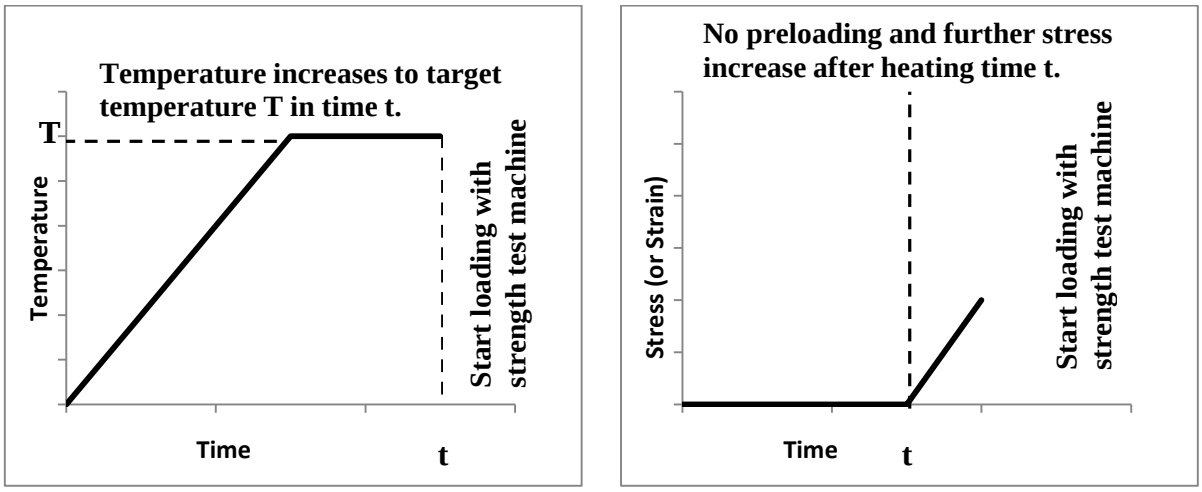

(a) Heating scheme (b) Loading scheme

Figure 3.12 – Schematics of temperature and stress increments as per unstressed test method.

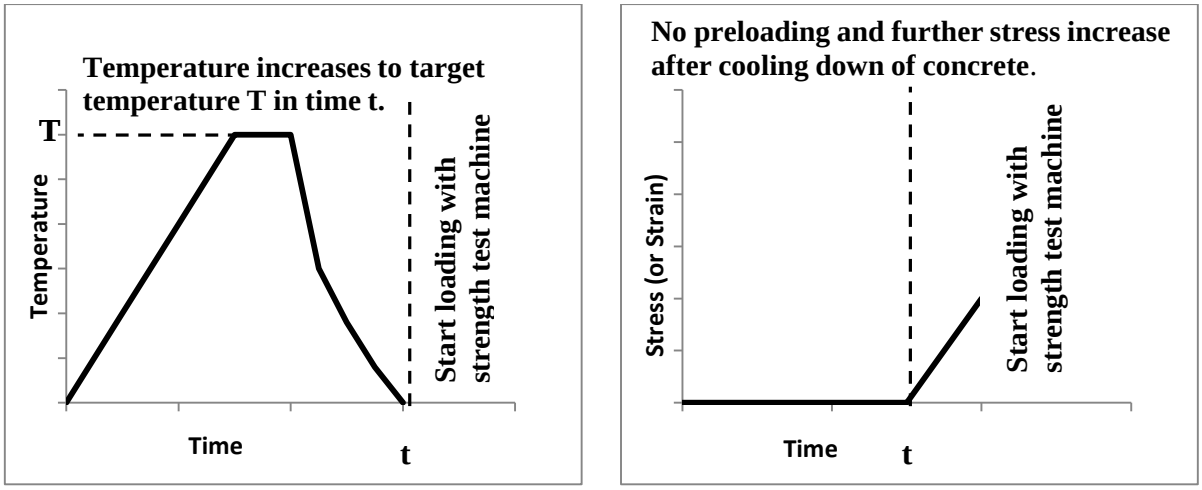

(a) Heating scheme (b) Loading scheme

Figure 3.13 – Schematics of temperature and stress increments as per residual test method.

The test procedures, such as hold time, loading and heating conditions were followed as per RILEM test procedures (1995; 2000). Under both unstressed and residual test conditions, an average heating rate of 5°C/min was maintained to achieve the desired target temperatures. Figure 3.14 illustrates the progression of temperature in the furnace, and on the surface of 100x200 mm test cylinder for the case of 600°C temperature. Three K type thermocouples (TC), two on the surface of the cylinder and one in the furnace (see Figure 3.3. (b)) were used to record the temperature in the furnace and on the surface of cylinder.

As the rise in temperature inside the specimen is slower than the surface and furnace temperature as discussed by Khaliq (2012), due to the low thermal conductivity of concrete, a hold time of at least 2 hours must be maintained to attain steady state equilibrium condition in the specimens at all target temperatures. To further validate that the temperature inside the cylinder is at steady state conditions (thermal equilibrium) the hold time was increased to 2 hours and 30 minutes at all target temperatures. This rise in temperature inside the furnace and the average of two temperature readings on the surface with respect to time can be seen in Figure 3.14.

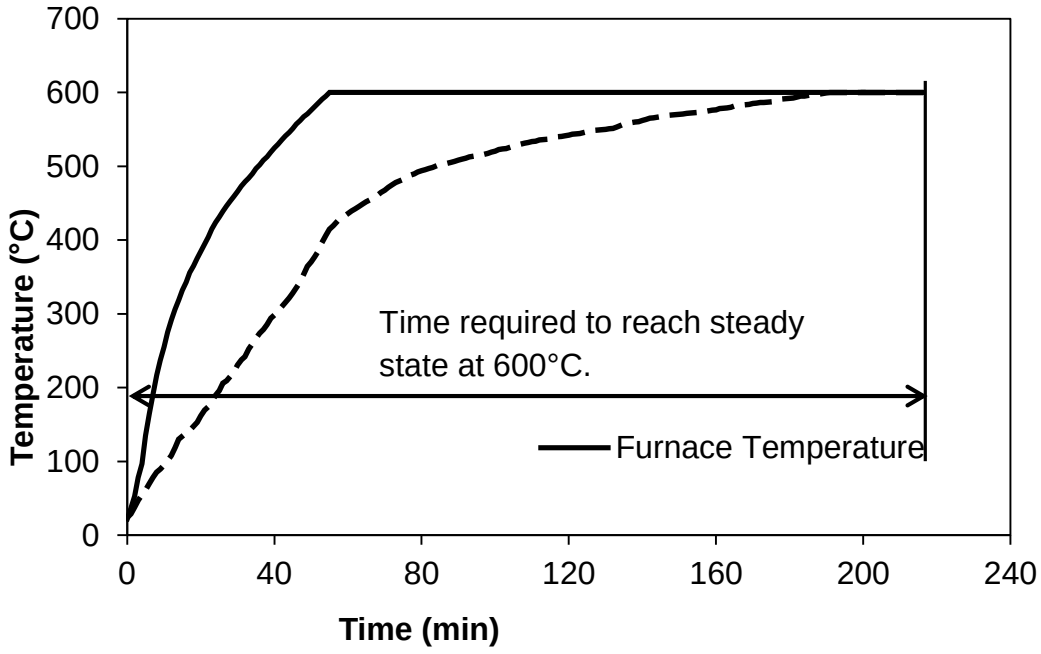

Figure 3.14 – Temperature rise recorded by thermocouple at different locations at 600°C.

3.4.3.2 Unstressed Test Method

3.4.3.2.1 General

In case of unstressed test method, the sample is allowed to heat up without any preload till the steady state equilibrium (uniform temperature distribution) is achieved. After that concrete cylinders are moved to the strength test machine for performing the material property tests as discussed in Figure 3.12.

3.4.3.2.2 Compressive Strength Test (f'_c)

After achieving steady state temperature condition, the cylinders were removed from the furnace and were wrapped tightly in 20mm thick thermal jacket to undertake the compression test and stress-strain test. The temperature measurements were pursued during the test

procedure till the completion of the tests. The specimens remained insulated in thermal jacket during tests and an average loss of temperature in a specimen was noted to be about 10°C. In the absence of specific test procedure for high temperature compression test, ASTM C 39 test procedure meant for room temperature was used for high temperature (unstressed) compressive strength. After the sample is transferred to the strength test machine, the sample is loaded at a loading rate of 0.2 MPa per second with a precision of ±1% as per ASTM C39 (2009), till failure is occurred and the failure load is recorded. Figure 3.15(a) shows, the sample prior to undertaking the strength test, whereas Figure 3.15(b) shows, the failed cylinder after compression test. For high temperature compressive strength (f'^{T}_{c}), one cylinder was tested at each target temperature. Test was repeated to confirm results at selected temperatures, where recorded result was unusual or lied outside the tolerance range. Compressive strength tests for NSC and CACC were carried out at different elevated temperatures (23°C, 200°C, 400°C, 600°C and 800°C). The details on the tested temperatures, cylinders and intervals for unstressed compressive strength can be seen in Table 3.7 and 3.8.

(a) (b)

Figure 3.15 – Arrangements prior of performing high temperature compressive strength test and tested cylinder.

3.4.3.2.3 Splitting Tensile Strength Test (f'_t)

After heating, the cylinders were placed in steel bracket assembly with proper insulations already placed to avoid any heat loss and were transferred to the strength test machine for undertaking splitting tensile strength test. The cylinders were gradually loaded at a loading rate of 0.025 MPa per second as per ASTM C496 (2004) test procedure, till failure occurred and then the failure load was recorded. Figure 3.16(a) show the sample ready for undertaking the splitting tensile strength test after being heated in the furnace, whereas Figure 3.16(b) shows, a failed cylinder after failure. Similar to compressive strength test one cylinder was tested at each target temperature to get the high temperature splitting tensile strength (f'^{T}_{t}). This test was repeated to confirm results at selected temperatures, where recorded results was unusual or lied outside the tolerance range. Splitting tensile strength tests for NSC and CACC were carried out at different elevated temperatures (23°C, 200°C, 400°C, 600°C and 800°C). The details on the tested temperatures, cylinders and intervals for unstressed splitting tensile strength can be seen in Table 3.7 and 3.8.

(a) (b)

Figure 3.16 – Arrangements prior of performing high temperature splitting tensile strength test and tested cylinder.

3.4.3.2.4 Stress-Strain Curve, Elastic Modulus and Toughness

Stress-strain curve test was also performed on both types of concrete, NSC and CACC to evaluate their response at different elevated temperatures (23°C, 200°C, 400°C, 600°C and 800°C). Figure 3.17 shows the cylinder prior to undertaking the stress-strain curve test. Test procedure similar to compressive strength test was adopted for stress-strain curve tests. Load-deformation data was recorded using data acquisition system by loading the cylinders at a rate of 0.2 MPa per second till the failure of the cylinders. In addition, the failure load was also observed from the control panel of strength test machine. The load-deformation curve was used to evaluate stress-strain curves for tested concrete cylinders. Secant elastic modulus (E_s) of NSC and CACC was calculated from the measured stress-strain curves. It is calculated at room temperature as the slope of compressive stress-strain curve corresponding to 40% of stress (ASTM C39, 2009). This approach is extended to measure the secant elastic modulus at elevated temperatures (E_s^T). Chord modulus of elasticity (E_c) for both types of concrete mixes is determined by Equation 3.1 as described in ASTM C469 (2002). This approach is extended to measure the chord modulus of elasticity at elevated temperatures (E_c^T). The details on the tested temperatures, cylinders and intervals for stress-strain curve tests can be seen in Table 3.7 and Table 3.8.

$$E_c = \frac{s_2 - s_1}{\varepsilon - 0.00005} \tag{3.1}$$

Where S_2 = Stress against 40% of ultimate load (f'_c) (MPa)

S_1= Stress against longitudinal strain of 0.00005

ε = Longitudinal strain against stress S_2

Toughness (T_c) of NSC and CACC was also calculated from the measured stress-strain curves. It is calculated at room temperature by measuring the area under the compressive stress-strain curve till the failure at peak stress which is the total energy absorbed prior to failure (Marar et al., 2011; Prabha et al., 2010). Equation 3.2 is used to calculate this energy per unit volume from stress-strain curves. Microsoft mathematics software was used for finding the areas under the curves. This approach is extended to measure the toughness at elevated temperatures (T_c^T).

$$T_c = \frac{Energy}{Volume} = \int_0^{\varepsilon} \sigma \, dx \qquad (3.2)$$

Where T_c = Compressive Toughness (J/m^3)

σ = Stress (N/mm^2)

ε = Strain at failure (mm/mm)

Figure 3.17 – LVDT and Load cell addition in the Controls strength test machine for stress-strain measurements.

3.4.3.2.5 Mass Loss

The variation in mass loss (ratio of mass at specified temperature M^T to mass at room temperature M_o) was measured following the room and high temperature mass and density calculations. After the specimens were heated to elevated temperature in furnace, they were allowed to stabilize to reach a steady state conditions at a specified target temperature. Then the heated specimens were quickly transferred to a sensitive balance (with accuracy of 1000^{th} of a kilogram) and weighed to record change in weight at that target temperature. This procedure was repeated for various target temperatures.

3.4.3.3 Residual Test Method

3.4.3.3.1 General

In case of residual test method, the sample is allowed to heat up without any preload till the steady state condition (uniform temperature distribution) is achieved. After achieving this equilibrium condition, that concrete cylinders are allowed to cool down till the ambient room temperature is achieved. After that concrete cylinders are loaded in the strength test machine till the failure to obtain the residual material properties of concrete, as shown in Figure 3.13.

3.4.3.3.2 Compressive Strength Test ($f'_{c\,res}$)

After achieving steady state temperature condition, the cylindrical specimens were allowed to cool down to the room temperature normally in air. The specimens were transferred to strength test machine to undertake the compression test and stress-strain test. There was no need for thermal jacket for transferring the sample to the strength test machine in case of this test method. Similar to the unstressed compressive strength test, the sample is loaded at a loading rate of 0.2 MPa per second with a precision of ±1% as per ASTM C39 (2009) test procedures, till failure is occurred and the failure load is recorded. Figure 3.18(a) shows the sample prior to undertaking the strength test whereas Figure 3.18(b) shows the failed cylinder after compression test. For high temperature compressive strength ($f'^{T}_{c\,res}$), one cylinder was tested at each target temperature. Test was repeated to confirm results at selected temperatures, where recorded result was unusual or lied outside the tolerance range. Compressive strength tests for NSC and CACC were carried out at different elevated temperatures (23°C, 200°C, 400°C, 600°C and 800°C). The details on the tested temperatures, cylinders and intervals for residual compressive strength can be seen in Table 3.7 and Table 3.8.

(a) (b)

Figure 3.18 – Arrangements prior of performing high temperature residual compressive strength test and tested cylinder.

3.4.3.3.3 Splitting Tensile Strength Test ($f'_{t\ res}$)

After achieving the ambient room temperature, the cylinders were placed in steel bracket assembly and were transferred to the strength test machine for undertaking splitting tensile strength test. Similar to the unstressed splitting tensile strength test, the cylinders were gradually loaded at a loading rate of 0.025 MPa as per ASTM C496 (2004) test procedure, per second till failure occurred and then the failure load is recorded. Figure 3.19(a) shows the sample ready for undertaking the splitting tensile strength test whereas Figure 3.19(b) shows a failed cylinder after failure. Similar to unstressed splitting tensile strength test one cylinder was tested at each target temperature. This test was repeated to confirm results at selected temperatures, where recorded results lied outside the tolerance range. Residual splitting tensile strength tests ($f'^{T}_{t\ res}$) for both CACC and NSC were carried out at 23°C, 200°C, 400°C, 600°C and 800°C elevated temperatures. The details on the tested temperatures, cylinders and intervals for residual splitting tensile strength can be seen in Table 3.7 and 3.8.

(a) (b)

Figure 3.19 - Arrangements prior of performing high temperature residual splitting tensile strength test and tested cylinder.

3.4.3.3.4 Stress-Strain Curve, Elastic Modulus and Toughness

Stress-strain curve test was also performed as per the residual test procedure to evaluate the response of both types of concrete, NSC and CACC at elevated temperatures (23°C, 200°C, 400°C, 600°C and 800°C). Figure 3.20 shows the cylinder prior to undertaking the stress-strain curve test after it has achieved the room temperature. Test procedure similar to residual compressive strength test was adopted for stress-strain curve tests. Load-deformation data was recorded using data acquisition system by loading the cylinders at a rate of 0.2 MPa per second till the failure of the cylinders. The load-deformation curve was used to evaluate stress-strain curves for tested concrete cylinders. Secant Elastic modulus ($E_{s\ res}$) of NSC and CACC was also calculated from the measured stress-strain curves. It is calculated at room temperature as the slope of compressive stress-strain curve corresponding to 40% of stress (ASTM C39, 2009). Whereas chord modulus of elasticity ($E_{c\ res}$) is calculated using Equation 3.1 as explained earlier. These approaches are extended to measure the secant ($E_s^T{}_{res}$) and chord modulus of elastic ($E_c^T{}_{res}$) at elevated temperatures. The details on the tested temperatures, cylinders and intervals for residual stress-strain curve tests can be seen in Table 3.7 and 3.8. As in unstressed test procedure, Toughness ($T_{c\ res}$) of NSC and CACC in residual test procedure was also calculated from the measured stress-strain curves. It is calculated at room temperature by measuring the area under the compressive stress-strain curve till the failure at peak stress.

Equation 3.2 is used to calculate this energy per unit volume from stress-strain curves. Microsoft mathematics software was used for finding the areas under the curves. This approach is extended to measure the residual toughness at elevated temperatures ($T_c{}^T{}_{res}$).

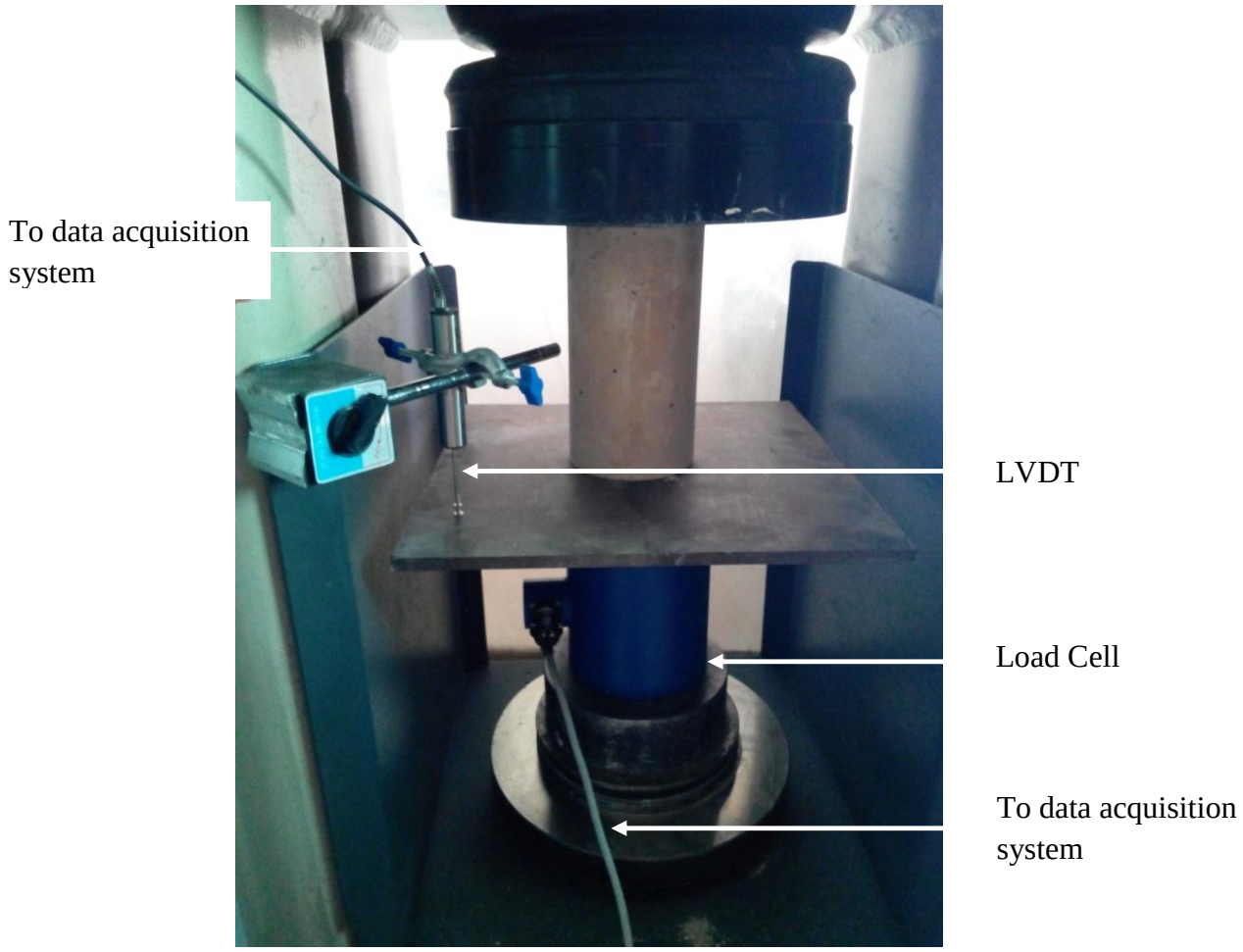

Figure 3.20 – LVDT and Load cell addition in the Controls strength test machine for residual stress-strain measurements.

3.4.3.3.5 Mass Loss

This material property was also evaluated after the concrete cylinders have attained ambient room temperature. Similar test procedure was adopted as in the case of unstressed test procedure i.e. the samples were transferred to a sensitive balance (with accuracy of 1000^{th} of a kilogram) and weighed to record change in weight at that target temperature. The variation in mass loss which is the ratio of mass at specified temperature ($M^T{}_{res}$) to mass at room temperature ($M_{o\ res}$) was measured following the room and high temperature mass and density calculations. This procedure was repeated for various target temperatures.

CHAPTER 4

RESULTS AND DISCUSSIONS

4.1 Introduction

In this chapter, the results of compressive strength, splitting tensile strength, stress-strain response, elastic modulus, compressive toughness, mass loss and microstructural studies are presented for both unstressed (hot state) and residual test procedures. These properties are presented to discuss the effect of elevated temperatures on the material properties of both normal strength concrete (NSC) and calcium aluminate cement concrete (CACC) after performing compressive strength, splitting tensile strength and stress-strain curve tests as explained in Chapter 3. The generated properties data was utilized to develop the high temperature material property relationships for various material properties as a function of temperature ranging from 23-800°C.

In addition, visual observations were also made to study the changes in the color and any signs of cracking and spalling after the samples were removed from the electric furnace. Scanning electron microscopy (SEM) was also performed to study the microscopic changes occurred in the concrete specimens due to the exposure to high temperatures.

4.2 Unstressed Material Properties

In case of unstressed test method, the samples are directly transferred from the electric furnace to the strength test machine to evaluate their material properties without any loss of heat at specified target temperatures as explained in chapter 2 and 3. This section presents the results of different material properties of NSC and CACC when exposed to elevated temperature using this test procedure.

4.2.1 Compressive Strength (f'_c)

The applied load in compression is computed at failure in case of both types of mixes, NSC and CACC after being exposed to elevated temperatures. The computed values of compressive strength ($f'_c{}^T$) at each temperature are plotted as a function of temperature for both CACC and NSC, as shown in Figure 4.1. It can be seen that, the compressive strength of both types of concrete decreases with the increase in temperature which can be attributed to the physical and chemical changes taking place in concrete as a result of elevated temperatures. If we compare the performance of both types of concrete in terms of compressive strength, we can see that CACC have given us much more strength with the similar mix proportion as compared to NSC at room temperature. However, the loss in compressive strength is gradual in case of CACC

after 200°C, as compared to NSC, where this loss is significant after 400°C. The strength loss observed till 200°C is due to the loss of mostly free and to some extent physically bound water present within the microstructure of concrete. The ultimate strength in CACC after it has been exposed to 800°C is much better as compared to NSC as shown in Figure 4.1.

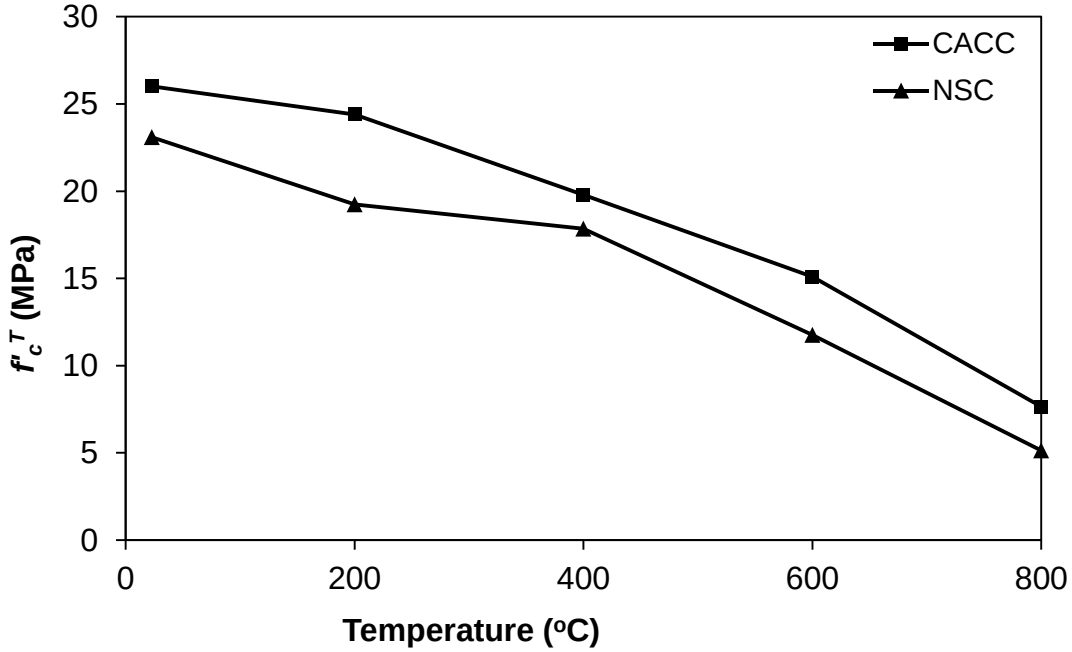

Figure 4.1 – Absolute unstressed compressive strength of CACC and NSC as a function of temperature

The relative compressive strength loss ($f'_c{}^T/f'_c$) in NSC and CACC follows similar trend to its absolute strength as shown in Figure 4.2. By observing the trend in this figure it is evident that CACC displays lesser loss of compressive strength ratio as compared to NSC. Further, NSC losses up to 78% of its strength when exposed to an elevated temperature of 800°C as compared to CACC where 29% of room temperature strength is retained.

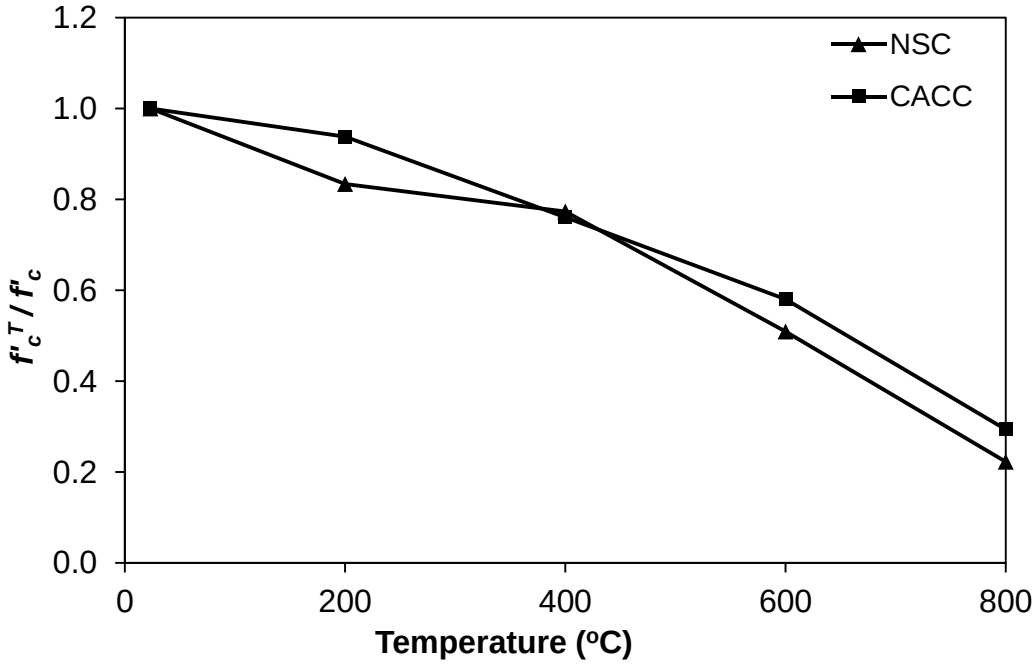

Figure 4. 2 – Relative unstressed compressive strength of CACC and NSC as a function of temperature

4.2.1.1 Calcium Aluminate Cement Concrete

The compressive strength ($f'_c{}^T$) of CACC which is also, plotted in Figure 4.1 and 4.2, decreases with the increase in temperature ranging from 20-800°C. It can be seen that, the compressive strength of CACC at room temperature is about 26 MPa i.e. 3 MPa more as compared to NSC with the similar mix design. At 200°C, the initial strength loss is monitored, which is due to the loss of moisture present in the mix. However, if we compare this loss with NSC it comes out be just 6% instead of 17% in case of NSC. This shows that, initial loss in strength is very minor as compared to NSC which is due to the physically bound moisture present in the concrete mix. Further, at this temperature the morphological and chemical changes in CACC modify the microstructure which includes the conversion of metastable hydrates into stable phases and the loss of chemically bound water occurred due to this reaction, as a result of which minor loss in strength was observed, unlike NSC (Scrivener et al., 1999). After 200°C, this loss in strength is gradual till 800°C which follows the same trend as in absolute strength. There is a noticeable retention in CACC when we compare it with NSC at 800°C i.e. around 29%. This observation confirms that, CACC has superior microstructure and therefore, displays better compressive strength even at higher temperatures.

4.2.1.2 Normal Strength Concrete

As shown in Figure 4.1 and 4.2, there is a gradual loss of compressive strength of NSC when exposed to elevated temperatures ranging from 23-800°C. There is an initial reduction in compressive strength up to 200°C due to the loss of moisture. After that the strength stabilizes up till 400°C with a minor slope. This minor loss in strength at 400°C i.e. up to 77% retention of room temperature strength is due to the reason that, NSC is usually not very dense and it allows the escape of pore water pressure without any cracking and spalling which results in a drastic loss in strength. After 400°C, significant loss in strength is observed by monitoring the trend of NSC curve. This major loss in strength of NSC i.e. just 22% retention at 800°C is due to the slow loss of chemically bound water and the deterioration of the cementing ability due to the dehydration and disintegration of calcium hydroxide (CH) and calcium silicate hydrate (C-S-H) in concrete (Chan et al., 1999). This level of strength retention is much lower than that observed in the same concrete mix produced by CACC. At 800°C, both CACC and NSC experience major loss in strength, which is around 29% with respect to strength at 600°C. This loss in strength is attributed to the dissociation of limestone (calcareous) aggregate (Khaliq, 2012).

4.2.2 Splitting Tensile Strength (f'_t)

The recorded applied load at which the cylinders failed were used to compute splitting tensile strength (f'_t) as per ASTM C496 (2004), using formula $f'_t=2P/\pi ld$, where (P) is the failure load, (l) is the length and (d) is the diameter of the tested cylinder. Absolute values of measured splitting tensile strength for both NSC and CACC are plotted in Figure 4.3 as a function of temperature. It is observed that both concretes experience loss in tensile strength with the increase in temperature. This loss in splitting tensile strength is dependent on the physical and chemical changes that occur at higher temperatures. If we compare the performance of NSC and CACC in terms of tensile strength, it is observed that the tensile strength of CACC is 23% more than that of NSC with an absolute value of 3.27 MPa. The loss in tensile strength of CACC is very gradual at elevated temperatures till 800°C as compared to NSC where there is a significant loss above 400°C. This loss is mainly due to the excessive thermal stresses beyond 400°C within the concrete matrix (Kowalski, 2010), and development of micro and macro cracks, which affect the tensile strength more as compared to compressive strength.

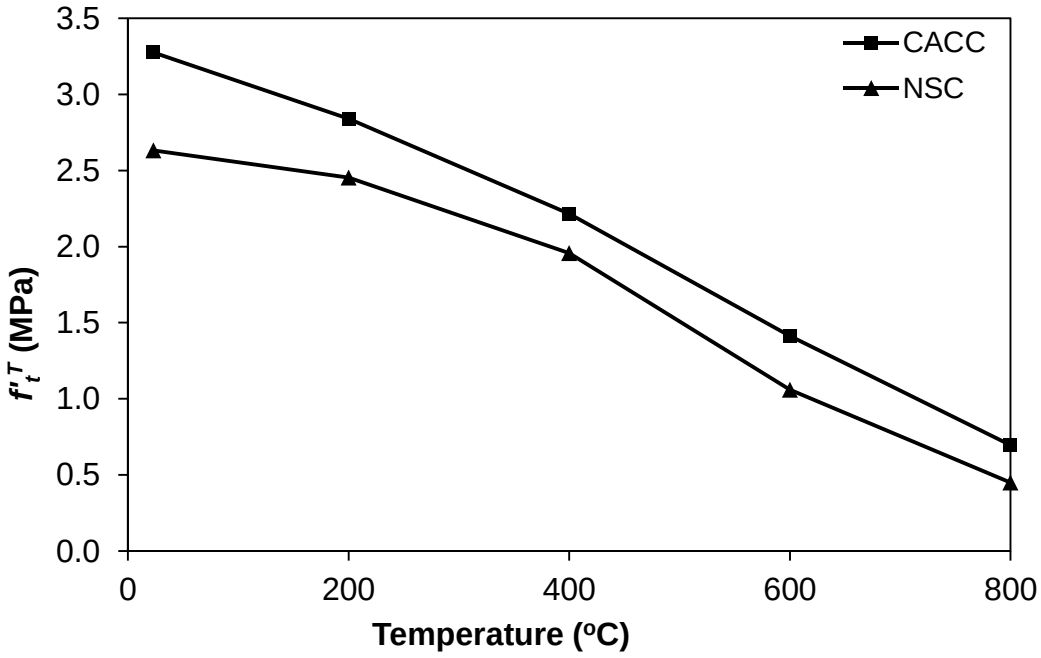

Figure 4.3 – Specified unstressed splitting tensile strength of CACC and NSC as a function of temperature

The relative splitting tensile strength (f'^{T}_{t}/f'_{t}) follows similar trend to its absolute strength is shown in Figure 4.4, for both NSC and CACC. CACC exhibits higher tensile strength ratio beyond 400°C. This increase in tensile strength is of much advantage in mitigating the fire induced spalling in CACC and therefore can enhance the fire resistance rating of RC members made of CACC.

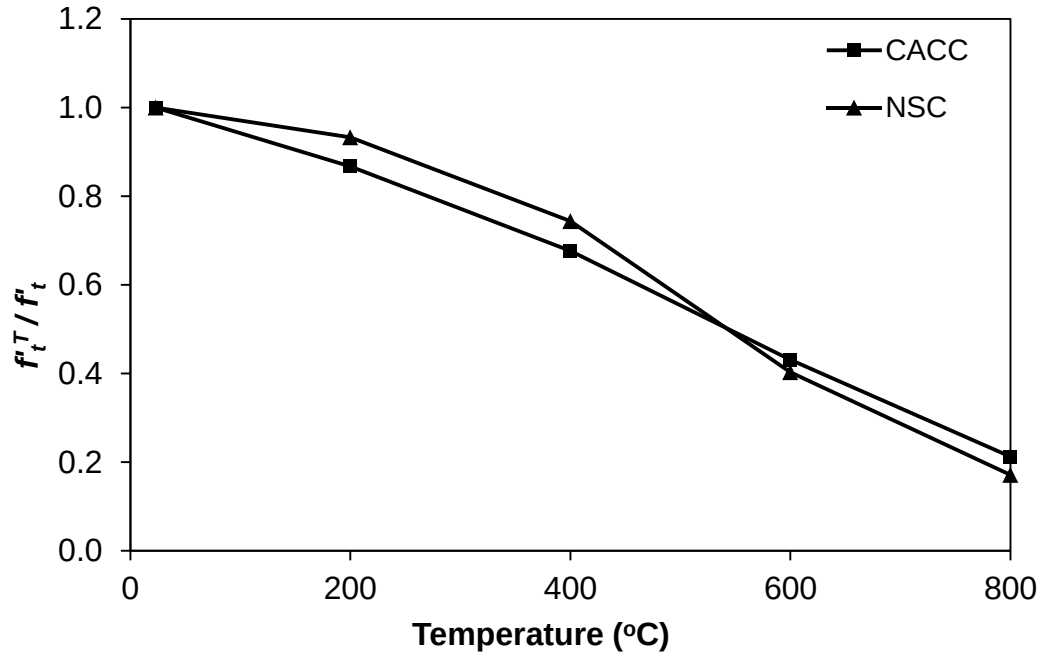

Figure 4.4 – Measured relative splitting tensile strength of CACC and NSC

4.2.2.1 Calcium Aluminate Cement Concrete

The splitting tensile strength ($f'_t{}^T$) of CACC which can be seen in Figure 4.3 and 4.4 decreases with the increase in temperature ranging from 20-800°C. In this concrete like in NSC, physical and chemical changes under high temperature lead to the reduction in tensile strength of concrete. By observing Figure 4.3, it can be seen that the tensile strength of CACC at room temperature with the same mix design is about 3.27 MPa i.e. around 23% higher as compared to NSC. This higher tensile strength of CACC is attributed to the improved microstructure as compared to NSC at room temperature. Upon heating, the free moisture in the concrete converts to vapor and this generates pore pressure which leads to the early strength loss up to 400°C which can be seen in Figure 4.4. However, the loss in tensile strength is a bit more i.e. around 32% till 400°C as that of room temperature strength, which is due to conversion reaction causing the hydrates of CACC to convert from low density metastable to stable hydrates having higher density and the release of water into the system causing increase in porosity of concrete. As a result, the exposure of CACC to elevated temperatures also results in the loss of chemically bound water due to this reaction. The loss in strength of NSC and CACC up to this limit is same i.e. the evaporation of pore water as vapor. Beyond 400°C, it is observed that the loss in strength of CACC is gradual without any abrupt decrease in strength till 800°C, unlike NSC. There is a noticeable retention in the tensile strength of CACC at 800°C i.e. around 21% instead of just 17% in case of NSC. However, at 800°C the tensile strength exhibited by CACC is around 1.54 times higher as compared to NSC. This is due to the increased binding strength of alumina present in the cement as a binder against C-S-H, which experiences major disintegration and collapse of microstructure at high temperature causing higher loss in tensile strength. This observation confirms that CACC has superior microstructure and displays better tensile strength even at higher temperatures.

4.2.2.2 Normal Strength Concrete

By observing the Figure 4.3 and 4.4, it can be seen that there is a gradual reduction in strength between 23-400°C. The steadiness in tensile strength up to 400°C is due to the dehydration of the cement matrix. This decrease in tensile strength is attributed to the weak microstructure of NSC i.e. it allows the cracks to initiate very easily from the microstructure to the surface. Beyond 400°C, there is a rapid decrease in tensile strength of NSC due to more prominent thermal damage in the form of micro and macro cracks in concrete. These cracks are generated due to the dehydration of CH and C-S-H in concrete which further reduces the tensile strength of concrete (Khaliq and Kodur, 2011), unlike CACC. Since the exposure of NSC to elevated

temperatures causes an expansion of aggregate resulting in weakening of bond between aggregate and paste (Castillo and Duranni, 1990). However, beyond 600°C both CACC and NSC suffered major loss in tensile strength, as a result of endothermic reaction causing the dolomite present in the calcareous aggregate to dissociate (Abrams, 1971).

4.2.3 Elastic Modulus

Generally, the elastic modulus of concrete is affected by the same factors which influence the compressive strength. It is dependent on moisture content and the microstructure of hydrated concrete products in paste (Bažant and Kaplan, 1996). With the increase in temperature, physical and chemical changes occur in concrete due to which elastic modulus degrades. Data generated from the compressive stress-strain curves was used to obtain the secant modulus and the chord elastic modulus of concrete for both types of concrete at elevated temperatures. Figure 4.5 represents the secant elastic modulus of NSC and CACC at different high temperatures (E_s^T), which is evaluated as the slope of compressive stress-strain curve corresponding to 40% of stress (ASTM C39, 2009). Figure 4.6 represents the chord elastic modulus of concrete at different temperatures (E_c^T), which is evaluated using Equation 3.1. The relative secant modulus (E_s^T/E_s) and chord modulus (E_c^T/E_c) of both types of concrete follows similar trend to its absolute strength as shown in Figure 4.7 and 4.8. The loss in modulus of elasticity with temperature depends upon factors namely water-cement ratio, type of aggregate, exposure temperature, and microstructure of concrete. Microstructure of concrete is usually linked with the type of binder used and quantity of cement. It can be seen that, in both the cases the elastic modulus of concrete keeps on decreasing till 800°C, whereas CACC gives a much higher values beyond 400°C till 800°C.

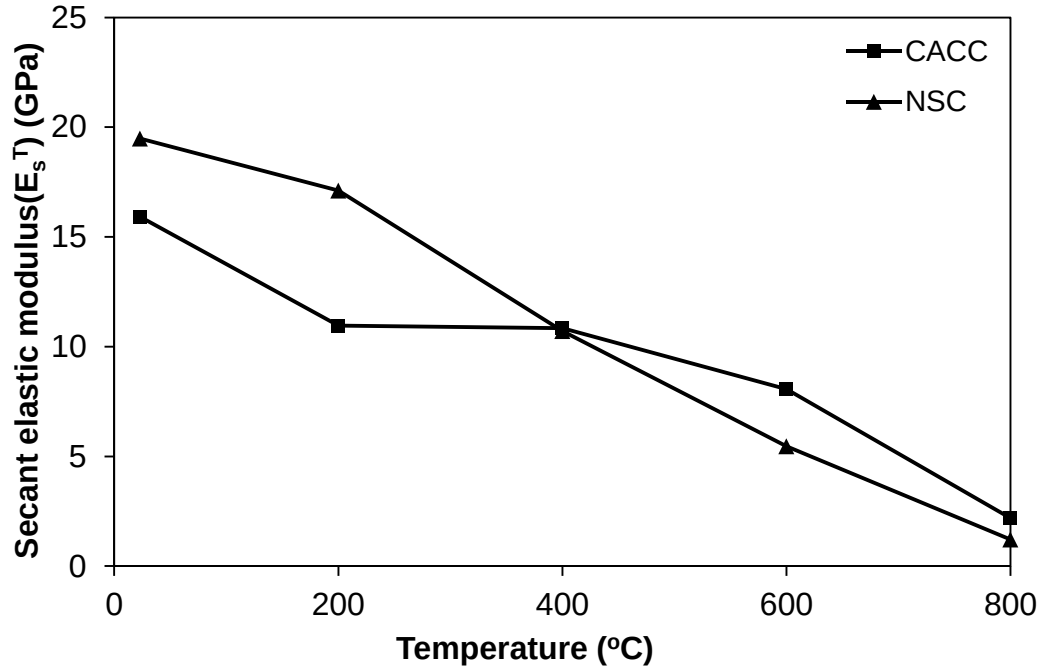

Figure 4.5 – Unstressed secant elastic modulus of CACC and NSC as a function of temperature

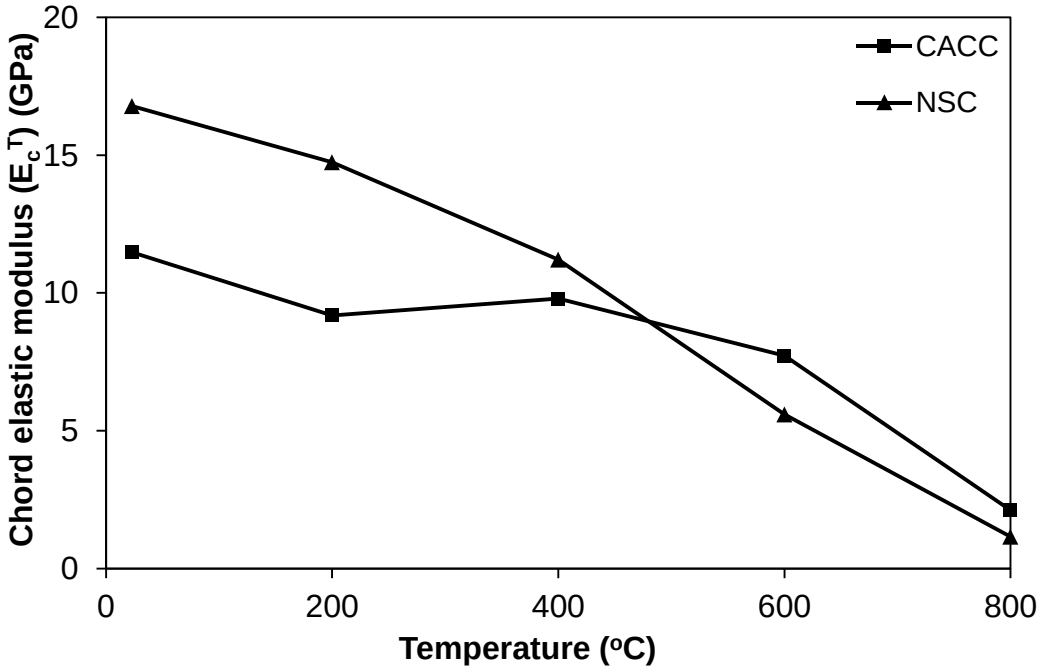

Figure 4.6 – Unstressed chord elastic modulus of CACC and NSC with respect to temperature

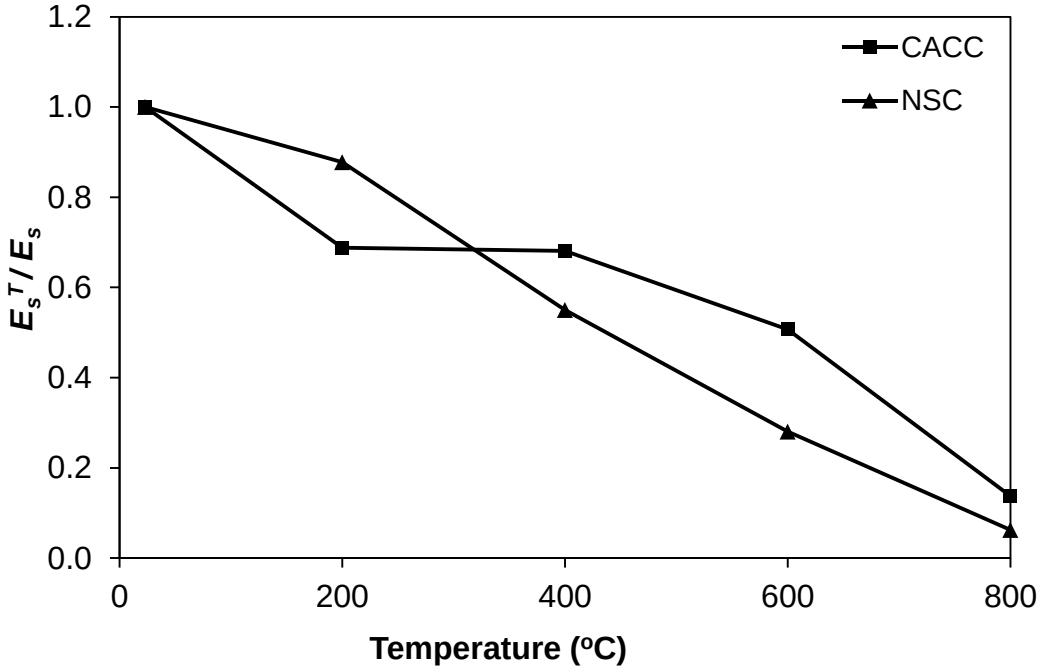

Figure 4.7 – Measured relative unstressed secant elastic modulus of CACC and NSC

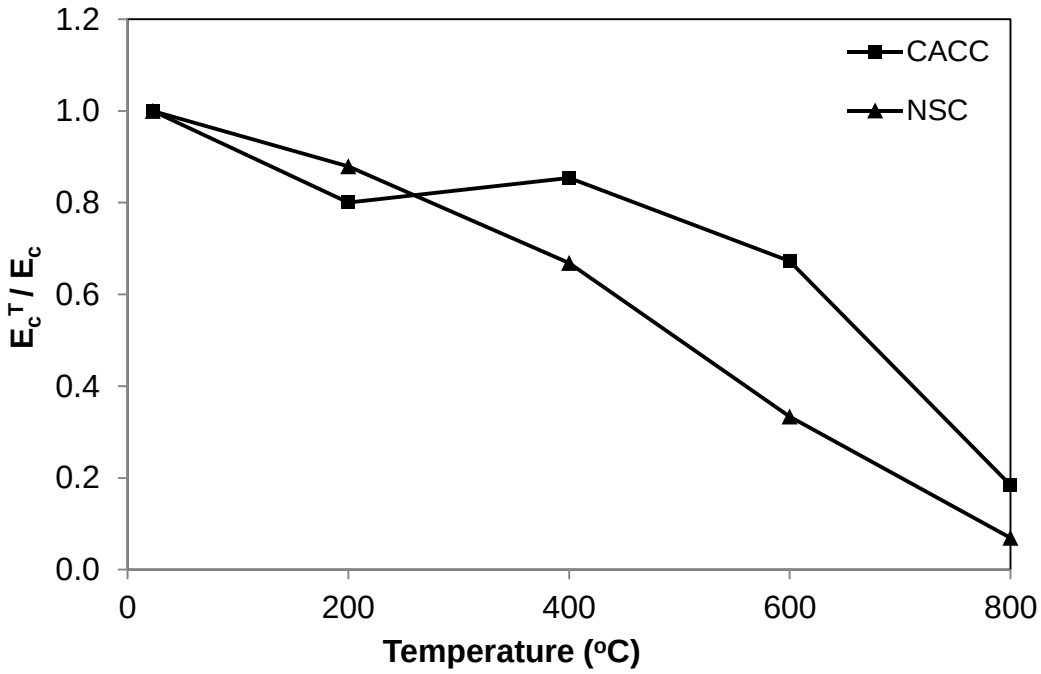

Figure 4.8 – Measured relative unstressed chord elastic modulus of CACC and NSC

4.2.3.1 Calcium Aluminate Cement Concrete

It can be seen from Figure 4.5 and 4.6 that, the elastic modulus of CACC observed is lesser as compared to NSC at room temperature. Further, there is a gradual loss in elastic modulus till 200°C which is due to the loss of moisture present in the mix. This initial loss in elastic modulus of CACC is attributed to the conversion of hydrates present in the microstructure of concrete causing an increase in porosity and ultimately the loss of chemically bound water generated

due to this reaction (Scrivener and Capmas, 1998). By observing Figure 4.7 and 4.8, the secant elastic modulus after 200°C remains almost constant at 69% without any further loss, which is not the case in NSC. This proves that CACC is much more stable in terms of loss of elastic modulus till 400°C due to much advanced morphology. The decrease in modulus beyond 400°C observed in NSC and CACC is attributed to the increase in porosity and internal microcracking with a drastic loss after 600°C, which can be observed from the slope of Figure 4.7 and 4.8. However at 800°C, almost 14-18% of modulus is retained, as compared to 6-7% in case of NSC. This higher elastic modulus observed in CACC at elevated temperatures can be attributed to the superior and dense microstructure due to alumina as compared to NSC where major dissociation and breakdown of CH crystals have taken place causing the development of microcracks extending up till the surface.

4.2.3.2 Normal Strength Concrete

The elastic modulus of NSC keeps on decreasing in 20-800°C temperature range. As the temperature increases beyond 200°C the stress strain curve becomes flatter till 600°C. As a result, elastic modulus keeps on decreasing with the increase in temperature. The recorded secant modulus of elasticity of NSC at 200°C, 400°C, 600°C and 800°C were about 88%, 55%, 28% and 6% of the original unheated values, respectively. This loss in elastic modulus of NSC is due to the loss of hydrated water in concrete, in addition to the increase in porosity of concrete which is attributed to the chemical and physical changes in concrete microstructure. Degradation of microstructure due to the development of micro and macro cracks also leads to the degradation of concrete's elastic modulus (Castillo and Duranni, 1990).

4.2.4 Stress-Strain Curves

The recorded load-deformation data in compressive stress-strain test is utilized to generate the stress-strain curve of NSC and CACC at 23, 200, 400, 600 and 800°C temperatures. The stress-strain response was obtained by measuring load-deformation through load controlled technique; as a result the descending branch of most of the curves was not captured. The complete compressive stress-strain curve of CACC for different temperatures is shown in Figure 4.9, whereas the stress-strain response of NSC is shown in Figure 4.10. With the increase in temperature, an increase in peak strain and decrease in compressive strength was observed. Therefore, the shape of the stress-strain curve becomes flatter as compared to the unheated concrete. Further, the strain corresponding to peak stress keeps on increasing significantly with the increase in temperature especially beyond 400°C in case of NSC, whereas

beyond 600°C in case of CACC. However, the performance of CACC is much better in terms of peak stress observed in stress-strain curve at elevated temperatures. Further, CACC depicts much higher peak strain as compared to NSC at elevated temperature which represents the ductility of concrete, as shown in Figure 4.9 and 4.10.

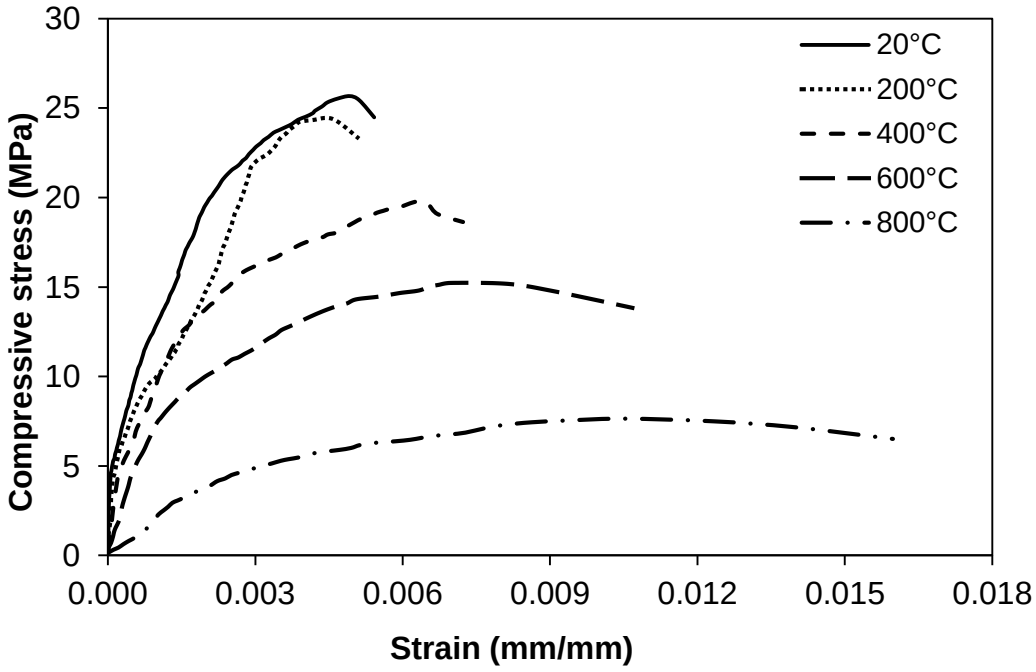

Figure 4.9 – High temperature unstressed stress-strain curve of CACC

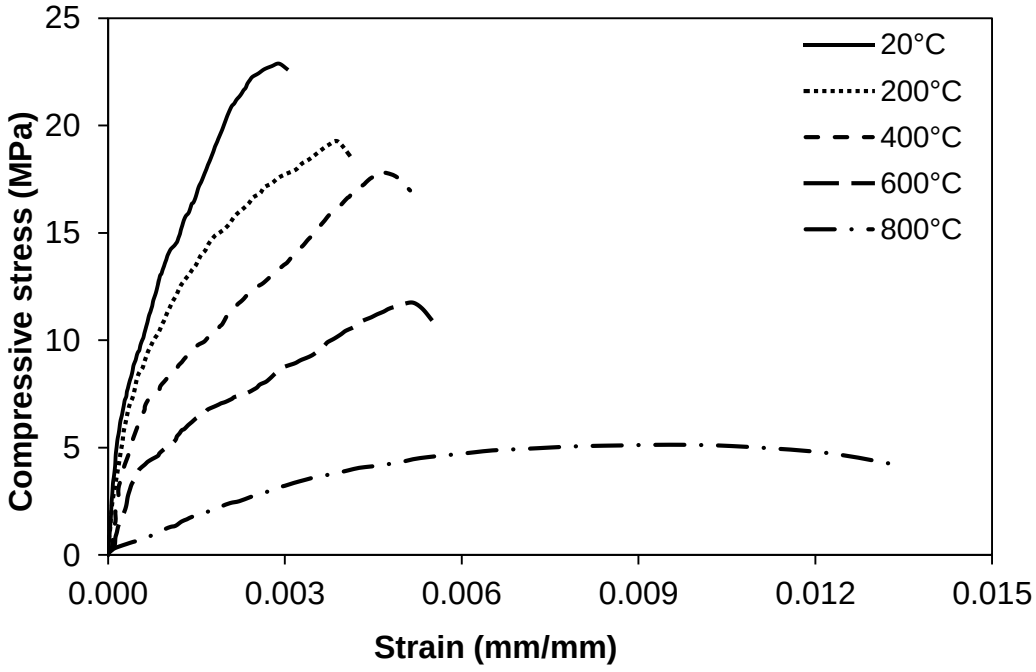

Figure 4.10 – High temperature unstressed stress-strain curve of NSC

4.2.4.2 Calcium Aluminate Cement Concrete

Stress-strain response of CACC at different temperatures can be seen in Figure 4.9. As in the case of NSC, with the increase in temperature the compressive strength and modulus of elasticity of CACC also decreases. As a result the stress-strain curve becomes flatter. By comparing the unstressed stress-strain response of both the concrete at different temperature, it is observed that the peak compressive stress and strain of CACC is much higher as compared to NSC. Besides this, peak strain keeps on increasing with the increase in temperature ranging from 0.0049 at 23°C to 0.0105 at 800°C. This rapid increase in peak strain beyond 400°C can be attributed to the increased cracks resulting from high temperature exposure and movement of pore water. In addition to that, the plotted total strain is mainly composed of mechanical strain due to loading and thermal strain due to temperature. As the tested cylinders were not loaded during heating i.e. unstressed test method, therefore the creep and transient strains are not significant in the measured (total) strain. It was observed that, major micro cracks were observed on the surface of the CACC which leads to the rapid increase in strain after 600°C. Therefore, higher peak strain can be attributed to additional thermal strain caused by easy diffusion of pore water facilitated due to higher porosity and increase in micro cracks due to burning at elevated temperature.

4.2.4.2 Normal Strength Concrete

Figure 4.10 shows the complete stress-strain behavior of NSC at different temperature levels. As discussed earlier that, with the increase in temperature physical and chemical changes takes place in the microstructure of NSC. These changes include the loss of moisture present in the mix up to 200°C after that some minor microcracking due to the degradation of CH and C-S-H up to 600°C (Chan et al., 1999). These changes results in major micro and macro cracking resulting in the loss in stiffness and brittleness of concrete up to 800°C which is shown in Figure 4.9. This loss is also attributed to the loss of mass, and degradation of microstructure. It can be seen from the above figure that, the strain at peak stress keeps on increasing from 0.0029, 0.0039, 0.00455, 0.0052 and 0.00952 with the increase in temperature at 23°C, 200°C, 400°C, 600°C and 800°C respectively. This rapid increase in peak strain after 400°C is attributed to the major cracks which are observed on the surface of the cylinder due to burning at elevated temperature and easy diffusion of pore water due to the increase in porosity and decrease in the mass of concrete.

4.2.5 Compressive Toughness (T_c)

After computing the stress-strain response of both types of concrete in unstressed test conditions, compressive toughness (T_c) was derived from these stress-strain curves and defines the energy absorbing capacity of concrete and is a measure of its ability to resist fracture in compression (Marar et al., 2011). It is calculated as the area under the stress-strain curve of NSC and CACC up to peak strain at failure by using Equation 3.2. The measured values of compressive toughness as a function of temperature can be observed in Figure 4.11. As it is a derived property, so it depends upon the stress-strain response of concrete. It can be seen that, the energy absorbed by CACC before rupturing was 2.30 times higher as compared to NSC which is due to higher peak strain at failure in compression. It was observed that, the value of T_c in CACC decreases in the beginning between 23-200°C temperature ranges because of the loss in compressive strength. However there was a drastic increase up to 400°C which is due to the reason that the loss in strength was not much at this temperature but the increase in strain is noteworthy.

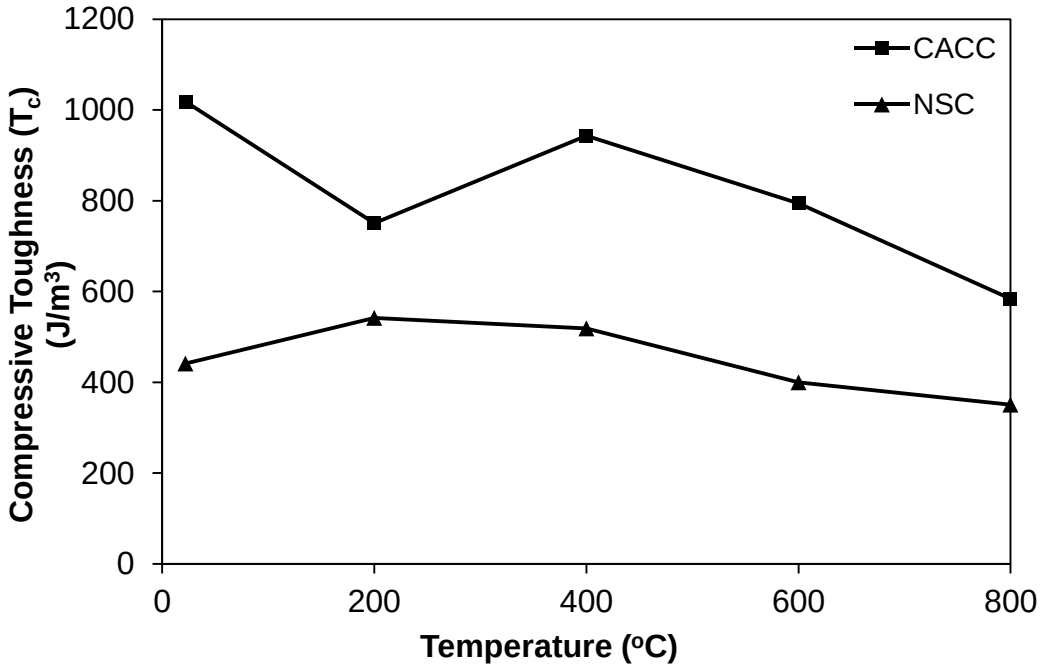

Figure 4.11 – Absolute unstressed compressive toughness of CACC and NSC as a function of temperature

The relative compressive toughness (T_c^T/T_c) follows the similar trend to its absolute as shown in Figure 4.12, for NSC and CACC. It can be seen that CACC exhibits lesser ratio of toughness, however, the absolute value of compressive toughness was much higher, especially with in 400 to 800°C temperatures range. This increase in compressive toughness characterize

the concrete's ability to resist fracture and sustain inelastic deformations without substantial decreases in the load carrying capacity which is of much advantage in mitigating the fire induced spalling in CACC and therefore can enhance the fire resistance rating of RC members made of CACC.

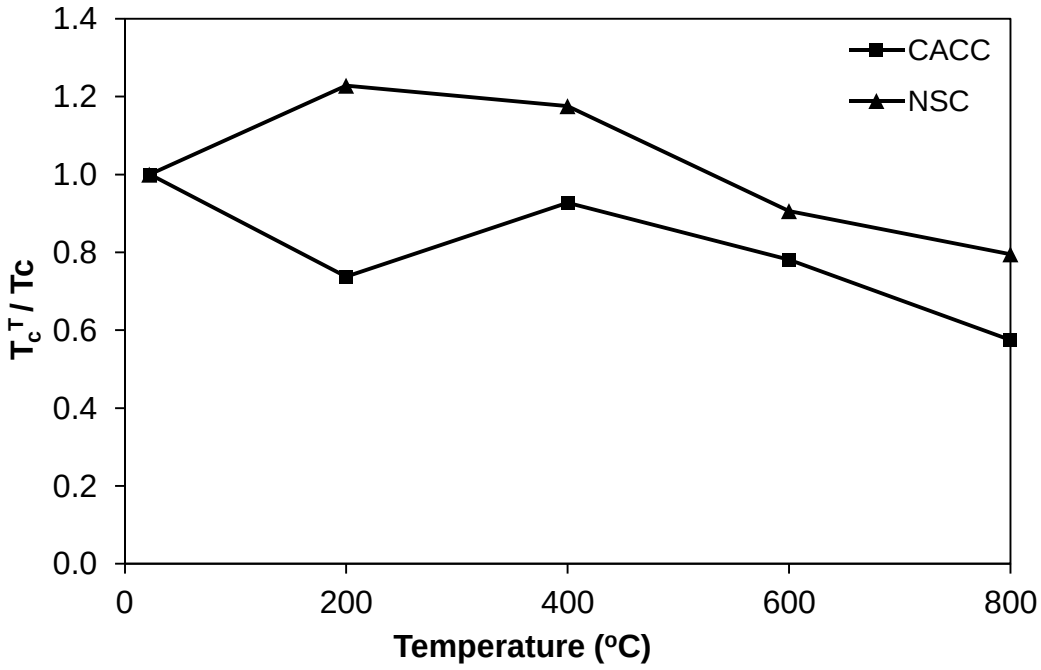

Figure 4.12 – Relative unstressed compressive toughness of CACC and NSC

4.2.5.1 Calcium Aluminate Cement Concrete

The compressive toughness (T_c) of CACC can be studied in Figure 4.11 and 4.12, which shows the impact of elevated temperature ranging from 23-800°C on it. The energy required to fail the specimen of CACC in compression at room temperature was 2.30 times higher as compared to NSC. Further, in case of unstressed test procedure the observed values of compressive toughness in CACC were 38-130% higher than that of NSC within the entire temperature range. This means that the CACC has a much better ability to absorb energy before failure in compression. However, major loss of around 26% in toughness is observed at 200°C in case of CACC, unlike NSC where 23% increase is observed at this temperature. This loss in toughness is linked with the major chemical and morphological changes taking place within the microstructure of CACC in the form of conversion reaction. The moisture changes resulting from this reaction in CACC lead to these abnormalities at 200°C. Similar, behavior at 200°C is also observed in other high temperature properties of CACC. However, an escalation in T_c was observed till 400°C i.e. around 26% increase in relative toughness with respect to that at 200°C. This is further validated that no major and minor cracks were observed in CACC

cylinders, unlike NSC, where minor cracks starts emerging at this temperature due to which no major loss in strength is evaluated in compression. Afterwards, gradual loss in toughness was estimated with the increase in temperature from 400°C till 800°C. This gradual loss is due to the physical deterioration of CACC at higher temperature. However, if we observe that how much energy absorbing capacity is retained at 800°C, CACC retains around 57% whereas in case of NSC 80% is retained. But if we compare the overall absolute capacity, CACC absorbs 1.66 times more energy before rupturing as compared to NSC at 800°C.

4.2.5.2 Normal Strength Concrete

By observing the Figure 4.11 and 4.12, it is estimated that the compressive toughness of NSC was improved with the increase in temperature till 200°C. This is due to the increase in peak strain from 0.0029 to 0.0039 with a very little decrease in strength. This results in an increase in energy absorption capacity from 441 to 542 J/m^3. Further, with the increase in temperature there is a minor loss in T_c till 400°C. However, sudden drop in energy absorbing capacity of NSC is observed which is linked with the peak compressive stress and strain at failure. Further, this loss in toughness is due to major loss in load carrying capacity of concrete after 400°C, which is linked with the micro cracking and degradation of microstructure after 400°C. The total loss observed at 800°C was 20.5% of the original unheated values i.e. 351 J/m^3 of energy was absorbed by the sample before rupturing in compression.

4.2.6 Mass Loss

The deviation in mass loss i.e. the ratio of mass evaluated at specified temperature level to the mass at room temperature is obtained from tests and is plotted in Figure 4.13 as a function of temperature, for both NSC and CACC. The change in mass at elevated temperatures depends on the hydration products and type of aggregates used in concrete, with a very little influence of type of cement (Kodur and Sultan, 2003). It is observed that with the increase in temperature the loss in density is observed in both types of concrete. It can be seen from this figure that no significant mass loss is observed in both types of concrete till 600°C. However, higher mass loss of about 17% of room temperature is observed within 600-800°C temperature range in case of NSC, whereas 13.5% of mass loss takes place in CACC. As both types of concrete are made up of limestone, so this major loss of mass in concrete is due to the calcination of calcareous aggregate (Abrams, 1971; Lie and Kodur, 1996).

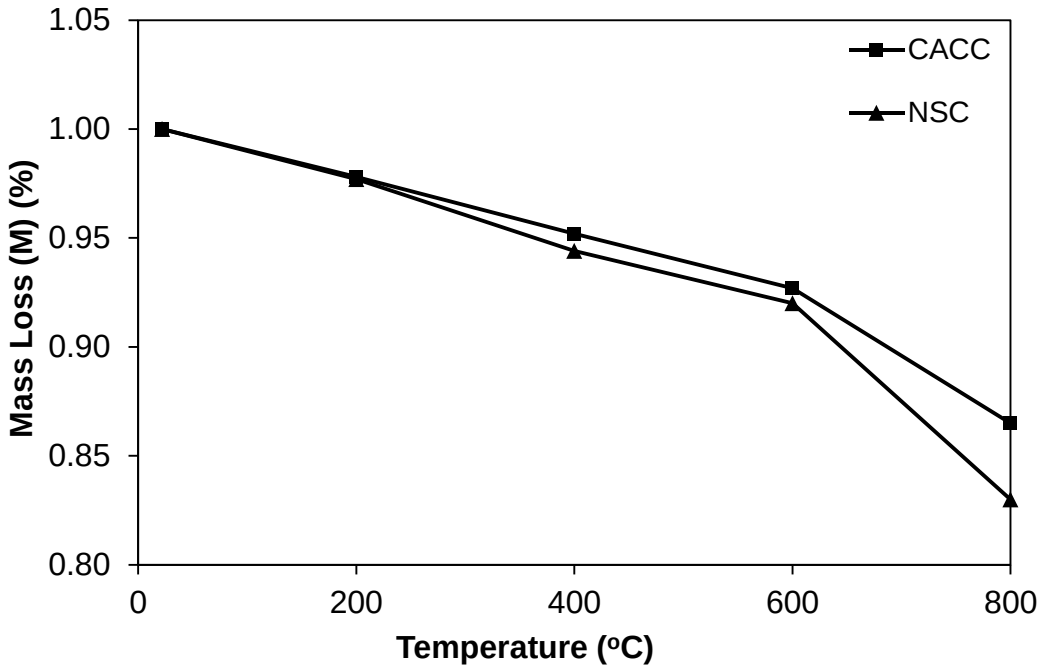

Figure 4.13 – Measured unstressed mass loss as a function of temperature for CACC and NSC

4.2.6.1 Calcium Aluminate Cement Concrete

Similarly from the above figure, it can be seen that around 7% loss of mass is observed till 600°C. However, slightly moderate loss in mass takes place till 800°C i.e. around 13%. As explained in the literature review, mass loss of the concrete at an elevated temperature depends upon the type of aggregate (Kodur and Sultan, 2003). As both concretes are made up of calcareous aggregate i.e. limestone, so no major difference in this material properties of concrete is observed. However, a slight difference in mass loss is throughout till 800°C, which is due to the different microstructure and permeability of concrete. However, the sudden loss of mass beyond 600°C in both the cases is due to dissociation of calcium carbonate present in the limestone aggregate.

4.2.6.2 Normal Strength Concrete

By studying Figure 4.13, it can be clearly observed that minor loss of mass takes place in NSC till 600°C which is around 8% of the mass observed at room temperature. This minor loss is due to the dehydration of concrete microstructure. However, a sudden drop of mass of around 17% is observed after 600°C, which can be seen in the above figure with a major increase in slope. This sudden drop of mass is due to the loss of moisture which is chemically bound and the dissociation of limestone aggregate present inside concrete. Further, the mass loss of NSC

is almost the same as that of CACC from which it can be seen that no significant effect of binder on mass loss of these concrete is observed at elevated temperatures.

4.3 Residual Material Properties

As explained in chapter 2 and 3, this test procedure involves the concrete sample to be exposed to elevated temperatures till the steady state is achieved. After that, the sample is removed from the furnace and allowed to cool down to the room temperature to develop the residual stresses. Afterwards, the sample is ready to be tested in strength test machine to evaluate their mechanical and material properties. This section discusses the results of different material properties of NSC and CACC when exposed to elevated temperature, according to this test procedure.

4.3.1 Compressive Strength ($f'_{c\,res}$)

The applied compressive load is computed at failure against both types of concrete mixes, NSC and CACC at different elevated temperatures. This failure load is computed when the samples temperature is reach to a uniform room temperature after being exposed to elevated temperature for a specified time. Figure 4.14 shows the residual compressive strength ($f'_{c\,res}$) of NSC and CACC as a function of temperature ranging from 23°C to 800°C. By studying this figure, it is observed that the compressive strength of both types of concrete decreases with the increase in temperature as a result of physical and chemical changes taking place in concrete at elevated temperatures. This loss in strength is gradual in case of CACC up to 600°C, whereas in case of NSC rapid loss in strength is observed beyond 400°C. In addition, if we compare the performance of both in terms of residual compressive strength, it can be seen that, major difference is present in strength at 800°C, which confirms that the overall performance of CACC is much better at higher temperature. The relative residual compressive strength loss ($f'_{c}{}^{T}{}_{res}/f'_{c\,res}$) in NSC and CACC follows similar trend to its absolute strength as shown in Figure 4.15. By observing the trend in this figure, it is evident that CACC displays lesser loss of compressive strength ratio as compared to NSC at 600°C, whereas at lower temperature NSC performs much better with the lesser loss in ratio. However, it can be further observed that NSC losses up to 78% of its absolute strength when exposed to elevated temperatures of 800°C whereas CACC losses 72% of its strength at such a high temperature, which further validates the performance of CACC at higher temperature.

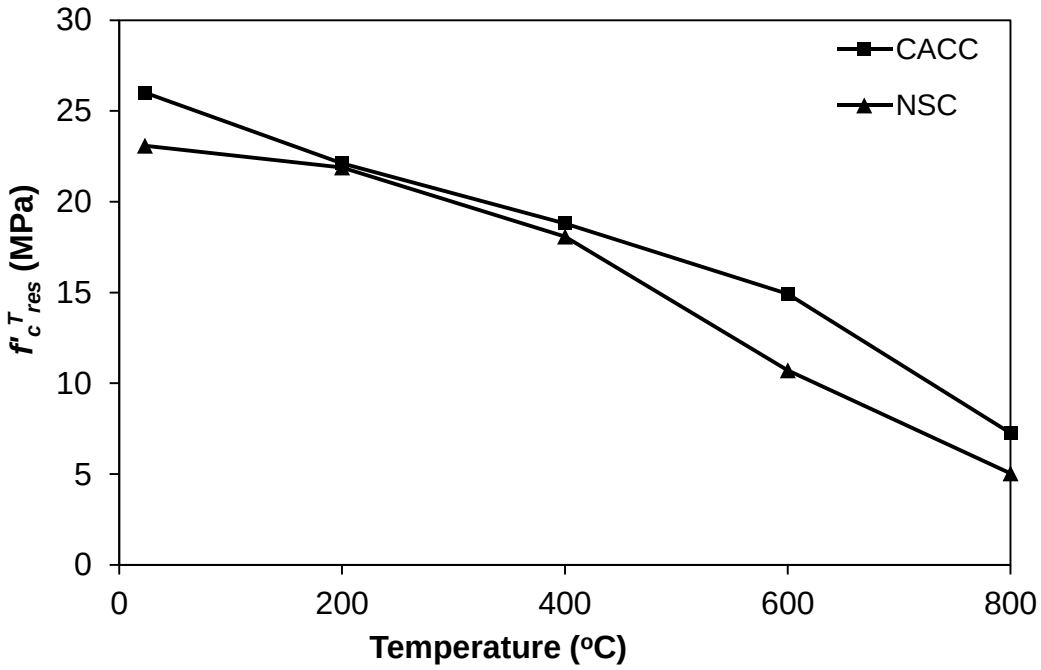

Figure 4.14 – Residual compressive strength of CACC and NSC as a function of temperature

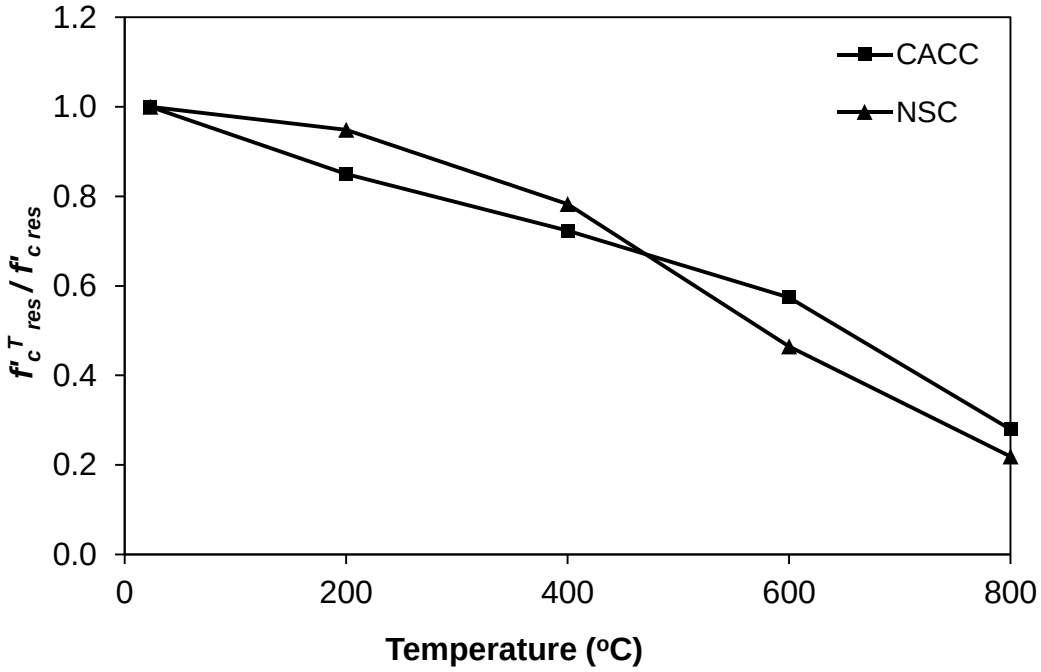

Figure 4.15 – Residual relative compressive strength of CACC and NSC

4.3.1.1 Calcium Aluminate Cement Concrete

By studying the Figure 4.14 and 4.15, the gradual loss in residual compressive strength of CACC is observed against different elevated temperatures between 23°C and 800°C. As the temperature increases, the physically bounded moisture escapes the matrix of the concrete resulting in the increase in porosity and decrease in strength, which can be seen from the above figures, that just 72% retention in compressive strength is observed at 400°C. Further at 600°C,

the minor loss in strength is observed which is much lesser i.e. around 43%, unlike NSC. However, when the strength is observed after exposing the sample to 800°C and allowing it to stabilize its temperature to room temperature a major loss is observed, which can be further validated from the slope of the curve beyond 600°C. At this temperature, major surface cracks were also observed which show damage occurred after exposure to elevated temperatures. In this scenario, only 28% strength is retained of that of original unheated values i.e. around 7.26 MPa. However, this strength is much better as compared to NSC i.e. 5.04 MPa. This major loss is due to the calcination of limestone aggregate used in CACC and dehydration of concrete causing deterioration of microstructure.

4.3.1.2 Normal Strength Concrete

The residual compressive strength of NSC can be observed from the Figure 4.14 and 4.15, which shows that an ongoing loss in strength is occurred with the increase in temperature. Initially a minor loss is observed i.e. around 5% of unheated strength at 200°C which is due to the loss of moisture. After that, the strength stabilizes up till 400°C with a minor loss. This slight loss in strength at 400°C i.e. around 22%, is due to the escape of pore water pressure present as physically bound water and the loss of bond between aggregate and cement paste. Beyond 400°C, there is a significant loss in strength which can be observed by investigating the slope of NSC curve resulting in 54% loss of unheated strength at 600°C. This major loss in strength of NSC is due to the degradation of microstructure resulting in minor cracks extending up to the surface. At 800°C, just 22% of room temperature strength is retained which is due to the slow loss of chemically bound water, degradation of microstructure and deterioration of cementing ability due to the dehydration and disintegration of CH and C-S-H in concrete (Khaliq and Kodur, 2011).

4.3.2 Splitting Tensile Strength ($f'_{t\,res}$)

This test tells us about the post-fire tensile strength of both types of concrete after being exposed to different levels of temperature. The performance of NSC and CACC in terms of residual tensile strength can be observed from the Figure 4.16. As this property tells us about the tensile strength and the damage to concrete in tension at elevated temperature, so this property is crucial in investigating the generation of micro cracks. Firstly, it is examined that the tensile strength of both types of concrete at different temperatures is little as compared to compressive strength of concrete. Secondly, that all concrete types experience loss in tensile strength with the increase in temperature. By observing the curve, it can be seen that the loss

in tensile strength of CACC is gradual till 800°C as compared to NSC, where there is significant loss in strength after 400°C. This major loss in concrete's tensile strength is attributed to development of minor and major cracks in concrete which results in the progressive micro cracking within the microstructure. This loss in strength is also attributed to the loss of moisture till 400°C, which results in the shrinkage of concrete matrix due to dehydration of water from cement paste and expansion caused by temperature rise which ultimately results in micro cracking and strength loss.

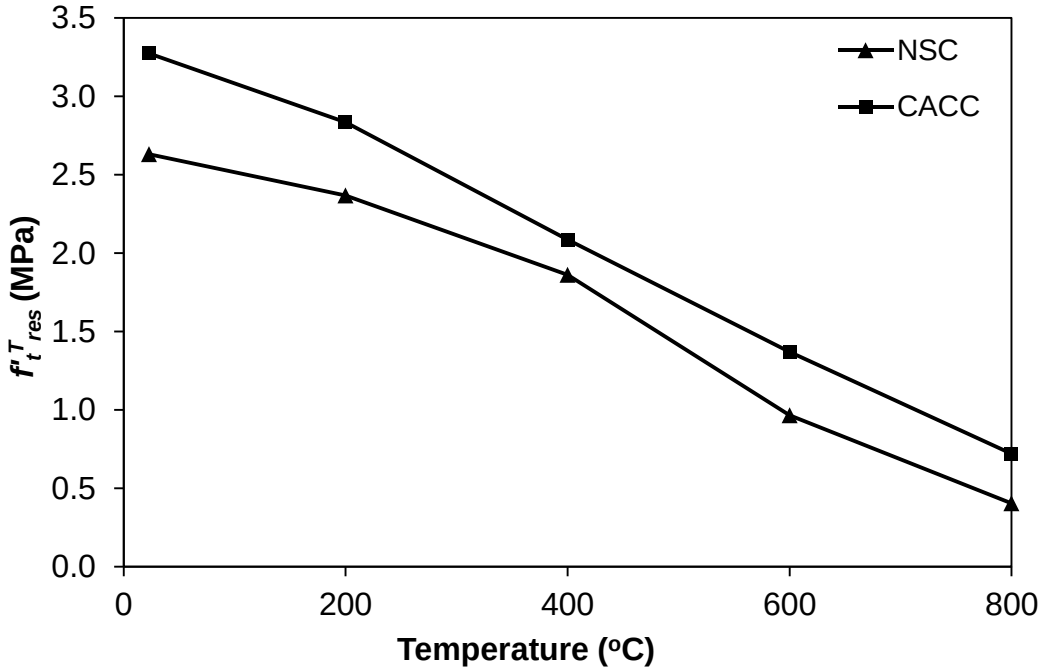

Figure 4.16 – Measured residual splitting tensile strength of CACC and NSC

The relative residual splitting tensile strength ($f'^{T}_{t\,res}/f'_{t\,res}$) follows similar trend to its absolute strength as shown in Figure 4.17, for both NSC and CACC. It can be seen that the loss in the strength in case of CACC is gradual till the end, unlike NSC. After 400°C, major loss in strength is observed in case of NSC, which can be further validated from the sudden drop in slope of NSC curve. This results in 34% loss in strength unlike CACC where just 22% loss is observed between 400°C to 600°C. This post-fire performance of CACC especially in the temperature range between 400°C till 800°C is noteworthy and therefore can help in enhancing the fire resistance rating of RC members made of CACC.

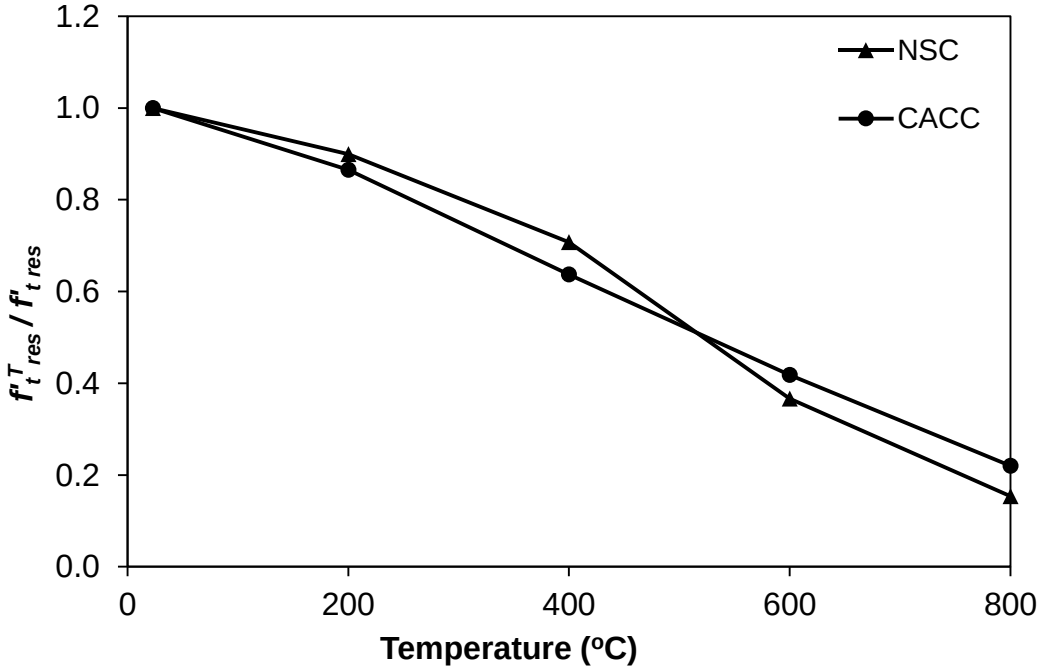

Figure 4.17 – Residual relative splitting tensile strength of CACC and NSC as a function of temperature

4.3.2.1 Calcium Aluminate Cement Concrete

By observing the trend of CACC in Figure 4.16 and 4.17, it is observed that the loss is tensile strength is unavoidable with the increase in temperature. This loss in tensile strength after being exposed to different elevated temperatures is very gradual and is attributed to the physical and chemical changes that take place in the CACC with the increase in temperature. By observing Figure 4.16, it can be seen that the tensile strength of CACC at room temperature with the same mix parameters is about 3.25 MPa i.e. about 23% more than NSC. Further, with the increase in temperature till 400°C, there is a loss of moisture from the cement paste which is physically bound which results in 36% strength loss as compared to room temperature strength. However, this loss is more i.e. around 7% additional when we compare it with NSC at 400°C. On the other hand, the loss in strength keeps on decreasing with the further increase in temperature, unlike NSC. This loss is attributed to the major chemical changes which takes place in CACC, where the chemically bound water is removed and the hydrates are transformed from metastable CAH_{10},C_2AH_8 in to more stable phases like residual C_3AH_6, CA, AH_3 and CA_2 (Martinović et al., 2012). However, this results in the loss of density and increase in the porosity of the concrete resulting in the weakening of the bond between the aggregates and paste, which causes the loss of strength and cracking at the microstructure visible at the surface of the concrete. Further, there is a noticeable retention in the tensile strength of CACC at 800°C i.e. around 22% instead of just 15% in case of NSC. This observation further confirms that CACC

has superior microstructure and therefore displays better tensile strength even at higher temperatures.

4.3.2.2 Normal Strength Concrete

The performance of NSC can be studied from Figure 4.16 and 4.17, by observing the slope of the curve depicting the tensile strength of NSC at different temperature levels. Increase in the exposure temperature results in the loss of tensile strength of concrete. This loss is minor till 400°C which is due to the physical changes in the concrete microstructure like loss of physically bound water from the paste resulting in the increase in the porosity of the concrete. However, after 400°C major loss in tensile strength is observed which is attributed to the increase in micro and macro cracks in the concrete microstructure and disintegration of CH and C-S-H hydrates (Mehta and Monteiro, 2006). This results in the increase in the porosity of the concrete and ultimately the loss in tensile strength of concrete. After the exposure of 800°C, the tensile strength is very limited and just 15% of the unheated tensile strength is retained, which confirms that the concrete is porous and does not respond very well after fire at room temperature.

4.3.3 Elastic Modulus

As described earlier, elastic modulus depends upon many factors in which the major importance is given to microstructure of concrete and hydrated products in concrete paste. Residual secant modulus and the chord elastic modulus of concrete is obtained from the compressive stress-strain curves after exposing the concrete cylinders (NSC and CACC) to elevated temperatures (23°C, 200°C, 400°C, 600°C, 800°C) and allowing it to cool down to room temperature to develop residual stresses. Figure 4.18 and 4.19, shows the absolute values of residual secant ($E_s{}^T{}_{res}$) and chord ($E_c{}^T{}_{res}$) elastic modulus of both types of concrete, respectively. By studying the curves it can be seen that the elastic modulus of both types of concretes degrades which shows that physical and chemical changes are taking place inside the concrete microstructure. Figure 4.20 and 4.21, shows the relative values of residual secant ($E_s{}^T{}_{res}/E_{s\ res}$) and chord ($E_c{}^T{}_{res}/E_{c\ res}$) elastic modulus as a function of temperature against different temperature levels respectively. It is observed that both types of concrete follows similar trend as that of its absolute values which continuously decreases with the increase in temperature till 800°C. However, at 800°C the difference between the observed values of NSC and CACC is minor, unlike lower temperature where major difference is observed.

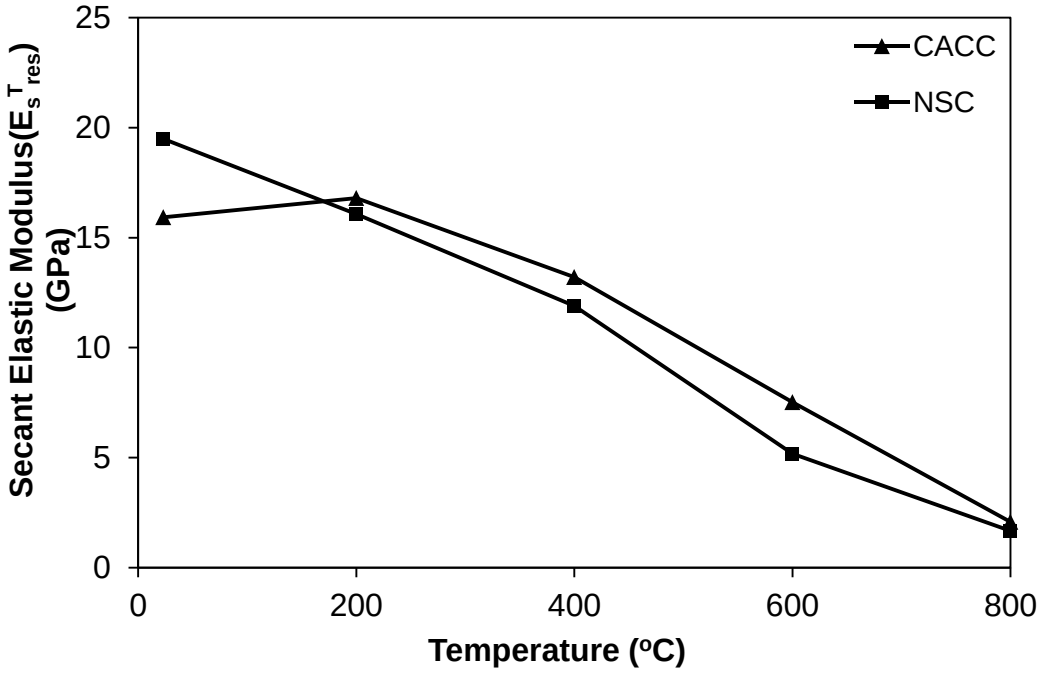

Figure 4.18 – Residual secant modulus of elasticity of CACC and NSC

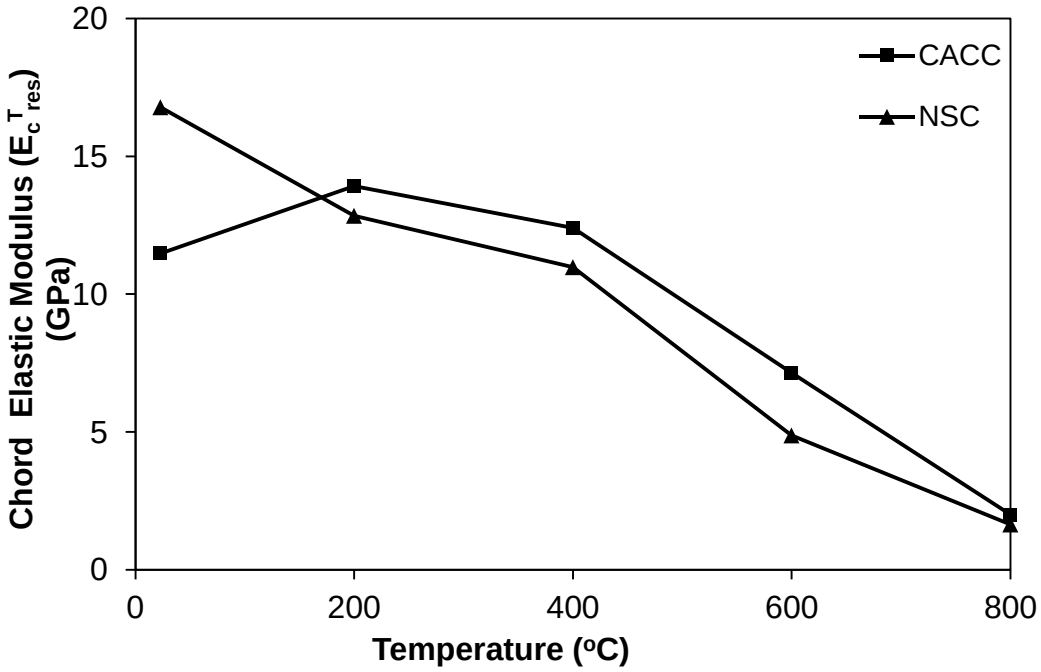

Figure 4.19 – Residual chord modulus of CACC and NSC as a function of temperature

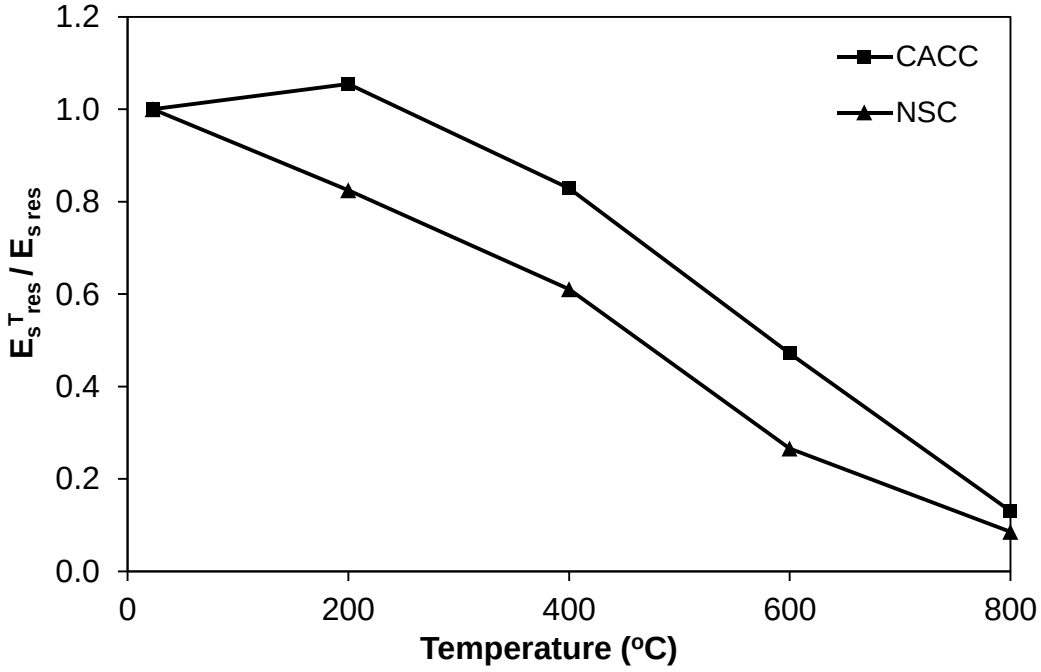

Figure 4.20 – Measured relative residual secant modulus of CACC and NSC as a function of temperature

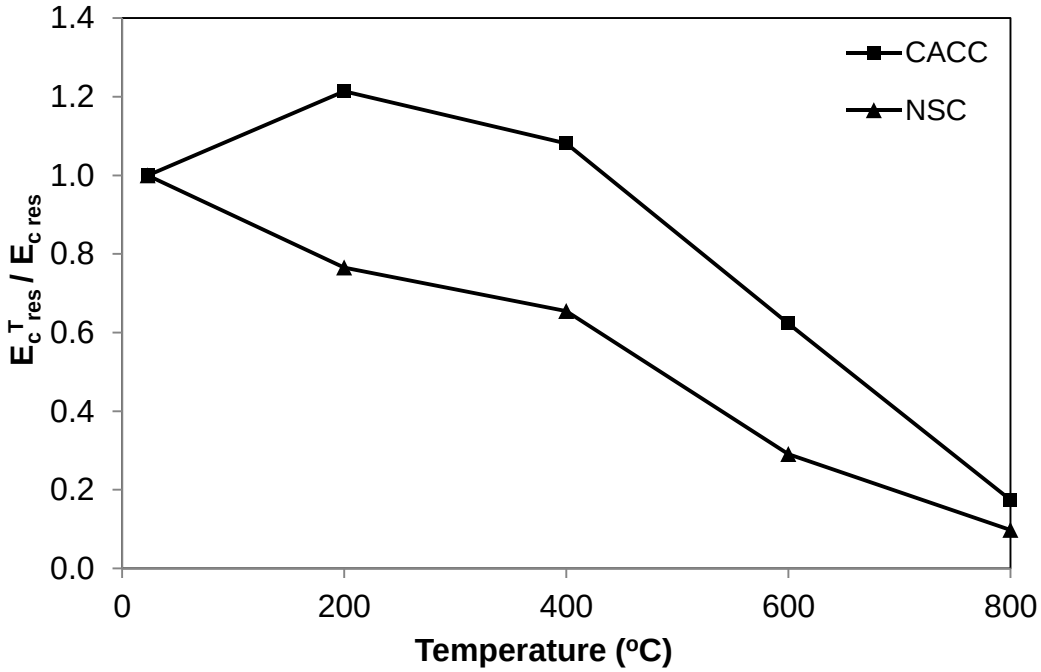

Figure 4.21 – Measured relative residual chord modulus of CACC and NSC as a function of temperature

4.3.3.1 Calcium Aluminate Cement Concrete

The absolute and the relative residual elastic modulus of CACC at different elevated temperatures can be seen in Figure 4.18, 4.19, 4.20 and 4.21. The elastic modulus of CACC in residual conditions exhibit a slight increase of around 7% - 8% at 200°C. This can be attributed

to regain of water due to moisture changes as a result of conversion reaction. In addition, CACC gives us 6% - 7% more post fire elastic modulus if we compare it with NSC at the same temperature. However, a gradual loss in modulus of elasticity can be seen after 400°C till 800°C. This initial loss is attributed to the conversion of hydrates present in the microstructure of concrete causing an increase in porosity and ultimately the loss of chemically bound water generated. In addition, no major cracks are observed on the surface of the concrete till 600°C but a loss in density is observed, which further validates that the loss in modulus with the increase in temperature is unavoidable. However, the estimated value of modulus of elasticity of CACC at 600°C is around 45% more than that of NSC. This higher elastic modulus observed in CACC at elevated temperatures can be attributed to the superior and dense microstructure as compared to NSC where major dissociation and breakdown of CH crystals have taken place causing the development of microcracks extending up till the surface.

4.3.3.2 Normal Strength Concrete

By observing figure 4.18 and 4.19, the absolute values of residual secant and chord modulus of NSC can be studied as a function of temperature. It can be seen that, a gradual loss in modulus of elasticity is observed till 400°C which can be linked to the loss of pore water present inside the microstructure of concrete. However, a major loss in elastic modulus takes place between 400°C and 600°C, which can be evaluated with the slope of curve in the above figures. This loss is due to minor and major micro cracks developed on the surface of the concrete and the degradation of microstructure which ultimately affects the stiffness of NSC considerably. However, this loss is a bit stabilized further after 600°C till 800°C in NSC, but this does not means that its ability to withstand external loading is improved. Further, Figure 4.20 and 4.21 show us the measured relative values of residual secant and chord modulus of NSC. It can be seen that, the recorded secant modulus of elasticity of NSC at 200°C, 400°C, 600°C and 800°C are 82%, 61%, 27% and 9%, whereas the chord modulus of elasticity of NSC at 200°C, 400°C, 600°C and 800°C are 77%, 65%, 29% and 10% of the original unheated values respectively.

4.3.4 Stress-Strain Curves

The complete compressive stress-strain curves are obtained after exposing the concrete cylinders to different elevated temperature levels and allowing it to cool down to the room temperature after achieving equilibrium at specified temperature. Figure 4.22 and 4.23 shows the stress-strain response of CACC and NSC at different temperature levels (23°C, 200°C, 400°C, 600°C and 800°C), respectively. By observing the curves, it is evident that the increase

in temperature causes a decrease in the load carrying capacity of the concrete. In addition to that, it also increases the ductility of the concrete. Besides, the stress-strain curve becomes flatter with the temperature, the peak strain increases from 0.0029 at room temperature to 0.00932 at 800°C in case of NSC. Similarly, in case of CACC there is a remarkable increase in peak strain from 0.00492 at 23°C to 0.01037 at 800°C. Further, in terms of strength loss and loss in the modulus of elasticity there are two major temperature ranges, 23°C to 400°C and 400°C to 800°C. This loss in strength is very different among these ranges and also varies a lot with respect to type of concrete. By studying these curves, it is evident that the performance of CACC is much better as compared to NSC. Firstly, the loss in strength after 400°C is much smaller as compared to NSC. Secondly, the peak strain in CACC is much more as compare to NSC which confirms the ductile behavior at elevated temperature i.e. in this case it will prolong the loss in failure in the load carrying capacity of concrete.

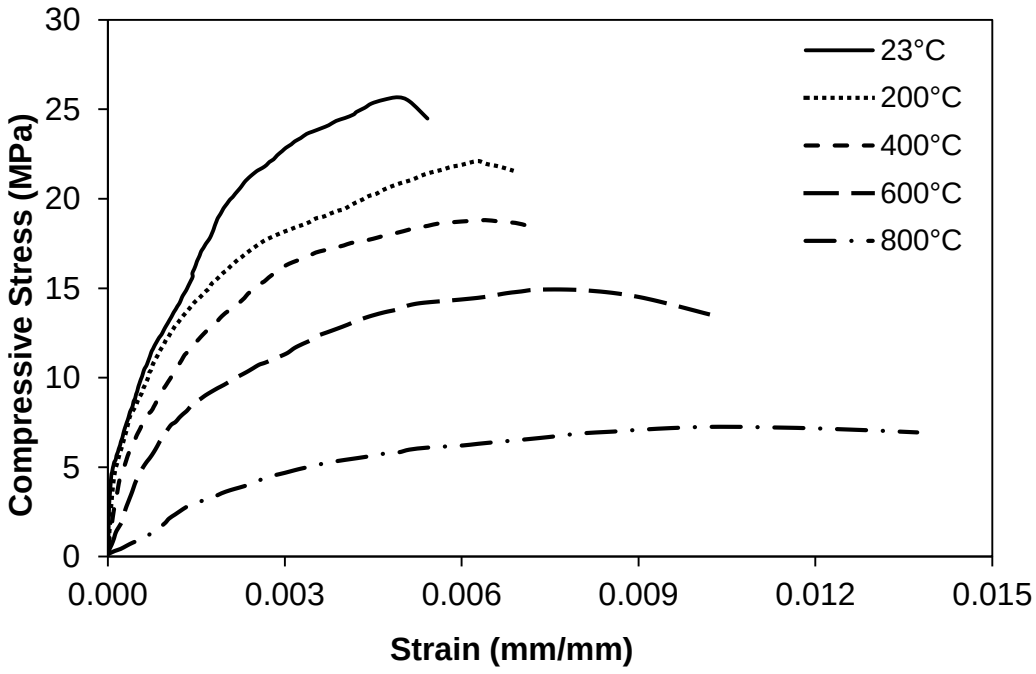

Figure 4.22 – High temperature residual stress-strain curve of CACC

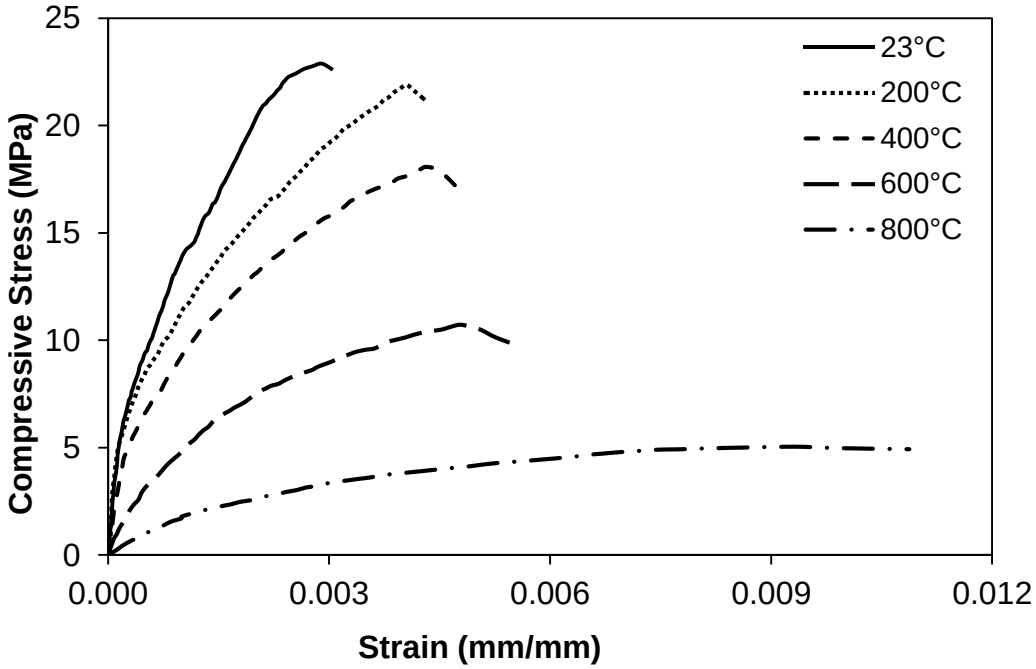

Figure 4.23 – High temperature residual stress-strain curve of NSC

4.3.4.1 Calcium Aluminate Cement Concrete

This high performance concrete (HPC) also undergoes the loss in the stiffness with the increase in temperature when exposed to elevated temperatures as shown in Figure 4.22. When it is exposed to elevated temperature, like every other concrete pore-structure deterioration also takes place in it. This is actually the changes in the concrete porosity as a result of which an increase in the concrete permeability takes place, which in returns affect the durability of concrete. However, this loss in concrete strength is not very critical in the range of 23°C to 400°C, because during this range in addition to the loss of physically bound water, major chemical changes also take place inside the concrete microstructure causing the transformation of hydrates from metastable CAH_{10} to stable C_3AH_6 phases (Scrivener et al., 1999). As this concrete, allows the loss of pore water pressure without any hurdle so the damage to concrete strength is minimum, which is evident from the slope of the concrete stress-strain curve. However, this loss in strength and durability remains gradual within the range of 400°C to 800°C, with an ultimate increase in the strain against peak stress from 0.0064 to 0.01037. This post-fire increase in the strain means that a major loss in the brittle nature of concrete has taken place. However, this increase in ductility, in terms of strain is almost the same in both the case i.e. NSC and CACC which is around 0.005 and 0.004 respectively, within this temperature range. The residual peak strains observed at 600°C and 800°C were 48% and 110% higher as compared to room temperature peak strain, whereas around 64% and 221% increase in peak

strain was observed in case of NSC at these temperature, respectively. Further, the residual peak strains of CACC at 600 and 800°C were 53% and 15% more as compared to NSC. Similarly, the failure compressive loads were 40% and 45% higher than NSC. These results confirm that, in addition to better response in terms of strength, CACC shows improved response in terms of ductility characteristics as well.

4.3.4.2 Normal Strength Concrete

By observing Figure 4.23, it can be seen that load carrying capacity of NSC vary remarkably with the increase in temperature. This residual stress-strain curve actually portrays post-fire load carrying capacity of NSC as a function of temperature to which it is exposed to. It can be seen that between 23°C to 400°C temperature range the fall in compressive strength is not very abrupt and ultimately the increase in peak strain is also very minor. This change in the shape of stress-strain curve can be linked with the loss of moisture present inside the microstructure resulting in an increase in porosity of the concrete. However, the loss in strength between 400°C to 800°C is abrupt and noteworthy. This is due to the chemical and physical changes that are taking place inside the concrete microstructure. In addition, the major and minor cracks which are produced due to thermal stresses on the surface and at the interfacial transition zone which also causes the loss in stiffness of concrete. Due to this reason the strain at the maximum stress in this temperature range increases from 0.0043 to 0.00932.

4.3.5 Compressive Toughness ($T_{c\ res}$)

As explained earlier, compressive toughness is a derived quantity which is obtained from the stress-strain response of concrete under compression. The post-fire response in terms of energy absorption capacity is dissimilar for both types of concrete at different temperatures, ranging from 23°C to 800°C. Figure 4.24 shows the residual absolute compressive toughness ($T_c{}^T{}_{res}$) values of concrete with respect to different elevated temperature, for both NSC and CACC. It can be observed that the energy absorbed by the CACC before rupturing is much more as compared to NSC which is due to higher strain at peak failure stress in compression. By studying the response of both types of concrete, it can be seen that a gradual increase in the toughness for both NSC and CACC is observed up to 200°C, after that both concrete suffers in terms of energy absorption capacity till 800°C. The compressive toughness of CACC at 800°C is around 60% more than that of NSC. This trend further validates the ductile nature of the concrete at such a high temperature.

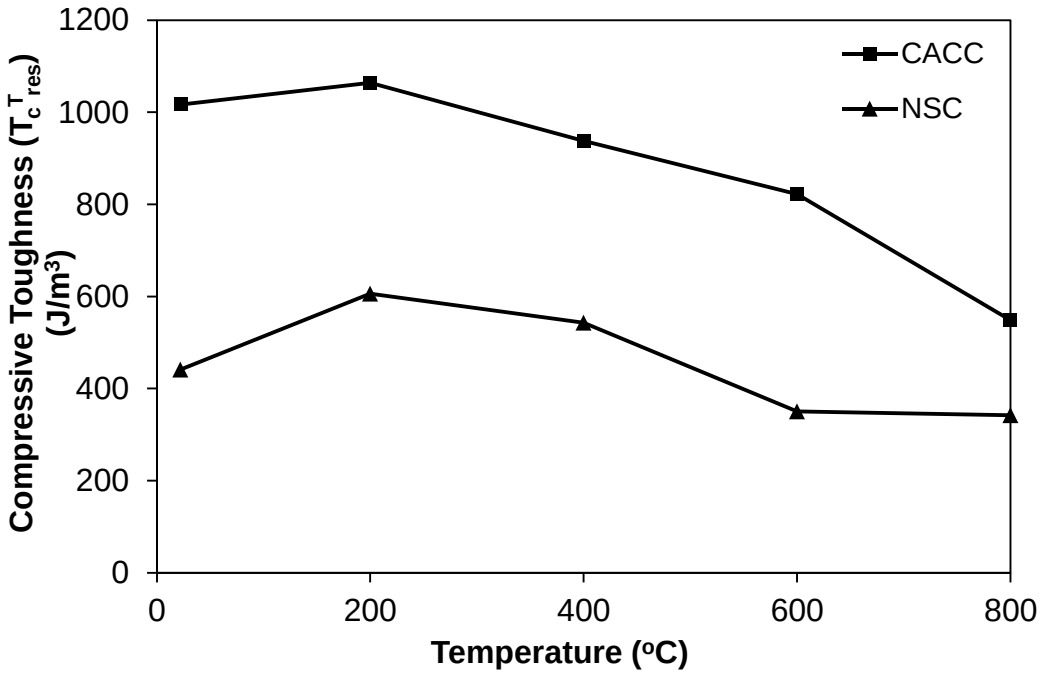

Figure 4.24 – Measured residual compressive toughness of CACC and NSC as a function of temperature

Figure 4.25 shows the relative post-fire trend of compressive toughness ($T_c^{T}{}_{res}/T_{c\ res}$), for NSC and CACC. The relative value follows the similar trend as that of an absolute value. It can be seen that, the change in energy absorption capacity of NSC is a bit sudden as compared to CACC till 800°C, which is very gradual. This abrupt change is linked with the stress-strain response of NSC, where a sudden loss in strength is observed with the increase in temperature (Figure 4.22).

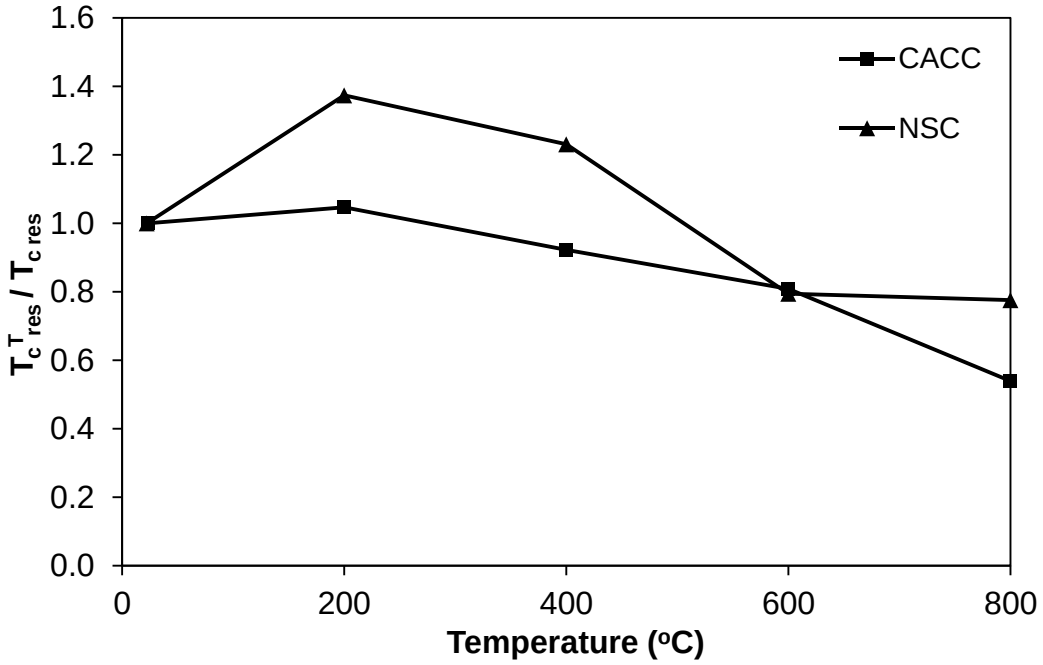

Figure 4.25– Relative residual compressive toughness of CACC and NSC

4.3.5.1 Calcium Aluminate Cement Concrete

The response of CACC in terms of energy absorbing capacity before failure is different as compared to NSC which can be seen from Figure 4.24 and 4.25. By studying these trends, it is observed, that there is a little increase in compressive toughness around 5% at 200°C as compared to room temperature toughness. This minor increase is due to the major increase in ductility in terms of peak strain of around 27% with minor loss in strength due to chemical changes within the microstructure of concrete which can be seen in Figure 4.22. Further, this increase can also be linked with the microscopic pictures taken to study the morphology of concrete microstructure at this temperature, where transformed stable hydrates are visible. However, there is a gradual loss in compressive toughness is observed between 200°C till 800°C, which is around 94% as compared to 200°C temperature toughness. This loss is attributed to the major chemical changes which takes place within CACC, where the chemically bound water is removed and the hydrates are transformed from metastable CAH_{10} in to stable phases like residual C_3AH_6, CA, A and CA_2 (Martinović et al., 2012). Further, these changes in the morphology of the hydrate can further be validated with the help of scanning electron microscopic pictures of the sample taken after being exposed to 600°C. In addition to that, this also results in the loss of density and increase in the porosity of the concrete resulting in the weakening of the bond between the aggregates and paste, which causes the loss of strength and cracking at the microstructure visible at the surface of the concrete. All these

chemical and physical changes results in the alteration of the shape of stress-strain curve of CACC, which results in the loss of energy absorbing capacity of concrete. However, if we compare the absolute value of compressive toughness at 800°C, CACC can absorb around 548 J/m^3 of energy 60% more as compared to NSC.

4.3.5.2 Normal Strength Concrete

By studying Figure 2.24 and 2.25, a rapid increase in toughness of around 37% is observed up to 200°C. This increase in toughness ($T_c{}^T{}_{res}$) can be linked with the stress-strain response of NSC at 200°C as shown in Figure 2.22, where a sharp increase in strain against peak stress is observed. However, from 200°C to 600°C a gradual loss in post-fire energy absorbing capacity is observed, which is around 73% of the toughness at 200°C. This is due to a gradual loss of strength which is linked with the increase in micro and macro cracks in the microstructure of concrete plus the loss of bond between the aggregate and paste. In addition, chemical changes like disintegration of CH and C-S-H hydrates also affect the overall performance of NSC in terms of energy absorption capacity before failure. However, after the exposure of NSC to 800°C, it is observed that it only absorbs 342 J/m^3 before failing in compression which means that 22% of the toughness at room temperature is lost. However, if major loss in toughness is observed against 200°C (which is the peak energy absorbing capacity of NSC) 77% of the energy absorbing capacity is lost.

4.3.6 Mass Loss

The variation in residual mass loss (ratio of mass at a specified temperature (M) to mass at room temperature (M_0)), as obtained from tests, is plotted in Figure 4.26 as a function of temperature for NSC and CACC. It can be seen that no significant mass loss takes place in both types of concrete till 600°C i.e. around 7%. However, major loss of around 15% takes place in case of NSC, whereas, 14% loss of mass was observed in case of CACC beyond 600°C up to 800°C. As discussed by (Kodur and Sultan, 2003; Lie and Kodur, 1996), the mass loss of concrete majorly depends upon the type of aggregate used. The performance of calcareous based aggregate (Limestone) is a bit poor as compared to siliceous based aggregate because of the dissociation of calcium carbonate.

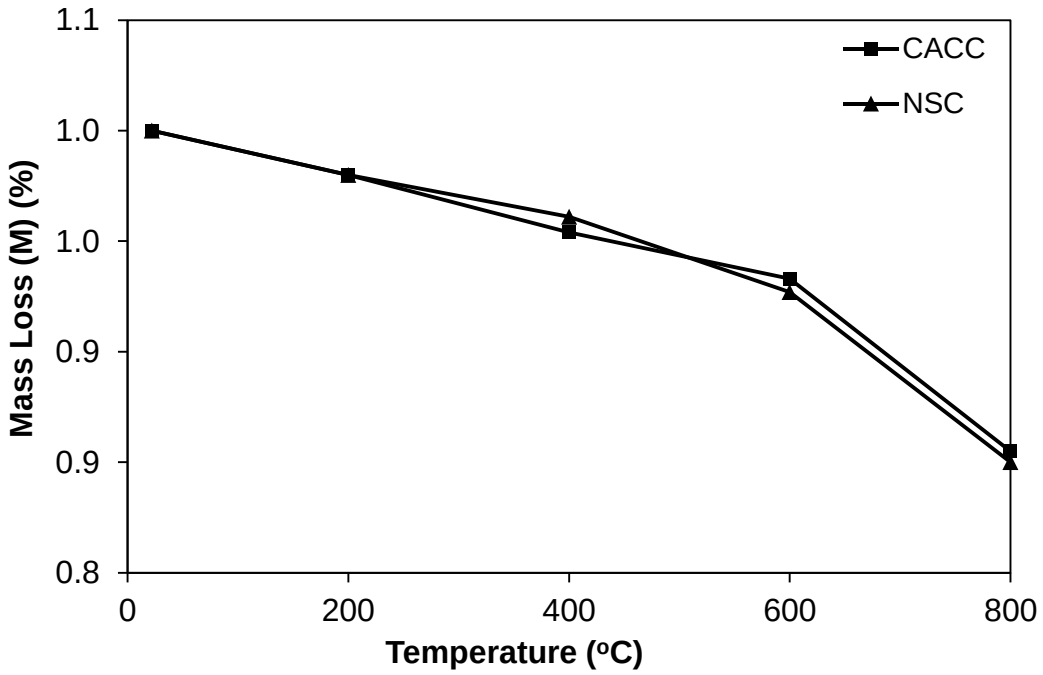

Figure 4.26 – Measured residual mass loss of CACC and NSC

It is observed, that mass loss is minimal in case of both types of concrete up to 600°C, which is attributed to easy loss of moisture form NSC and CACC due to their permeable microstructure. Further, a minor difference of 1% is also observed at 800°C which can be linked to the physical and chemical changes taking place in NSC at such a high temperature resulting in the loss of moss.

4.3.6.1 Calcium Aluminate Cement Concrete

The mass loss trend observed by CACC as shown in Figure 4.26 is similar to that of NSC, which confirms that reliance of mass loss majorly on the type of aggregate instead of the type of concrete. However, more compact and less permeable concrete like high performance concrete (HPC) does not allow the moisture to evaporate easily resulting in the higher thermal properties as compared to NSC (Khaliq, 2012). However, CACC is more permeable and allows the moisture to evaporate easily resulting in the loss of mass similar to NSC. Further, the chemical changes that take place inside limestone aggregate present in CACC after 600°C, causes reduction in density and increases the porosity of CACC. This results in the sudden major mass loss of 14% at 800°C.

4.3.6.2 Normal Strength Concrete

As shown in Figure 4.26, minor loss in mass around 7% was observed till 600°C which shows the similar trend observed by (Kodur and Sultan, 2003) for calcareous aggregate. The mass loss evaluated for carbonate type aggregate shows a different trend up to 600°C, in which

around 15.5% mass was lost due to dissociation of dolomite (Khaliq, 2012). However, sudden higher mass loss of 15% was observed after 600°C, which is due to the loss of hidden moisture present in the carbonate aggregate that vaporizes at temperature above 600°C due to dissociation of limestone. In addition to that, this chemical reaction also causes micro cracking and increase in porosity of the concrete. Further, this loss can also be linked with the loss of mass observed in NSC made with calcareous aggregate which is around 17% (Hu et al., 1993).

4.4 Relations for Material Properties

4.4.1 General

The material properties measured at elevated temperatures give physical constants in the form of mathematical equations that can be used as mathematical models for the fire resistance calculations of RC structures. The use of such equations facilitates the application of these mathematical models for the calculation of fire resistance rating of structures (Lie, 1992). Data produced from the material property tests is employed to develop mechanical property relations for both NSC and CACC against both types of test (unstressed and residual) procedures. These properties are expressed in the form of empirical relations over temperature range of 23-800°C in the form of empirical relations for compressive strength, splitting tensile strength, elastic modulus, compressive toughness and mass loss. These empirical relations are produced using linear regression. For regression analysis, measured material properties were used as a dependent variable with temperature as their independent variable. The method of linear fitting i.e. by fitting a straight line through a set of data points is used for estimating the parameters of any linear variable (Wackerly et al., 2008).

The least-squares procedure is used for fitting a line through a set of 'n' data points where it is desired that the differences between the observed values and corresponding points on the fitted line should be minimum. A convenient way to accomplish this, and one that yields estimators with good properties, is to minimize the sum of squares of the standard deviations from the fitted line. In this case the deviations are actually the errors in the values of material properties (dependent variable) given by the values of temperatures (independent variables) and to reduce these deviations in the dependent values sum of the square of error is utilized.

Commercial software, Minitab (Mintab, 2015) is used to carry out the regression analysis of the material properties experimental results. For regression analysis, coefficient of determination R^2 is evaluated to define the accuracy of the best fit equation (Wackerly et al., 2008). This R^2 is actually the proportion of total variation in the response that is explained by

the variable prediction in a simple regression model and represents the proportion of the sum of square of error about their independent variable. The values of coefficient determination R^2 obtained for unstressed material property equations lie between 0.75-0.97 whereas for residual material property equation it lies between 0.78-0.97 that represents a reasonably high confidence level in light of high variability in material properties.

The variation of compressive strength ($f'_c{}^T$), splitting tensile strength ($f'_t{}^T$), elastic modulus ($E_s{}^T$), compressive toughness ($T_c{}^T$) and mass loss (M) with temperature for NSC as per unstressed test procedure can be related by coefficient (α_T), which represents the ratio of respective strength at target temperature to that of room temperature (f'_c, f'_t, E_s, T_c and M_0) given by Equation 4.1 to 4.5. Similarly, the variation of these material properties with temperature for CACC as per unstressed test procedure can be related by coefficient (β_T) representing ratio of respective strength at target temperature to that of room temperature (f'_c, f'_t, E_s, T_c and M_0) given by Equation 4.6 to 4.10. In case of residual test procedure, the ratio of respective strength at target temperature to that of room temperature ($f'_{c\,res}$, $f'_{t\,res}$, $E_{s\,res}$, $T_{c\,res}$ and $M_{0\,res}$) for NSC is denoted by ($\alpha_{T\,res}$) whereas for CACC it is denoted by ($\beta_{T\,res}$) given in Equation 4.11 to 4.15 and 4.16 to 4.20, respectively. The strength reduction coefficient ratio (α_T, β_T, $\alpha_{T\,res}$, $\beta_{T\,res}$) equation for compressive strength, splitting tensile strength, elastic modulus, compressive toughness and mass loss is given as:

$$\alpha_{T,compressive} = \frac{f'_c{}^T}{f'_c} \tag{4.1}$$

$$\alpha_{T,tensile} = \frac{f'_t{}^T}{f'_t} \tag{4.2}$$

$$\alpha_{T,modulus} = \frac{E_s{}^T}{E_s} \tag{4.3}$$

$$\alpha_{T,toughness} = \frac{T_c{}^T}{T_c} \tag{4.4}$$

$$\alpha_{T,massloss} = \frac{M}{M_0} \tag{4.5}$$

$$\beta_{T,compressive} = \frac{f'_c{}^{T}}{f'_c} \tag{4.6}$$

$$\beta_{T,tensile} = \frac{f'_t{}^{T}}{f'_t} \tag{4.7}$$

$$\beta_{T,\mathrm{modulus}} = \frac{E_s{}^{T}}{E_s} \tag{4.8}$$

$$\beta_{T,toughness} = \frac{T_c{}^{T}}{T_c} \tag{4.9}$$

$$\beta_{T,massloss} = \frac{M}{M_0} \tag{4.10}$$

$$\alpha_{T\,res,\,compressive} = \frac{f'_c{}^{T}{}_{res}}{f'_{c\ res}} \tag{4.11}$$

$$\alpha_{T\,res,\,tensile} = \frac{f'_t{}^{T}{}_{res}}{f'_{t\ res}} \tag{4.12}$$

$$\alpha_{T\,res,\,\mathrm{modulus}} = \frac{E_s{}^{T}{}_{res}}{E_{s\ res}} \tag{4.13}$$

$$\alpha_{T\,res,\,toughness} = \frac{T_c{}^{T}{}_{res}}{T_{c\ res}} \tag{4.14}$$

$$\alpha_{T\,res,\,massloss} = \frac{M_{res}}{M_{0\ res}} \tag{4.15}$$

$$\beta_{T\,res,\,compressive} = \frac{f'_c{}^{T}{}_{res}}{f'_{c\ res}} \tag{4.16}$$

$$\beta_{T\,res,\,tensile} = \frac{f'_{t}{}^{T}{}_{res}}{f'_{t\ res}} \tag{4.17}$$

$$\beta_{T\,res,\,\mathrm{modulus}} = \frac{E_{s}{}^{T}{}_{res}}{E_{s\ res}} \tag{4.18}$$

$$\beta_{T\,res,\,toughness} = \frac{T_{c}{}^{T}{}_{res}}{T_{c\ res}} \tag{4.19}$$

$$\beta_{T\,res,\,massloss} = \frac{M_{res}}{M_{0\ res}} \tag{4.20}$$

In light of the equations, Table 4.1 and 4.2 shows the unstressed values of reduction factors α_T and β_T for compressive strength, splitting tensile strength, elastic modulus, toughness and mass loss for NSC and CACC respectively. Similarly, Table 4.3 and 4.4 shows the residual values of reduction factors $\alpha_{T\,res}$ and $\beta_{T\,res}$ for compressive strength, splitting tensile strength, elastic modulus, toughness and mass loss for NSC and CACC, respectively. Further, Equations 4.21 till 4.75 will show the equations to evaluate the values of respective material properties at different temperatures for both NSC and CACC. These equations are obtained by placing a trend line in such a way that the sum of the squares of deviation from the test data is minimal as shown in Figure 4.27 till 4.36.

Table 4.1– Unstressed Compressive strength, tensile strength, elastic modulus, toughness and mass loss reduction factors (α_T) at different temperatures for NSC

Temperature (°C)	**Reduction Factor (α_T)**				
	Compressive Strength ($f'_c{}^T$)	**Splitting Tensile Strength ($f'_t{}^T$)**	**Elastic Modulus ($E_s{}^T$)**	**Compressive Toughness ($T_c{}^T$)**	**Mass Loss (M)**
23	1	1	1	1	1
200	0.83	0.93	0.88	1.23	0.98
400	0.77	0.74	0.55	1.18	0.94
600	0.51	0.40	0.28	0.91	0.92
800	0.22	0.17	0.06	0.80	0.83

Table 4.2– Unstressed Compressive strength, tensile strength, elastic modulus, toughness and mass loss reduction factors (β_T) at different temperatures for CACC

Temperature (°C)	Reduction Factor (β_T)				
	Compressive Strength ($f'_c{}^T$)	Splitting Tensile Strength ($f'_t{}^T$)	Elastic Modulus ($E_s{}^T$)	Compressive Toughness ($T_c{}^T$)	Mass Loss (M)
23	1	1	1	1	1
200	0.94	0.87	0.69	0.74	0.98
400	0.76	0.68	0.68	0.93	0.95
600	0.58	0.43	0.51	0.78	0.93
800	0.29	0.21	0.14	0.57	0.87

Table 4.3– Residual Compressive strength, tensile strength, elastic modulus, toughness and mass loss reduction factors ($\alpha_{T\,res}$) at different temperatures for NSC

Temperature (°C)	Reduction Factor ($\alpha_{T\,res}$)				
	Compressive Strength ($f'_c{}^T{}_{res}$)	Splitting Tensile Strength ($f'_t{}^T{}_{res}$)	Elastic Modulus ($E_s{}^T{}_{res}$)	Compressive Toughness ($T_c{}^T{}_{res}$)	Mass Loss (M_{res})
23	1	1	1	1	1
200	0.95	0.9	0.82	1.48	0.98
400	0.78	0.71	0.61	1.23	0.96
600	0.46	0.37	0.27	0.79	0.93
800	0.22	0.15	0.09	0.78	0.85

Table 4.4– Residual Compressive strength, tensile strength, elastic modulus, toughness and mass loss reduction factors ($\beta_{T\,res}$) at different temperatures for CACC

Temperature (°C)	Reduction Factor ($\beta_{T\,res}$)				
	Compressive Strength ($f'_c{}^T{}_{res}$)	Splitting Tensile Strength ($f'_t{}^T{}_{res}$)	Elastic Modulus ($E_s{}^T{}_{res}$)	Compressive Toughness ($T_c{}^T{}_{res}$)	Mass Loss (M_{res})
23	1	1	1	1	1
200	0.85	0.87	1.07	1.05	0.98
400	0.72	0.64	0.83	0.92	0.95
600	0.57	0.42	0.47	0.81	0.93
800	0.28	0.22	0.13	0.54	0.85

4.4.2 Relations for Compressive Strength

4.4.2.1 Unstressed Test Data

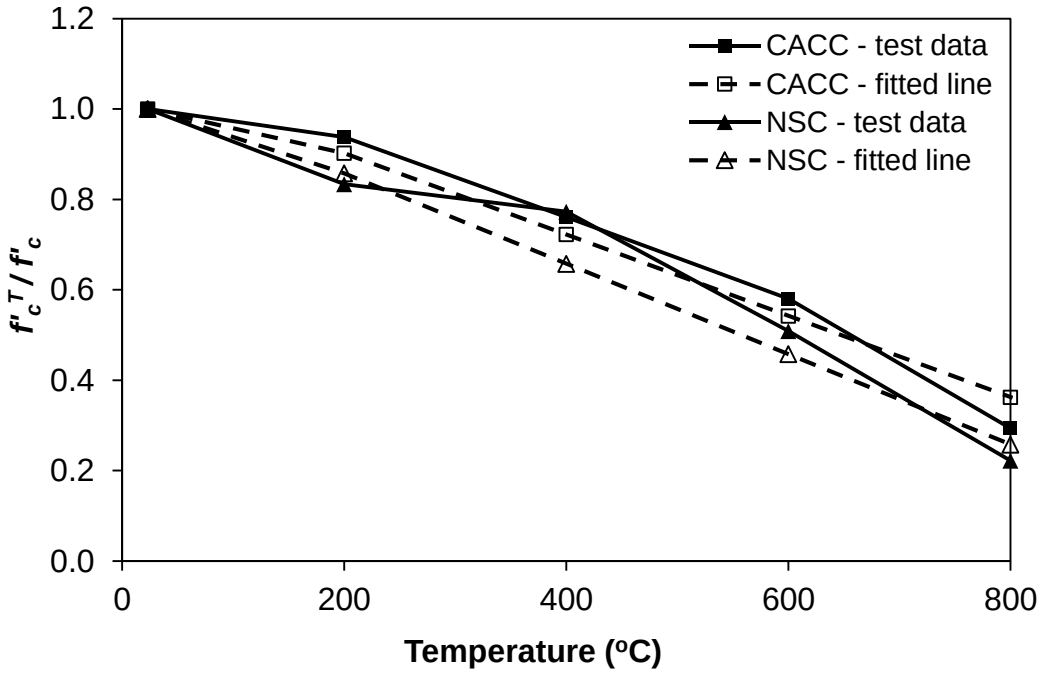

Figure 4.27 – Unstressed compressive test data of CACC and NSC compared with regression based fitted line

- **NSC**

$$\alpha_{T,compressive} = 1.0 \qquad 23°C \qquad (4.21)$$

$$\alpha_{T,compressive} = 1.058 - 0.001T \qquad 23°C < T \leq 800°C \qquad (4.22)$$

- **CACC**

$$\beta_{T,compressive} = 1.0 \qquad 23°C \qquad (4.23)$$

$$\beta_{T,compressive} = 1.082 - 0.0009T \qquad 23°C < T \leq 800°C \qquad (4.24)$$

4.4.2.2 Residual Test Data

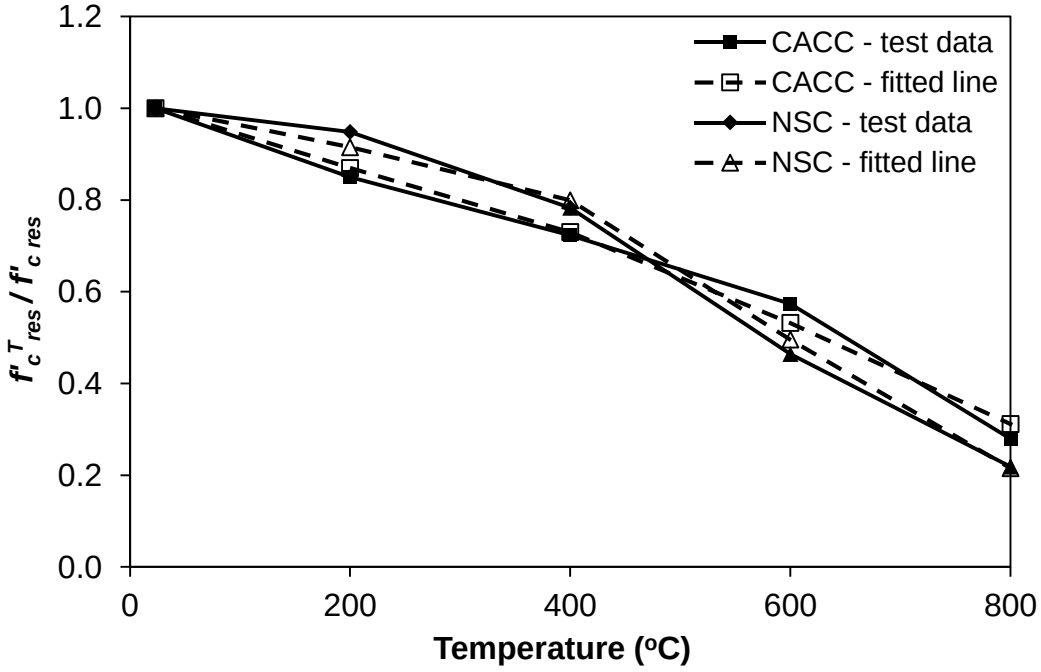

Figure 4.28 – Residual compressive test data of CACC and NSC compared with regression based fitted line

- **NSC**

$$\alpha_{T\,res,\text{compressive}} = 1.0 \qquad 23°C \qquad (4.25)$$

$$\alpha_{T\,res,\text{compressive}} = 1.032 - 0.0006T \qquad 23°C < T \leq 400°C \qquad (4.26)$$

$$\alpha_{T\,res,compressive} = 1.3353 - 0.0014T \qquad 400°C < T \leq 800°C \qquad (4.27)$$

- **CACC**

$$\beta_{T\,res,compressive} = 1.0 \qquad 23°C \qquad (4.28)$$

$$\beta_{T\,res,compressive} = 1.0097 - 0.0007T \qquad 23°C < T \leq 400°C \qquad (4.29)$$

$$\beta_{T\,res,compressive} = 1.1916 - 0.0011T \qquad 400°C < T \leq 800°C \qquad (4.30)$$

4.4.3 Relations for Splitting Tensile Strength

4.4.3.1 Unstressed Test Data

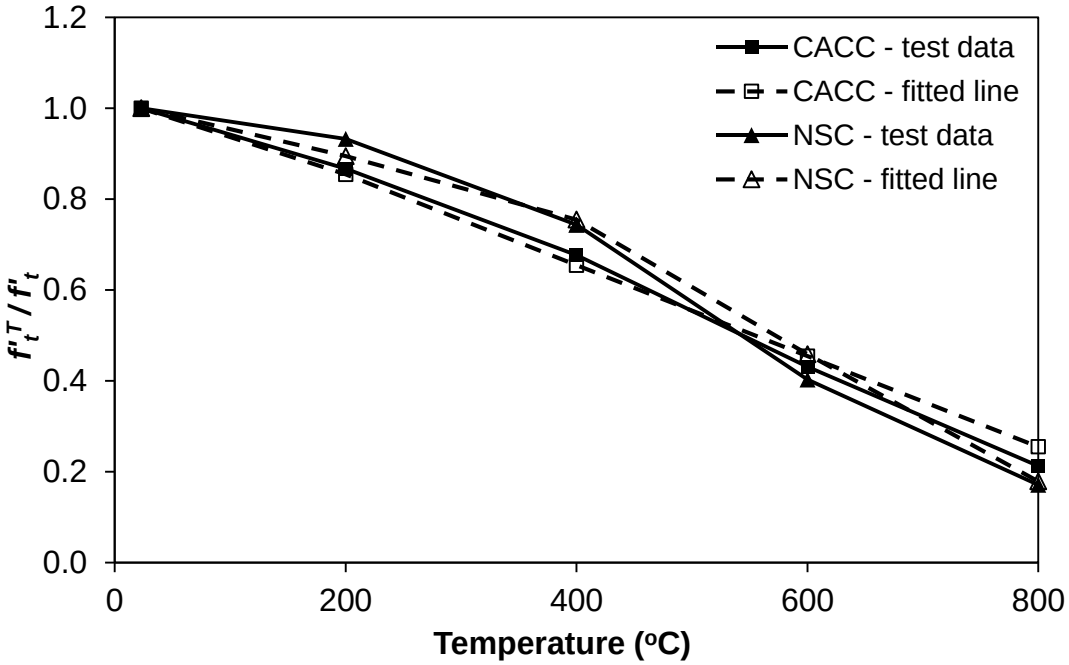

Figure 4.29 – Unstressed splitting tensile strength test data of CACC and NSC compared with regression based fitted line

- **NSC**

$$\alpha_{T,tensile} = 1.0 \qquad 23°C \qquad (4.31)$$

$$\alpha_{T,tensile} = 1.0346 - 0.0007T \qquad 23°C < T \leq 400°C \qquad (4.32)$$

$$\alpha_{T,tensile} = 1.2984 - 0.0014T \qquad 400°C < T \leq 800°C \qquad (4.33)$$

- **CACC**

$$\beta_{T,tensile} = 1.0 \qquad 23°C \qquad (4.34)$$

$$\beta_{T,tensile} = 1.054 - 0.0010T \qquad 23°C < T \leq 800°C \qquad (4.35)$$

4.4.3.2 Residual Test Data

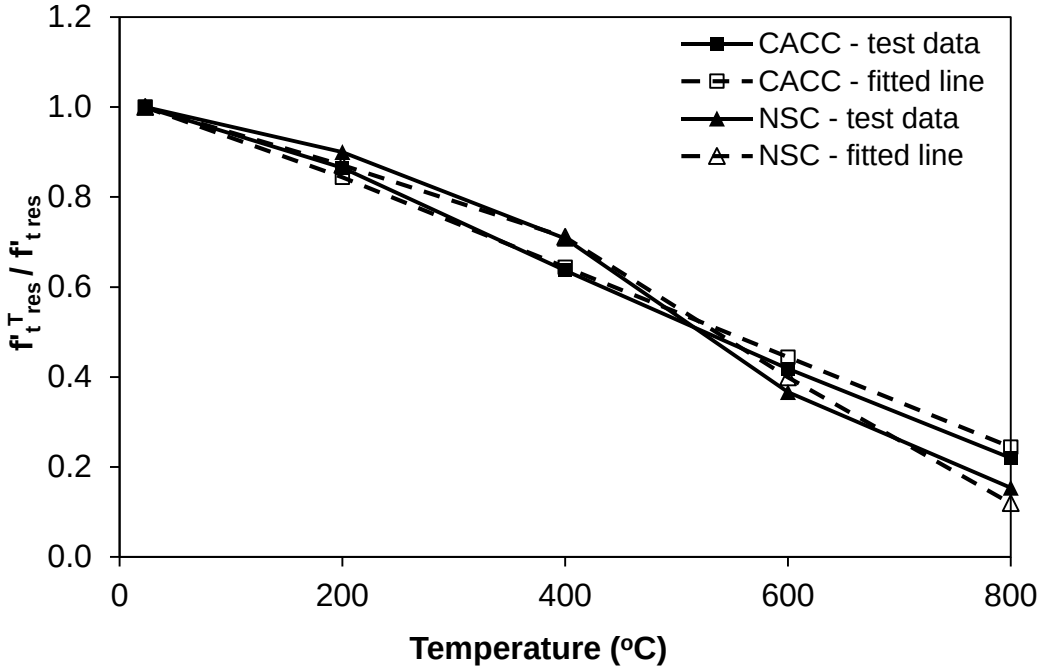

Figure 4.30 – Residual splitting tensile strength test data of CACC and NSC compared with regression based fitted line

- **NSC**

$$\alpha_{T\,res,tensile} = 1.0 \qquad 23°C \qquad (4.36)$$

$$\alpha_{T\,res,tensile} = 1.0311 - 0.0008T \qquad 23°C < T \leq 400°C \qquad (4.37)$$

$$\alpha_{T\,res,tensile} = 1.2392 - 0.0014T \qquad 400°C < T \leq 800°C \qquad (4.38)$$

- **CACC**

$$\beta_{T\,res,tensile} = 1.0 \qquad 23°C \qquad (4.39)$$

$$\beta_{T\,res,tensile} = 1.044 - 0.001T \qquad 23°C < T \leq 800°C \qquad (4.40)$$

4.4.4 Relations for Modulus of Elasticity

4.4.4.1 Unstressed Test Data

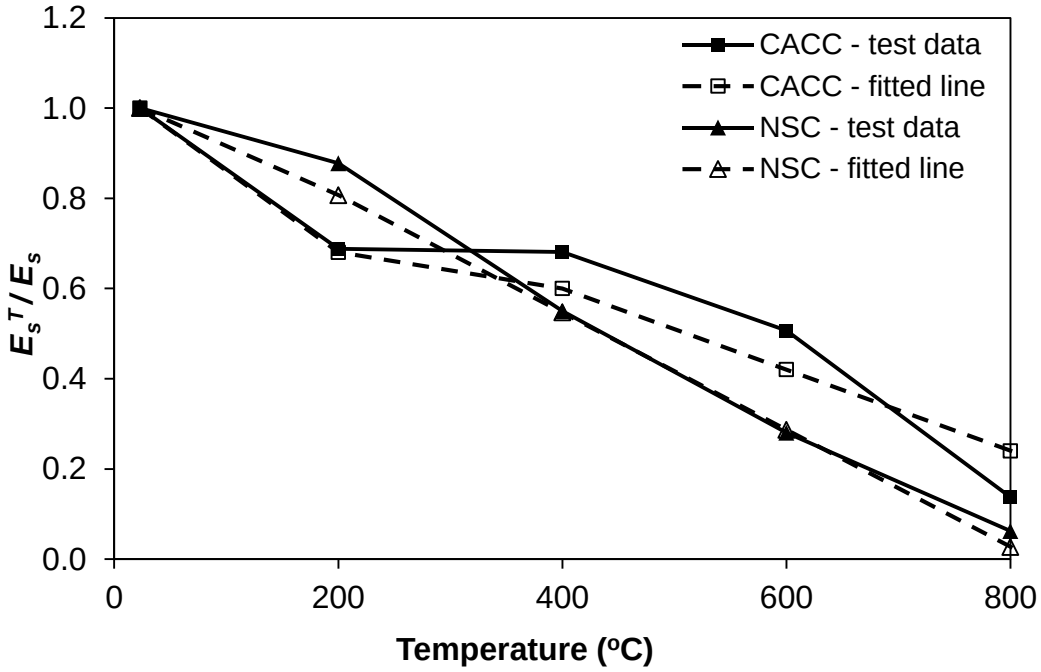

Figure 4.31 – Unstressed elastic modulus test data of CACC and NSC compared with regression based fitted line

- **NSC**

$$\alpha_{T,\text{modulus}} = 1.0 \qquad 23°C \qquad (4.41)$$

$$\alpha_{T,\text{modulus}} = 1.0671 - 0.0013T \qquad 23°C < T \leq 800°C \qquad (4.42)$$

- **CACC**

$$\beta_{T,\text{modulus}} = 1.0 \qquad 23°C \qquad (4.43)$$

$$\beta_{T,\text{modulus}} = 1.041 - 0.0018T \qquad 23°C < T \leq 200°C \qquad (4.44)$$

$$\beta_{T,\text{modulus}} = 0.9602 - 0.0009T \qquad 200°C < T \leq 800°C \qquad (4.45)$$

4.4.4.2 Residual Test Data

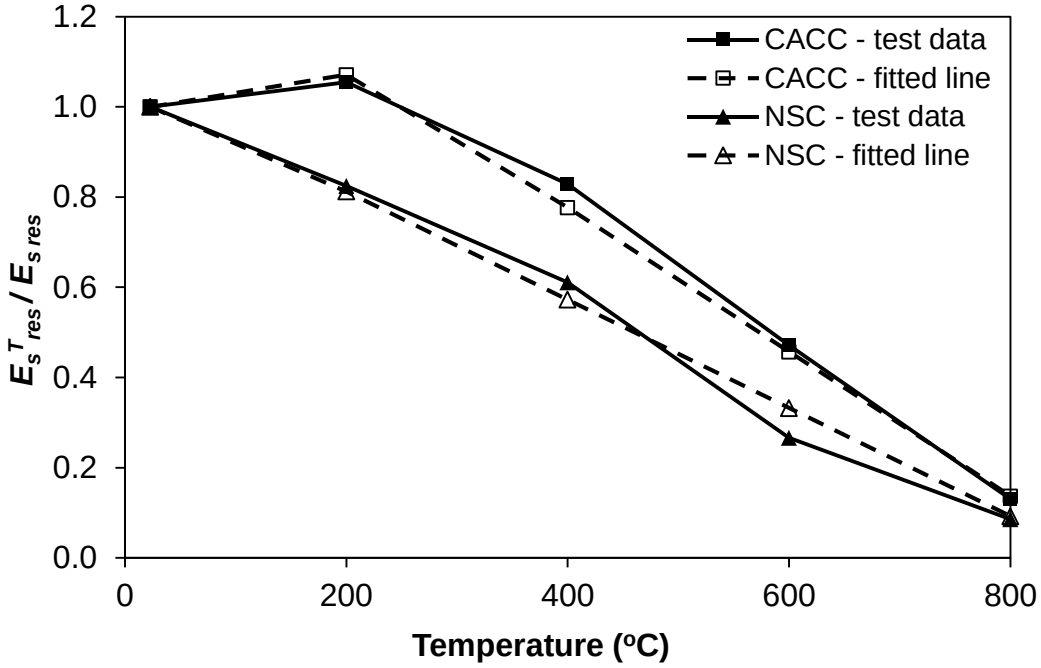

Figure 4.32 – Residual elastic modulus test data of CACC and NSC compared with regression based fitted line

- **NSC**

$$\alpha_{T\,res,\text{modulus}} = 1.0 \qquad 23°C \qquad (4.46)$$

$$\alpha_{T\,res,\text{modulus}} = 1.052 - 0.0012T \qquad 23°C < T \leq 800°C \qquad (4.47)$$

- **CACC**

$$\beta_{T\,res,\text{modulus}} = 1.0 \qquad 23°C \qquad (4.48)$$

$$\beta_{T\,res,\text{modulus}} = 0.9912 + 0.0004T \qquad 23°C < T \leq 200°C \qquad (4.49)$$

$$\beta_{T\,res,\text{modulus}} = 1.417 - 0.0016T \qquad 200°C < T \leq 800°C \qquad (4.50)$$

4.4.5 Relations for Compressive Toughness

4.4.5.1 Unstressed Test Data

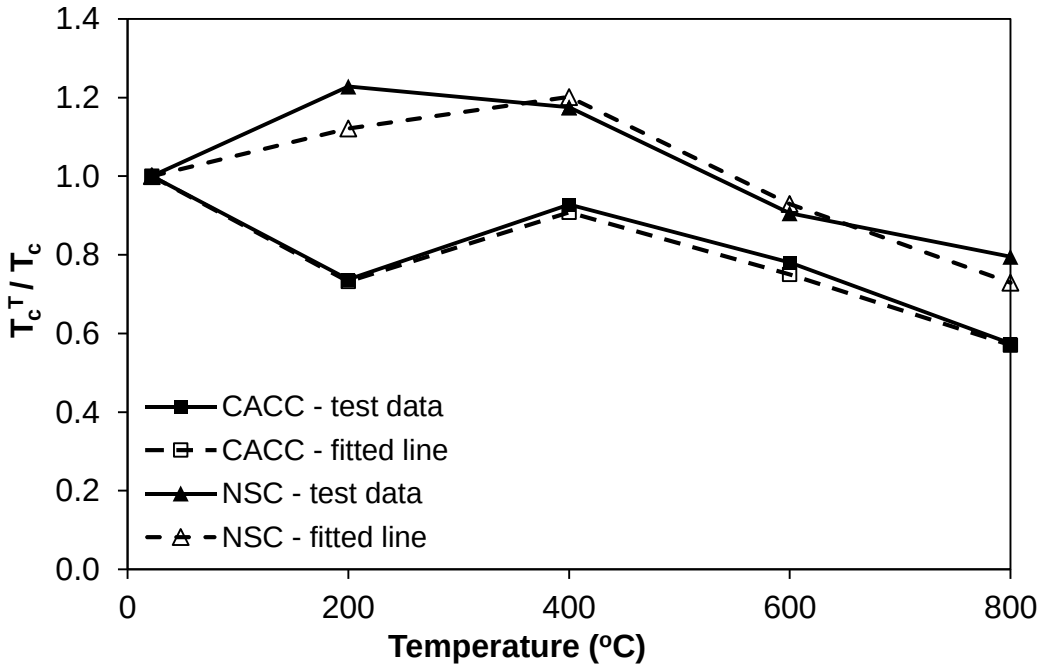

Figure 4.33 – Unstressed compressive toughness test data of CACC and NSC compared with regression based fitted line

- **NSC**

$$\alpha_{T,toughness} = 1.0 \qquad 23°C \qquad (4.51)$$

$$\alpha_{T,toughness} = 1.0415 + 0.0004T \qquad 23°C < T \leq 400°C \qquad (4.52)$$

$$\alpha_{T,toughness} = 1.53 - 0.0010T \qquad 400°C < T \leq 800°C \qquad (4.53)$$

- **CACC**

$$\beta_{T,toughness} = 1.0 \qquad 23°C \qquad (4.54)$$

$$\beta_{T,toughness} = 1.0324 - 0.0015T \qquad 23°C < T \leq 200°C \qquad (4.55)$$

$$\beta_{T,toughness} = 0.548 + 0.0009T \qquad 200°C < T \leq 400°C \qquad (4.56)$$

$$\beta_{T,toughness} = 1.29 - 0.0009T \qquad 400°C < T \leq 800°C \qquad (4.57)$$

4.4.5.2 Residual Test Data

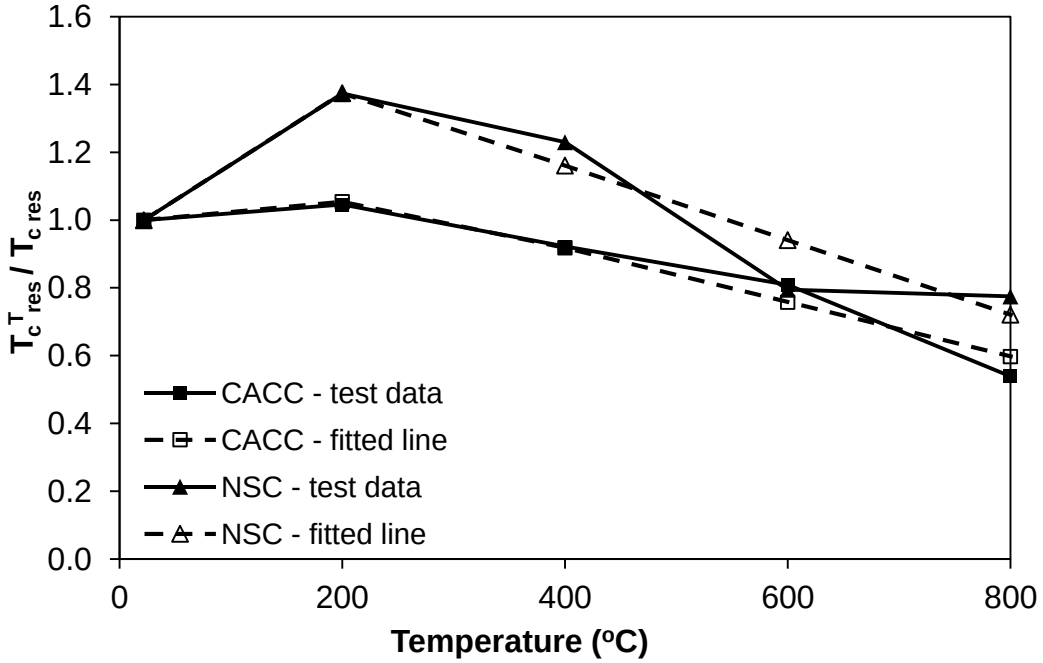

Figure 4.34 – Residual compressive toughness test data of CACC and NSC compared with regression based fitted line

- **NSC**

$$\alpha_{T\,res,toughness} = 1.0 \qquad 23°C \qquad (4.58)$$

$$\alpha_{T\,res,toughness} = 0.954 + 0.0021T \qquad 23°C < T \leq 200°C \qquad (4.59)$$

$$\alpha_{T\,res,toughness} = 1.60 - 0.0011T \qquad 200°C < T \leq 800°C \qquad (4.60)$$

- **CACC**

$$\beta_{T\,res,toughness} = 1.0 \qquad 23°C \qquad (4.61)$$

$$\beta_{T\,res,toughness} = 0.9943 + 0.0003T \qquad 23°C < T \leq 400°C \qquad (4.62)$$

$$\beta_{T\,res,toughness} = 1.238 - 0.0008T \qquad 400°C < T \leq 800°C \qquad (4.63)$$

4.4.6 Relations for Mass Loss

4.4.6.1 Unstressed Test Data

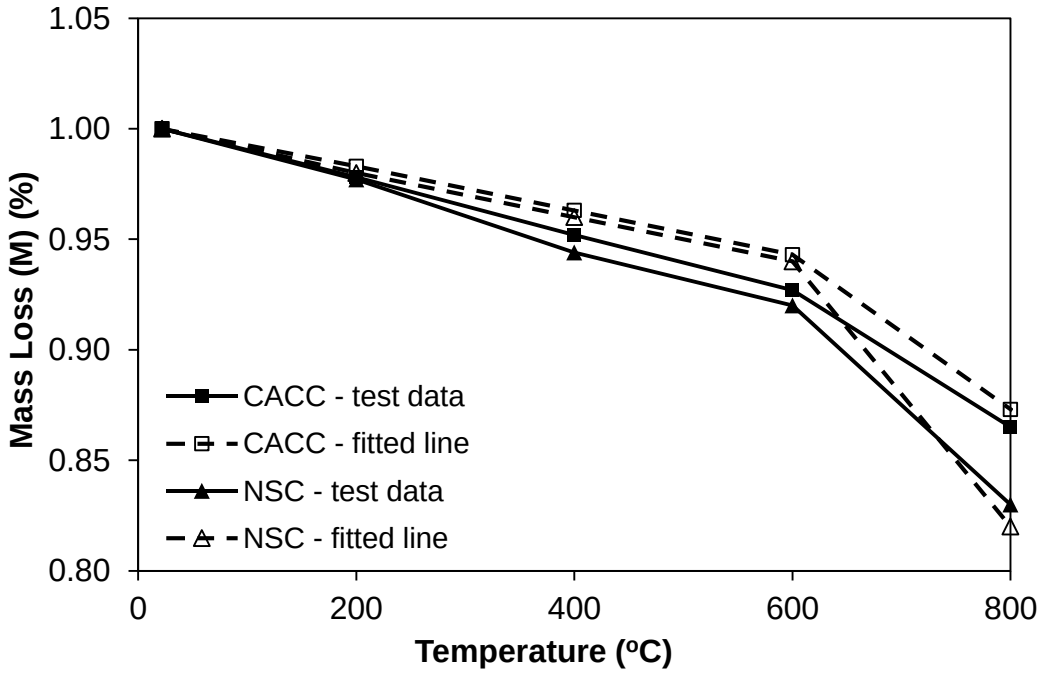

Figure 4.35 – Unstressed mass loss data versus regression based fitted line for CACC and NSC

- **NSC**

$$\alpha_{T,mass\,loss} = 1.0 \qquad 23°C \qquad (4.64)$$

$$\alpha_{T,mass\,loss} = 1.0004 - 0.0001T \qquad 23°C < T \leq 600°C \qquad (4.65)$$

$$\alpha_{T,mass\,loss} = 1.22 - 0.0005T \qquad 600°C < T \leq 800°C \qquad (4.66)$$

- **CACC**

$$\beta_{T,mass\,loss} = 1.0 \qquad 23°C \qquad (4.67)$$

$$\beta_{T,mass\,loss} = 1.003 - 0.0001T \qquad 23°C < T \leq 600°C \qquad (4.68)$$

$$\beta_{T,mass\,loss} = 1.113 - 0.0003T \qquad 600°C < T \leq 800°C \qquad (4.69)$$

4.4.6.2 Residual Test Data

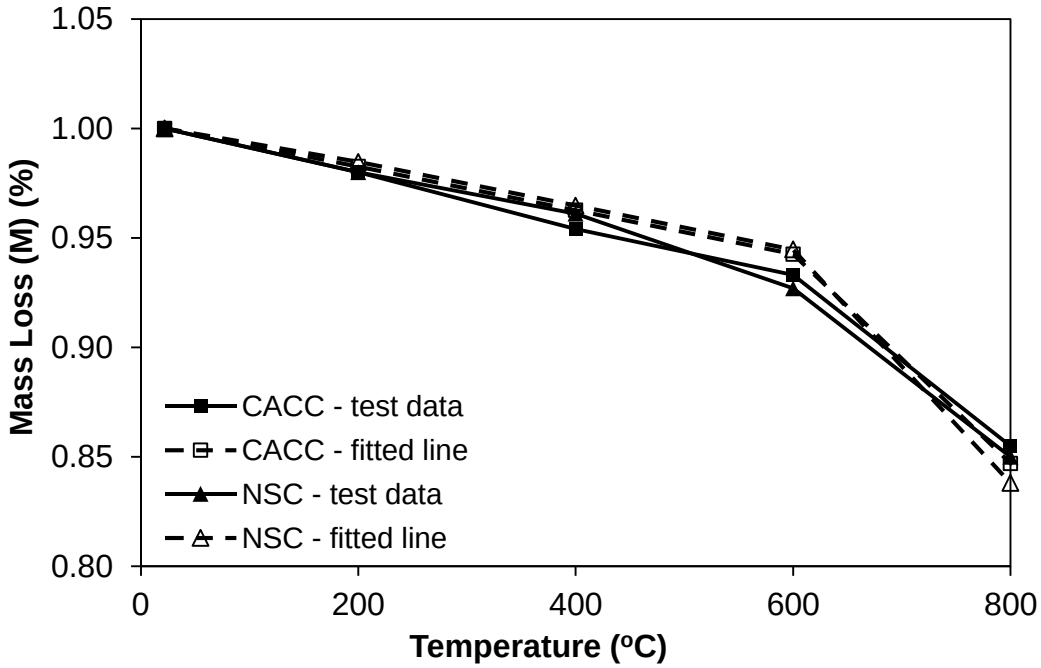

Figure 4.36 – Residual mass loss data versus regression based fitted line for CACC and NSC

- **NSC**

$$\alpha_{T\,res,mass\,loss} = 1.0 \qquad 23°C \qquad (4.70)$$

$$\alpha_{T\,res,mass\,loss} = 1.0047 - 0.0001T \qquad 23°C < T \leq 600°C \qquad (4.71)$$

$$\alpha_{T\,res,mass\,loss} = 1.158 - 0.0004T \qquad 600°C < T \leq 600°C \qquad (4.72)$$

- **CACC**

$$\beta_{T\,res,mass\,loss} = 1.0 \qquad 23°C \qquad (4.73)$$

$$\beta_{T\,res,mass\,loss} = 1.0026 - 0.0001T \qquad 23°C < T \leq 600°C \qquad (4.74)$$

$$\beta_{T\,res,mass\,loss} = 1.167 - 0.0004T \qquad 600°C < T \leq 800°C \qquad (4.75)$$

4.5 Visual Assessment of Heated Concretes

The visual assessment of both CACC and NSC cylinders includes observation of color change, cracking and crazing. This physical assessment started after removing the samples from the furnace i.e. after exposing the samples to elevated temperatures. Color of the sample provides

a broader view of the exposure temperature. Whereas the crazing and cracking caused by dehydration of cement paste, the loss of physical bound water and disintegration of the concrete microstructure, were general signs of temperature to which concrete has been exposed (Georgali and Tsakiridis, 2005).

4.5.1 Calcium Aluminate Cement Concrete (CACC)

The visual inspection of CACC showed different response as compare to NSC. No major color change was observed in the cylinders till 400°C. However, at 600°C minor change in color, from dark brownish to light brownish, was observed in CACC. Minor surface cracks were also observed but they are not in abundance as shown in Figure 4.37(a). However, at 800°C some major changes take place in CACC cylinder starting with the change of color from light brownish to light grayish. In addition to that, some longitudinal cracks parallel to the axis of cylinder were also observed strengthening the argument that high temperature is the main cause of loss in strength and durability in concrete at elevated temperatures, as shown in Figure 4.37(b). These major physical changes were due to the chemical changes taking place inside the concrete microstructure which includes, the conversion of some metastable phases to cubical stable phases at 600°C, the loss of physically and chemically bound water by breaking the hydraulic bond inside the concrete microstructure causing an increase in porosity and decrease in strength (Martinović et al., 2012).

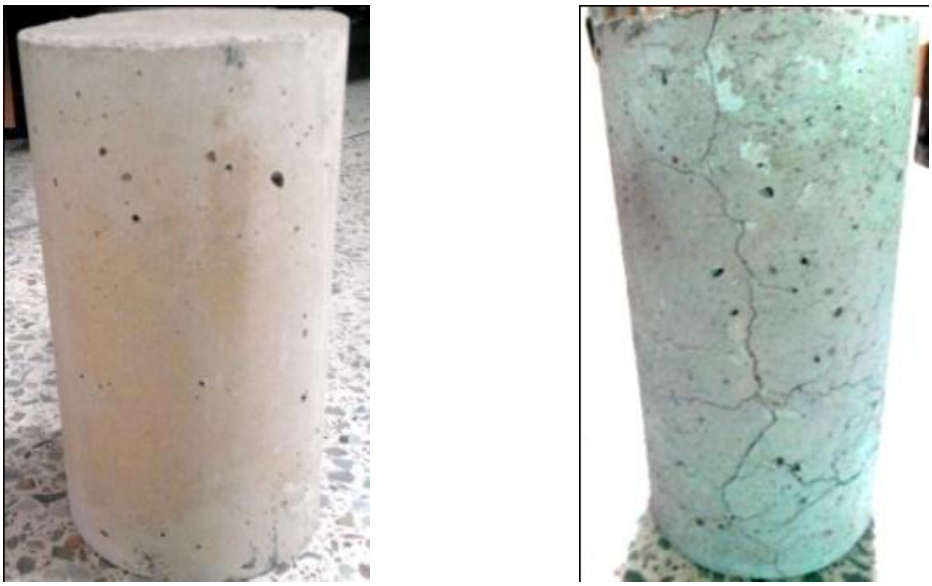

(a) 600°C (b) 800°C

Figure 4.37 – CACC cylinders after exposure to elevated temperatures

4.5.2 Normal Strength Concrete (NSC)

On heating the concrete above 300°C, changes in color of the concrete takes place. In the beginning, color of the concrete observed was light grayish with a dense surface and no micro or macro cracks on the surface till 400°C. However, after the exposure of NSC to 600°C the color of the NSC changes from light grayish to dark, in addition to that surface crazing and minor cracks were also observed as shown in Figure 4.38(a). These surface crazing and minor cracks can be attributed to the differing thermal expansions causing weakening of the bond between aggregate and cement paste (Castillo and Duranni, 1990). In addition to that, disintegration of CH crystal to CaO after 500°C also takes place, making this a critical temperature ranges for the NSC (Mehta and Monteiro, 2006). Figure 4.38(b) shows the NSC cylinder after being exposed to 800°C. After exposure to this temperature the NSC cylinder experienced some major widening of these cracks extending up to the surface of the concrete. In addition, the color change from dark grayish to light brownish (buff) was also observed. These major cracks were due to the generation of minor cracks after 400°C as a result of dehydration of concrete. These randomly oriented cracks also contribute in loss of compressive and tensile strength of concrete at elevated temperatures.

(a) 600°C (b) 800°C

Figure 4.38 – NSC cylinders after exposure to elevated temperatures

4.6 Scanning Electron Microscope (SEM) Imaging

The shape, size and morphology of the hydration products are quite important parameter for understanding the material properties of both types of concrete specimens at elevated temperature. In addition, these images also tell us about effect of temperature on the level of porosity and morphological changes in the microstructure of concrete specimens. SEM images were taken for both NSC and CACC at two resolutions of 5μm and 1μm samples to study the changes in microstructure of both concrete types, exposed to different temperature ranging from room temperature to 600°C.

4.6.1 Calcium Aluminate Cement (CACC)

SEM images of CACC samples after exposure to elevated temperature ranging from 23°C to 600°C can be seen in Figure 4.39. As discussed by Scrivener et al. (1999), that with the increase in temperature the hydrates of CAC converts from metastable hydrates CAH_{10}, C_2AH_8 to stable hydrates C_3AH_6 (cubic) and AH_3 (crystalline gel). This conversion reaction results in an increase in porosity which is due to the difference in the relative volume of the phases and ultimately decreases the strength of the concrete (Mostafa et al., 2012). Figure 4.39(a), shows the microstructure of CACC at room temperature without any exposure to elevated temperature. It can be seen, that a well-developed crystalline formation can be observed with a much denser microstructure. Hexagonal plates of C_2AH_8 were also observed embedded in amorphous gel of AH_3 resulting in a denser microstructure. However, after the exposure of CACC to elevated temperature some morphological changes can be seen as shown in Figure 4.39(b) and (c). At 200°C, densely packed crystals of C_3AH_6 and AH_3 can be seen with a gel covering the pores within the hydrates making an elaborate and dense microstructure, as shown in Figure 4.39(b). Figure 4.39(c) shows the microstructure of CACC at 600°C exposure temperature. Clear dried cubic crystals of C_3AH_6 with a little amount of amorphous AH_3 gel are visible. Further it can be seen, that due to the exposure of specimen to such a high temperature the evaporation of chemically bound crystalline water takes place, which results in the creation of skeletal and empty spaces in the microstructure leading to an increase in porosity (Martinović et al., 2012). However, at 600°C microstructure of CACC still presents denser microstructure as compared to NSC with minor cracks and voids due to the presence of AH3 gel covering the C_3AH_6 crystals. In addition, these morphological changes depicting the conversion of metastable to stable hydrates can be seen in Fig. 4.39 and validates the changes in material properties of CACC with the increase in temperatures.

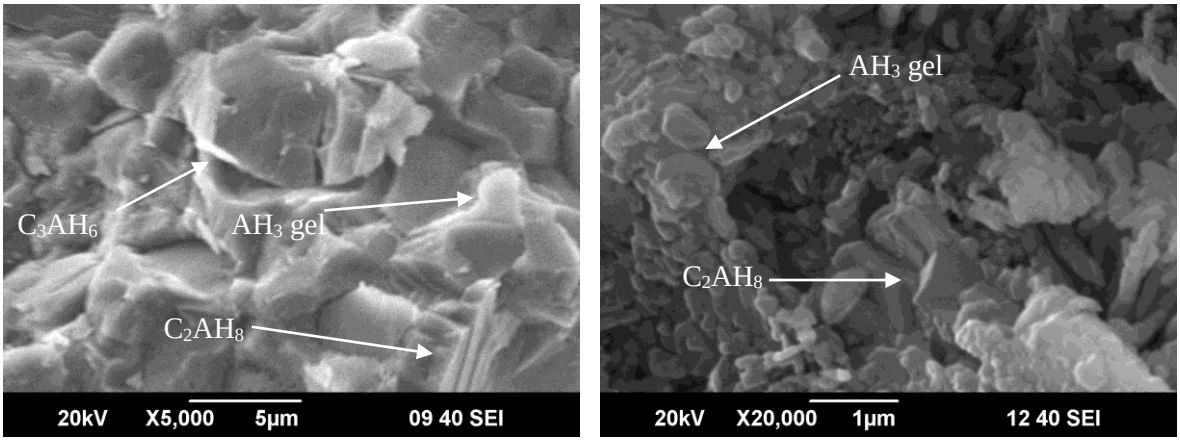

(a) 23°C

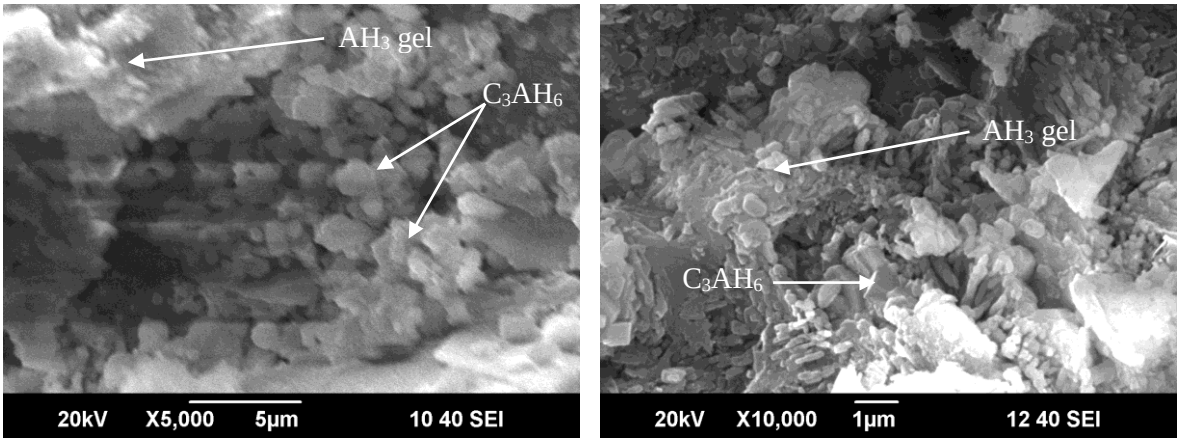

(b) 200°C

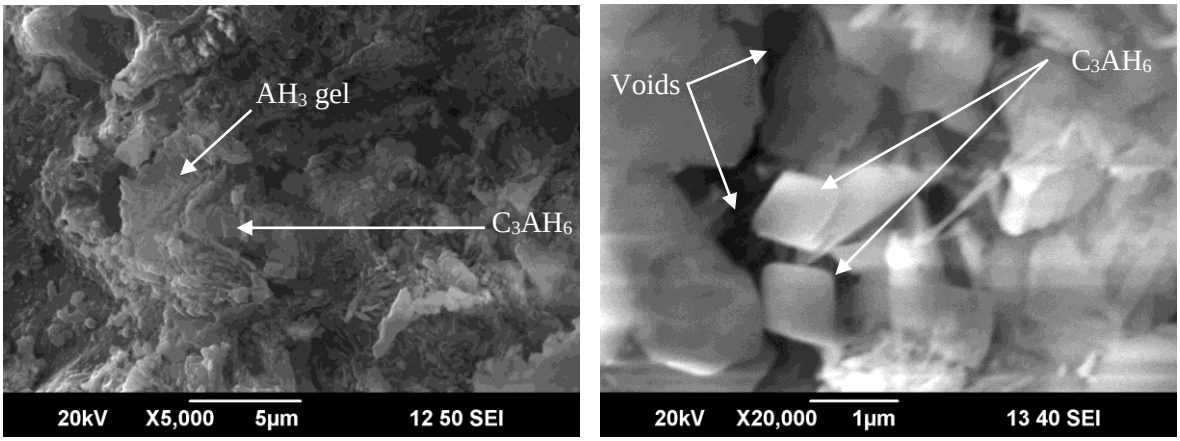

(b) 600°C

Figure 4.39 – SEM images of CACC after exposure to different temperatures

4.6.2 Normal Strength Concrete (NSC)

Figure 4.40 shows the SEM images of NSC samples after being exposed to elevated temperature to observe the microstructure. Figure 4.40(a) shows, the image of the sample with

a very dense microstructure at room temperature. By studying this figure, nearly amorphous C-S-H gel along with CH crystals in the form of tightly packed grains can be clearly seen. In addition, slender needle like crystals of ettringite were also observed in the NSC sample. Further, at 200°C the microstructure of NSC is fuller and dense with closely knit ettringite present within C-S-H gel in addition to some pores as shown in Figure 4.40(b). Further, no major deterioration was observed in the microstructure at this temperature. However, at 600°C a major cavity can be seen in the microstructure of the concrete as shown in Figure 4.40(c), which shows a weak microstructure with appearance of pores and micro cracks. In addition, CH crystals were also not observed in the microstructure due to the disintegration of CH crystals into CaO at such a high temperature, due to the loss of chemically bonded water (Eglinton, 1998). No significant damage to the cement paste was observed at this temperature. However, increase in cracking and pore structure intensifying can be seen representing the partial decomposition of the formed phases, which confirms the loss of compressive and splitting tensile strength of concrete at this temperature.

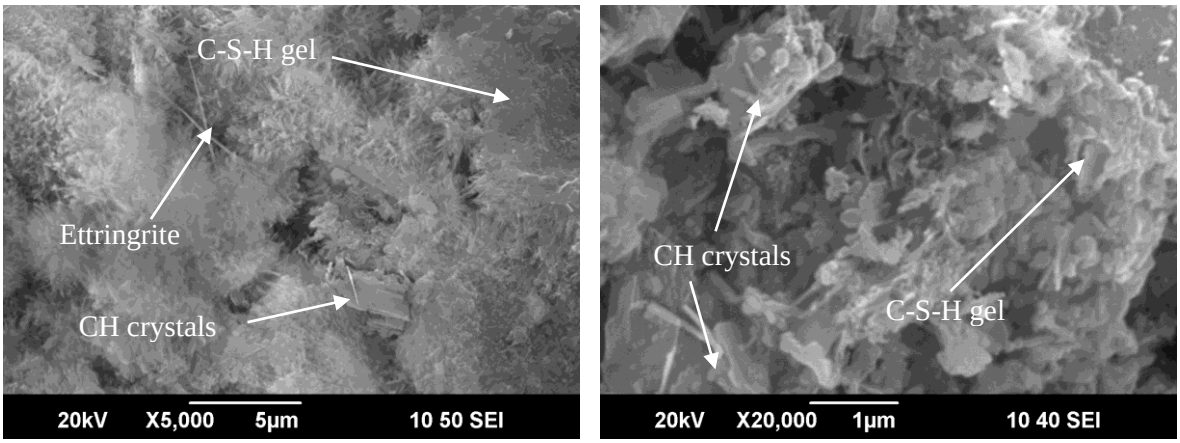

(a) 23°C

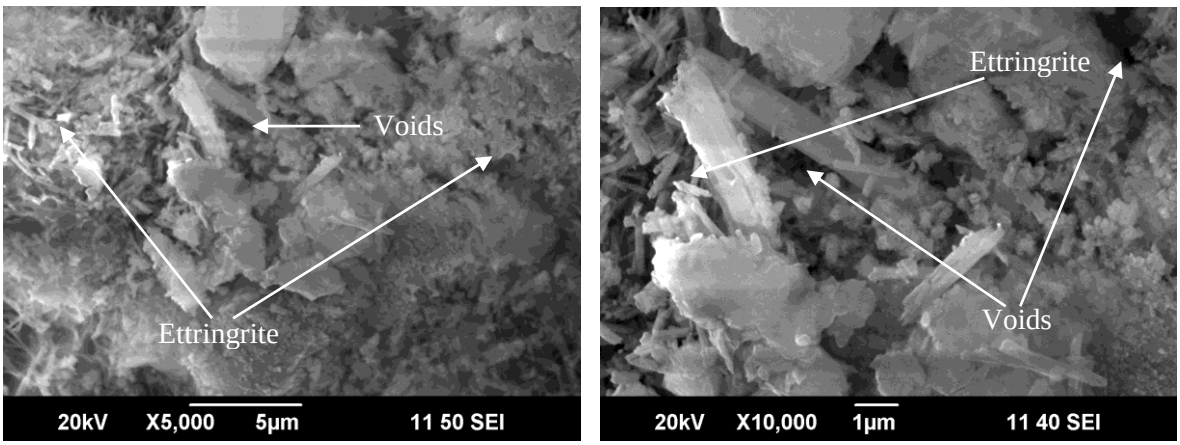

(b) 200°C

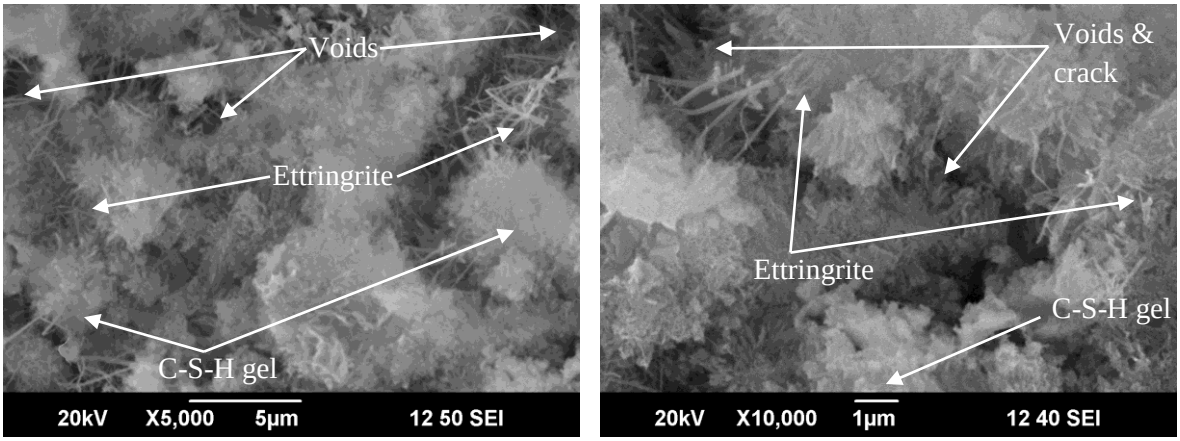

(c) 600°C

Figure 4.40 – SEM images of NSC after exposure to different temperatures

4.7 Analysis of Results

In this section, the unstressed material properties of CACC and NSC are compared with residual material properties which include compressive strength, tensile strength, elastic modulus, stress-strain curve, toughness and mass loss. The performance of all these properties is evaluated as a function of elevated temperatures ranging from 23°C till 800°C.

4.7.1 Comparison of Unstressed and Residual Compressive Strength

The effect of temperature on the compressive strength of NSC and CACC for two test conditions namely, unstressed and residual can be observed in Figure 4.41. It can be seen, that with the increase in temperature the strength keep on decreasing for both types of concrete irrespective of the test method. However, for NSC the loss of strength is sudden beyond 400°C which is due to the dehydration of the cement paste resulting in the gradual disintegration. Further it is observed, that the residual strength is slightly lower than the unstressed strength for both types of concrete, which conforms to results reported by Abrams (1971), and Castillo and Duranni (1990). This additional loss in strength can be attributed to mechanical damage resulting from self-stabilizing stresses induced in the concrete as a result of transient heat flow when it is allowed to cool down to room temperature (Abramowicz and Kowalski, 2007; Kowalski, 2010). There is very little difference between unstressed and residual compressive strength of CACC which can be attributed to slow cooling of specimens after exposure to elevated temperatures (Abramowicz and Kowalski, 2005). However in NSC, during cooling CH crystals which are decomposed into CaO at around 600°C, again convert to CH and result in expansion of volume (Karokoc, 2013). This expansion attributes to additional loss in residual strength of NSC through weakening of aggregate-paste bond at elevated temperatures, which

is not the case with CACC. Due to this reason, the absolute strength of NSC observed at 600°C is much lesser than CACC. However, at higher temperatures, this additional degradation is almost the same as both the systems have suffered a major loss in terms of deterioration of microstructure.

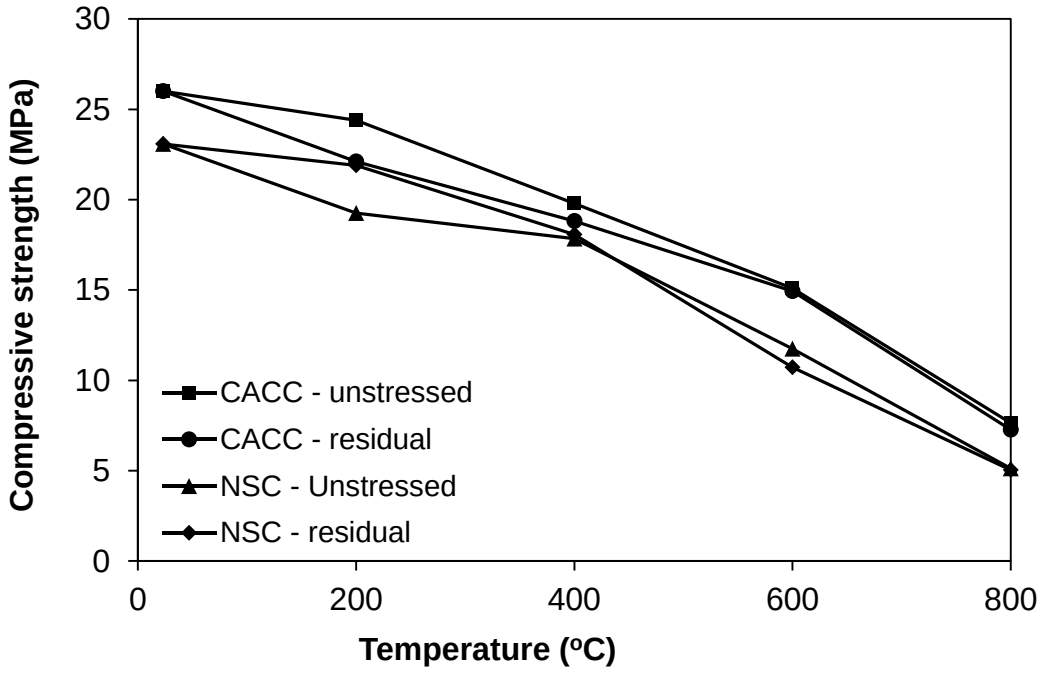

Figure 4.41 – Comparison of absolute values of compressive strength against temperature

Further, Figure 4.42 shows the relative strength of CACC and NSC against elevated temperatures for residual and unstressed test programs. It can be clearly seen that the relative strength follows the same trend as that of absolute values. Further, in case of NSC, the difference between the residual and unstressed strength at 200°C is around 12% of the strength at room temperature, which is due to the stabilization of strength in case of residual while cooling down to room temperature, which is not the case in unstressed test where sample is tested hot. However, at 400°C this difference is reduced to minimum as a result of dissociation of CH crystals around 400°C (Kowalski, 2010). Similarly in case of CACC, the difference between unstressed and residual strength is around 9% at 200°C which keeps on decreasing till 600°C with just a difference of 1% at this temperature. This additional degradation of strength in case of residual test for CACC is due to the additional thermal stresses inside the system trying to self-equilibrate it. However, at higher temperature this additional degradation is almost the same as both the systems have suffered a major loss in terms of degradation and dissociation of microstructure as observed in microscopic images (see Figure 4.38, 4.39 & 4.40).

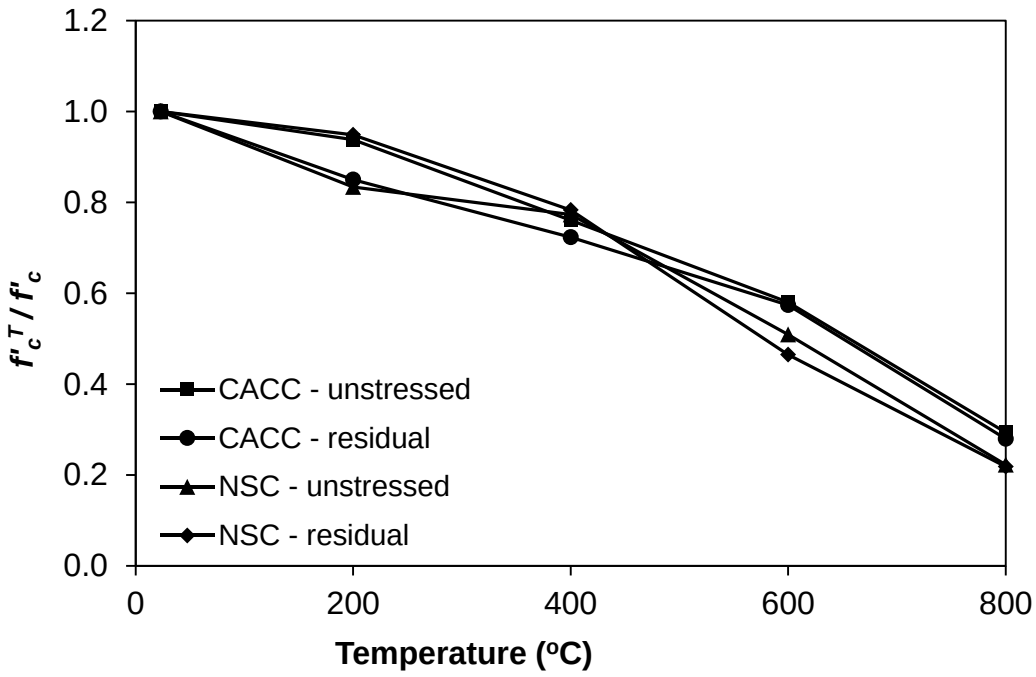

Figure 4.42 – Relative compressive strength values against elevated temperature

4.7.2 Comparison of Unstressed and Residual Splitting Tensile Strength

The tensile strength of concrete depends upon the ease of crack propagation under tensile load. When concrete is exposed to elevated temperatures, the microstructure of the concrete deteriorates resulting in the loss of tensile strength of concrete which is governed by micro cracking (Khaliq and Kodur, 2011). Figure 4.43, shows the loss of tensile strength of NSC and CACC as a function of temperature for unstressed and residual test method. It can be clearly observed that, with the increase in temperature both types of concrete suffer a major loss in their tensile strength. However, the absolute tensile strength of CACC is much higher than NSC at all levels of elevated temperatures. Further, the difference between the tensile strength of NSC for residual and unstressed test varies between 2-3% throughout the temperature range with the maximum difference around 3.5% at 400°C. In addition, the tensile strength of NSC drops suddenly beyond 400°C in both the cases due to the increase in micro cracking after 400°C. Similarly, in case of CACC the tensile strength varies throughout the temperature range with the maximum difference between the two test procedures at 400°C which is around 4%, as shown in Figure 4.43. This additional degradation of residual tensile strength is due to the thermal stresses induced in the microstructure of concrete while self-equilibrating (Abramowicz and Kowalski, 2005). However, this difference in the loss of tensile strength reduces to almost 0.5% at 800°C the microstructure is almost degraded, which is attributed to the dissociation and disintegration of limestone aggregate.

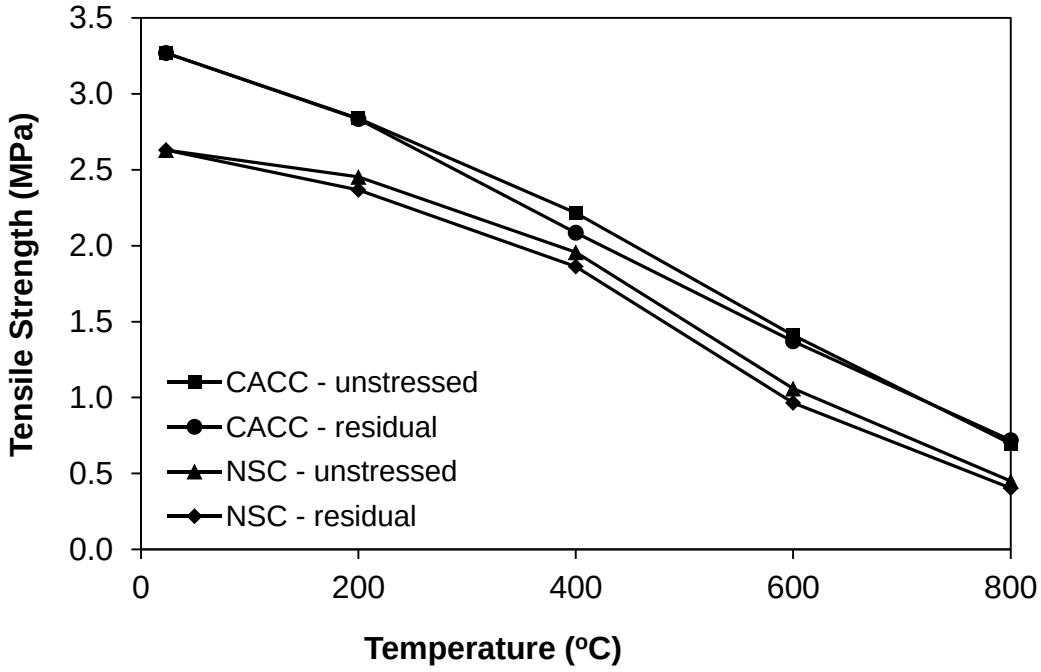

Figure 4.43 – Comparison of absolute tensile strength against different levels of temperature

The relative splitting tensile strength of NSC and CACC for unstressed and residual test follows similar trend to its absolute strength as shown in Figure 4.44. It can be seen that the loss in the strength in case of CACC is gradual till the end unlike NSC, which drops suddenly after 400°C. This loss in strength is linked with the degradation of microstructure at different levels of elevated temperature. However, the loss observed in CACC is steadier as compared to NSC which confirms the improved microstructure, as validated by SEM images. Further, after 600°C the loss in tensile strength is reduced to minimum for both the test procedures, which is due to the dissociation and disintegration of calcium carbonate present in limestone aggregate. This results in just 15-17% retention of tensile strength in NSC at 800°C as compared to 21-22% in case of CACC, as shown in Figure 4.44.

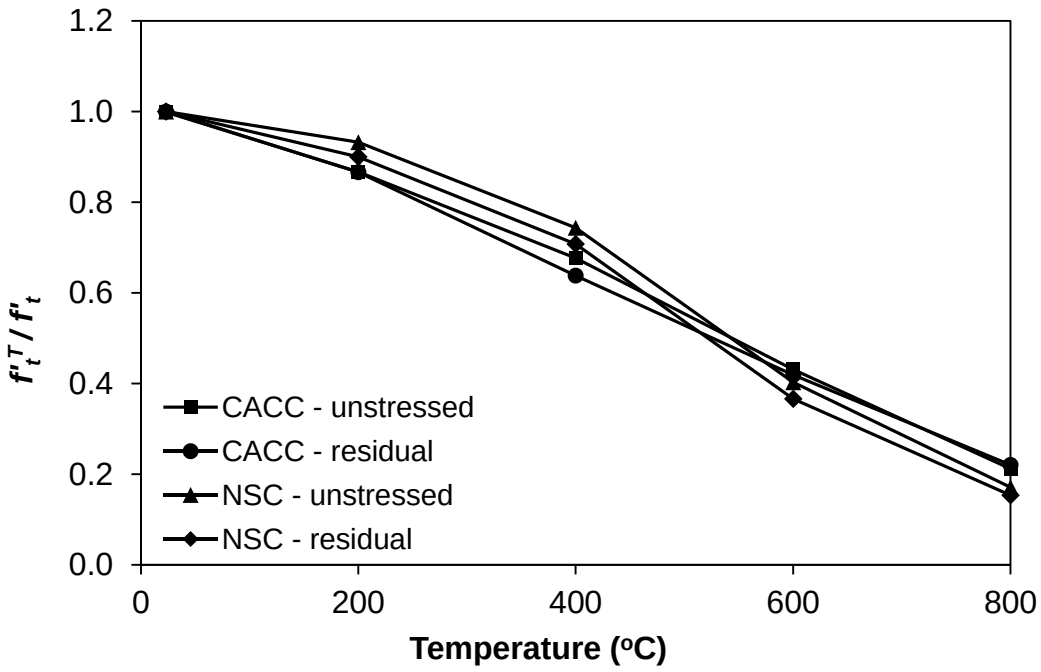

Figure 4.44 – Comparison of relative tensile strength at different elevated temperatures

4.7.3 Comparison of Unstressed and Residual Elastic Modulus

The trend of elastic modulus with respect to increase in temperature for NSC and CACC can be observed from Figure 4.45 and 4.46. The absolute values of unstressed and residual elastic modulus can be compared for NSC and CACC in Figure 4.45. It can be seen, that modulus of elasticity of both NSC and CACC decreases with an increase in temperature, with an absolute elastic modulus of both at 800°C is almost the same. This loss in elastic modulus in the beginning up to 400°C is linked with the dehydration of the cement paste resulting in the degradation of the bond between paste and aggregate (Castillo and Duranni, 1990). Further, after 400°C there are major physical and chemical changes which take place in both types of concrete microstructure, resulting in a major drop in the stiffness of the concrete. These chemical changes include the dehydration of the concrete microstructure in the beginning till 400°C, after that till 600°C dissociation of CH crystals in case of NSC takes place unlike CACC where major dehydration takes place after the phase transformation to stable hydrates. However, around 800°C the decarbonation of limestone aggregate and cement paste is the main reason behind the sudden drop in the elastic modulus of concrete (Kowalski, 2010).

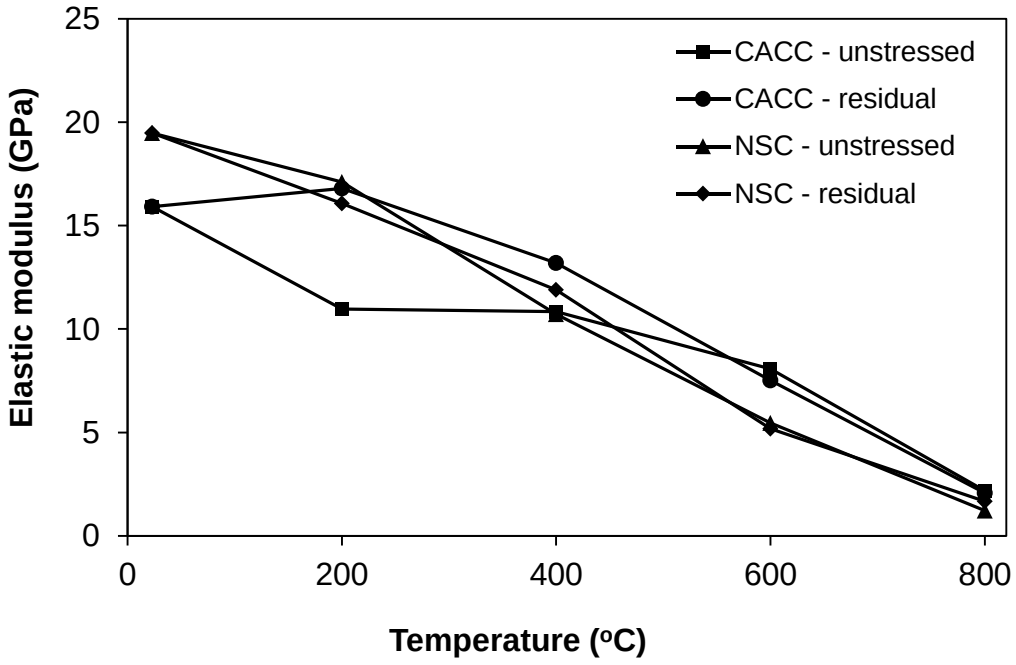

Figure 4.45 – Comparison of absolute unstressed and residual modulus of elasticity as a function of temperature

As observed in Figure 4.46, which represents the relative modulus of elasticity of NSC and CACC as a function of temperature for unstressed and residual test, it is seen that the trend followed by CACC is a bit different as compared for NSC for both the test procedures. The difference in the loss of modulus in case of NSC is almost the same with the maximum difference of 6% at 200°C and 400°C. Further, with the increase in temperature this difference reduces to just 3% at 800°C. In case of CACC, there is an increase in residual modulus of elasticity at 200°C, resulting in a major difference of 37% between the unstressed and residual modulus of elasticity. The moisture changes resulting from this reaction in CACC lead to these abnormalities at 200°C. Similar, behavior at 200°C is also observed in other high temperature properties of CACC. However, this difference reduces to just 1% at 800°C. At lower temperature, the loss of modulus is due to the evaporation and dehydration of the water present inside the microstructure of CACC, which is regained when the sample is allowed to cool down in the moist environment of relative humidity of 45-50% resulting in the regain of stiffness which is not the case in unstressed test procedure. Further, with an increase in temperature to higher temperatures, there are morphological changes inside the concrete microstructure in to more stable hydrate and the dehydration of adsorbed water within the pores which causes irreversible reduction in elastic modulus of concrete. These microscopic changes in the microstructure of concrete, results in the reduction of difference between the loss of elastic modulus, as shown in Figure 4.45 and 4.46. In addition to that, at 800°C the difference between

NSC and CACC is almost disappeared to just 4-8%, because both concrete (NSC and CACC) suffer the calcination of limestone aggregate at this temperature.

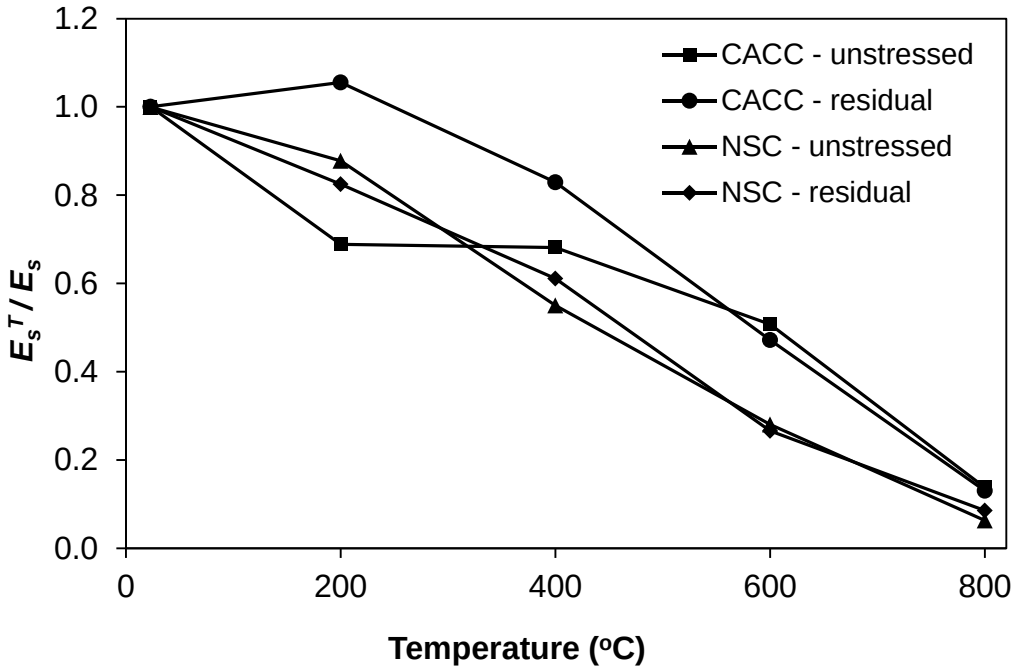

Figure 4.46– Comparison of relative unstressed and residual modulus of elasticity as a function of temperature

4.7.4 Comparison of Unstressed and Residual Stress-Strain Curves

The effect of high temperature on the stress-strain behavior of both the NSC and CACC was observed and was very much different throughout the range of test temperatures. Typical stress-strain response of NSC and CACC at different temperatures are shown in Figure 4.47 to 4.51. It is observed, that the peak load of CACC was around 12% more than that of NSC at room temperature. In addition to that, the strain at failure was around 69% higher than that of NSC. However, the response of both types of concrete at peak load did not vary significantly up to 200°C as compared to room temperature with a minor variation depending on the type of test procedure adopted. This minor variation in the load carrying capacity of NSC and CACC is majorly dependent on the loss of moisture present in the concrete at 200°C.

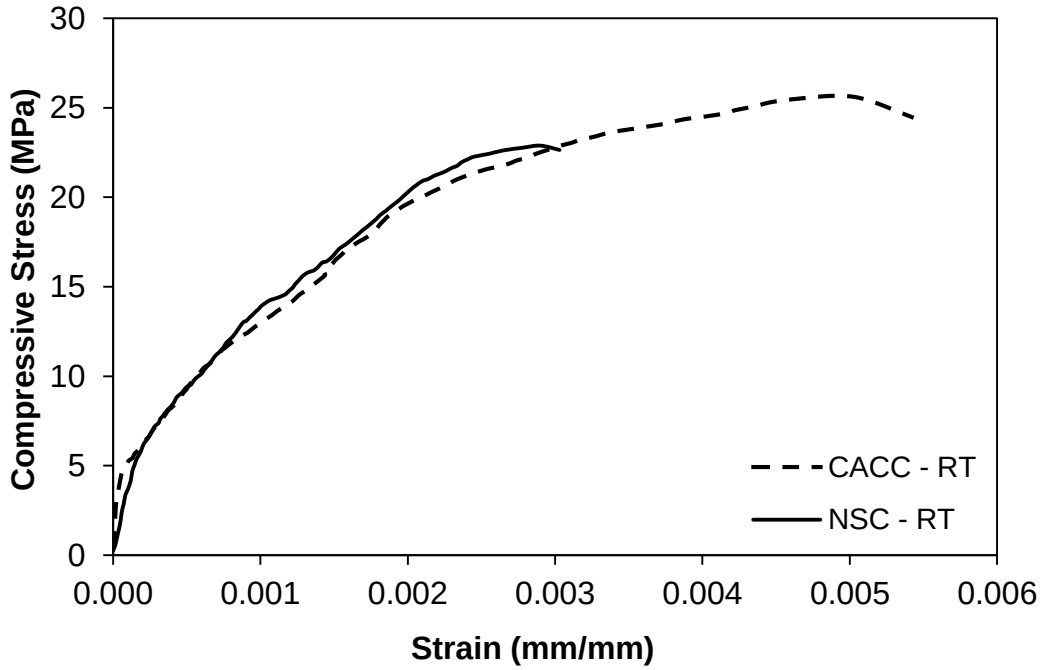

Figure 4.47 – Stress-strain response of CACC and NSC after 28 days at room temperature

In case of NSC, around 5-18% loss in stress was observed at 200°C as compared to room temperature. This variation in the load carrying capacity depends on the test procedure adopted. The overall load carrying capacity against unstressed test procedure was lower as compared to residual test procedure, unlike CACC. However, the overall performance of CACC observed is much better as compared to NSC at 200°C with a minor difference in their stress-strain response for residual and unstressed test procedure. Further, it is also observed that peak strain achieved in case of residual test at 200°C was around 37% more as compared to unstressed peak strain at the same temperature. In addition, residual peak strain was around 27% more than that of room temperature peak strain. This shows that, post-fire stress-strain response of CACC is a bit different as compared to that at elevated temperature. The residual peak stress at failure was reduced by around 10% as compared to unstressed peak stress, whereas the ductility in term of peak strain at failure is improved by 37%. This additional strength degradation is due to the thermal inertia inside the concrete which tries to self-equilibrate the system by generating additional stresses due to transient heat flow. However, if the response of CACC is evaluated in terms of stress-strain response at this temperature it is still brittle in nature.

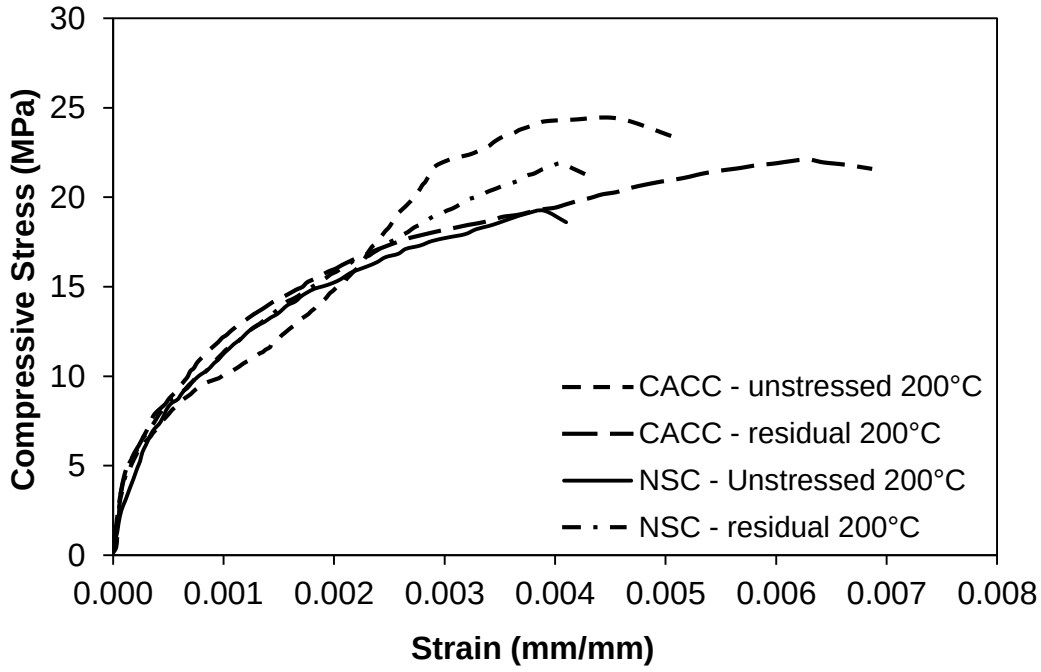

Figure 4.48 – Unstressed and residual stress-strain response of CACC and NSC at 200°C temperature

The stress-strain response of CACC and NSC for residual and unstressed test procedure at 400°C can be studied from Figure 4.49. It is evident that the overall performance of CACC is much better as compared to NSC however the difference in the strength is very minor at this temperature. The load carrying capacity of CACC is around 11% more as compared to NSC at this temperature with an additional advantage of ductility which is portrayed in terms of peak strain as shown in Figure 4.49. However, if residual performance of CACC is compared with unstressed stress-strain response, very minor difference of just 4.5% is observed in terms of peak stress and strain. This confirms that the effect of elevated temperature at and after the exposure to 400°C is almost the same with some minor difference. However, if this trend in stress-strain response of NSC and CACC is compared with that at 200°C (Figure 4.48), then decrease in load carrying capacity is observed with the increase in strain resulting in more flat curve. This flatness in stress-strain curve is attributed to the reason that at higher temperature thermal stresses are developed which causes internal micro cracking due to which the slope of the stress-strain curve was decreased i.e. ultimately the modulus of elasticity of the concrete is affected.

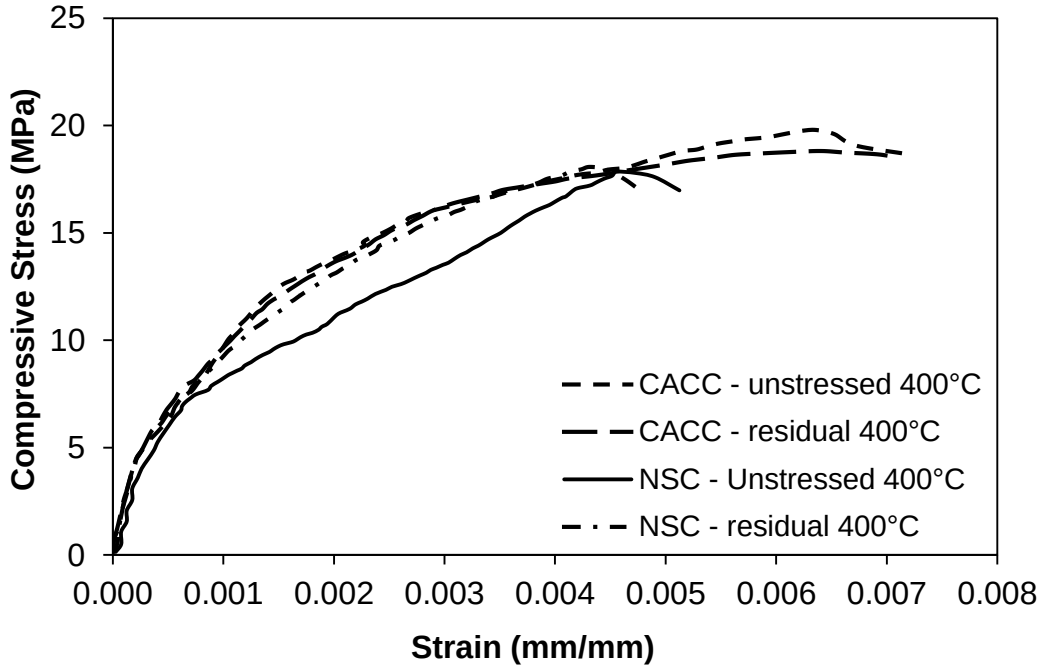

Figure 4.49 – Unstressed and residual stress-strain response of CACC and NSC at 400°C temperature

Further, at 600°C the response of NSC start degrading at a much faster rate as compared to CACC. This major degradation at elevated temperature of NSC is due to the loss of bond strength between aggregate and cement paste. The micro cracks turns into major cracks extending to the surface of the concrete. This trend can further be validated from the microscopic and visual examination of the NSC as discussed above. However, the performance of NSC at the elevated temperature is comparable with the post-fire examination in terms of stiffness as portrayed in stress-strain response. Around 9.5% additional degradation in strength, is observed in case of residual test results if compared with unstressed test due to the thermal inertia causing an additional increase in temperature after the heating is stopped (Abramowicz and Kowalski, 2007). However, if the performance of CACC is evaluated at this temperature, the presence of alumina as a binder protects the loss of stiffness with a minor cracking not extending to the surface of the concrete. The stress-strain response of both NSC and CACC can be observed in Figure 4.50, which further confirms that, the performance of CACC in terms of stress-strain is much more enhanced than NSC. This observation further substantiate that CACC has superior microstructure and therefore displays better stress-strain response even at higher temperatures. However, a minor difference stress-strain curve between the two test procedures, residual and unstressed is also observed as in NSC. This difference is due to the thermal inertia as discussed above.

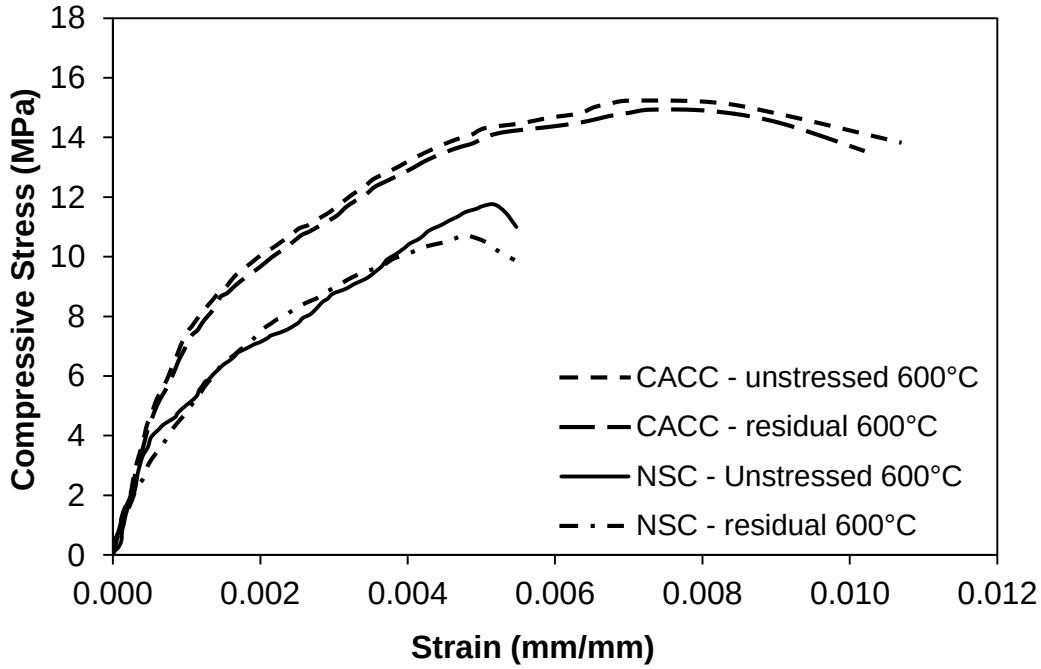

Figure 4.50– Unstressed and residual stress-strain response of CACC and NSC at 600°C temperature

The stress-strain response of NSC and CACC at 800°C for both residual and unstressed test procedure can be observed in Figure 4.51. It can be clearly seen that, both the concrete suffers major damage at this temperature resulting in the loss of stiffness in terms of modulus as observed by the flatness of the stress-strain curve. This major loss in strength is due to the calcination of the calcium carbonate present in the aggregate causing major dissolution of the concrete. However, the performance of CACC is better as compared to NSC because between temperature of 600°C and 800°C NSC also suffers from the disintegration of calcium hydroxide (CH) and calcium silicate hydrate (C-S-H) in concrete causing additional strength loss (Chan et al., 1999). Further, the peak stress and strain achieved in case of CACC is around 44-49% and 20-22% more as compared to NSC, respectively, confirming an improved microstructure. However in case of CACC, if the performance of residual test program is compared with unstressed test program in terms of stress-strain response, the CACC in unstressed condition gave much improved results for peak stress and strain with around 5.2% and 1.5% enhancement as compared to residual respectively, as shown in Figure 4.51.

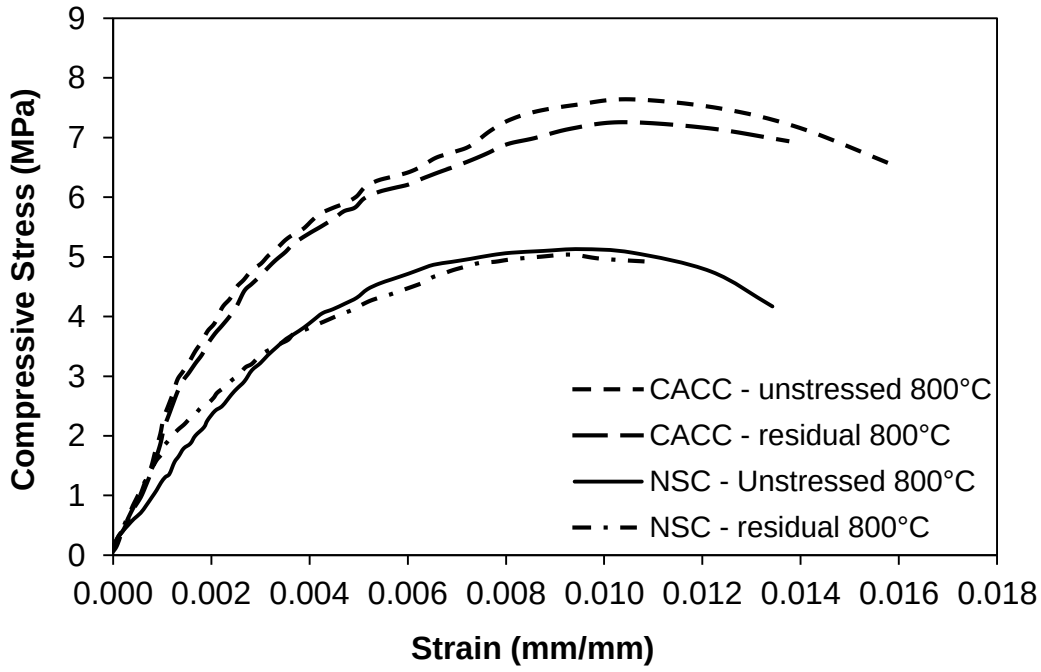

Figure 4.51 – Unstressed and residual stress-strain response of CACC and NSC at 800°C temperature

After carrying out the trend analysis and comparative study of stress-strain response of NSC and CACC at elevated temperatures, the difference between the two methods residual and unstressed test procedure was observed. The overall performance in terms of stress-strain response of CACC under unstressed condition was much better as compared to residual. This difference was due to the thermal inertia of the concrete causing additional loss in compressive strength (Kowalski, 2010). Further, the overall trend of loss of strength observed in case of CACC is much slower and gradual as compared to NSC in which an abrupt loss in strength and increase in ductility was examined after 400°C.

4.7.5 Comparison of Unstressed and Residual Compressive Toughness

The effect of elevated temperature on the energy absorbing capacity is evaluated in terms of compressive toughness for NSC and CACC. As explained earlier, toughness is a derived property and is evaluated as the area under the stress-strain curve till the complete failure of the material, so it also deviates with the variation of stress-strain response of the material. As it is observed that, the residual and unstressed compressive toughness changes with the change in temperature, so it is compared for both the test programs at different levels of temperature, as shown in Figure 4.52. The overall energy absorption capacity of CACC is much higher than NSC at all the levels of elevated temperature due to enhanced and superior microstructure. However, if it is compared for the test program adopted it is observed that, at 200°C major

variation between the energy absorbed is present. In case of NSC, there is an increase in the energy absorbed till 200°C with a maximum difference of 25% observed between residual and unstressed test procedure. However, after that this difference keeps on reducing to just 2% at 800°C. In case of CACC, there is a major difference in the energy absorbed at 200°C between the unstressed and residual test procedure. In case of unstressed test, a loss of 26% was evaluated in the toughness, unlike residual toughness where 5% increase was observed, which is due to the loss in strength with no increase in ductility. However, this increase in residual toughness is due to the major increase in ductility in terms of peak strain of around 27% with minor loss in strength due to chemical changes within the microstructure of concrete. However, afterward a regain of 19% was observed in unstressed toughness till 400°C, which is due to the increase in ductility with a minor loss in strength. After that, no major difference between the two test program results was observed till 800°C as shown in Figure 4.48.

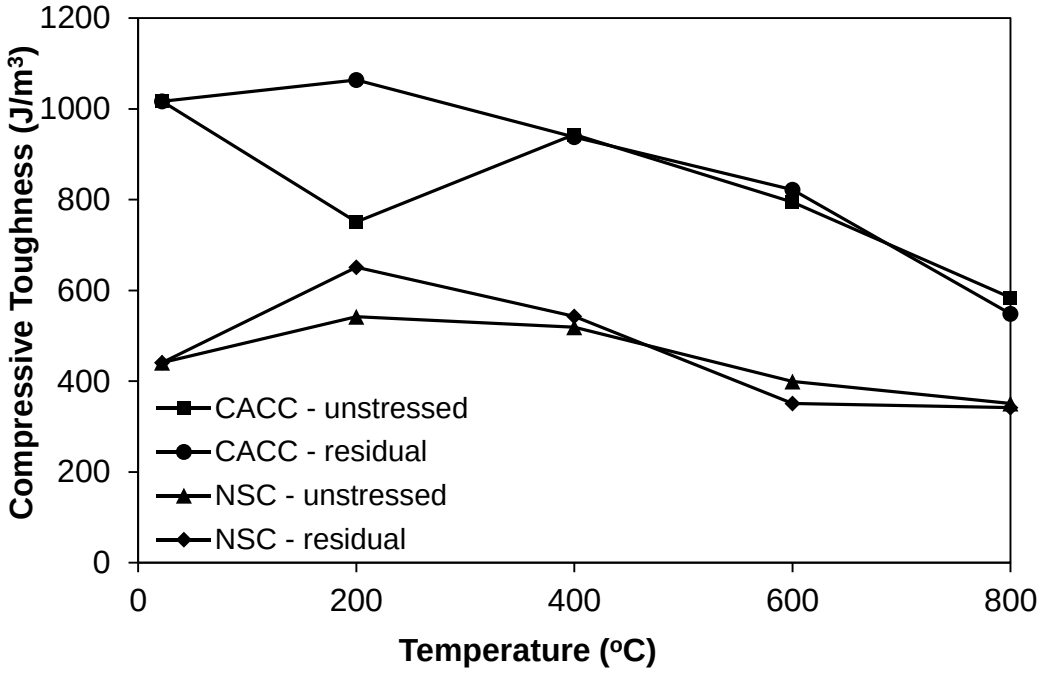

Figure 4.52– Comparison of measured absolute unstressed and residual compressive toughness as a function of temperature

The absolute trend in the toughness is further analyzed in the form of relative loss of energy absorbing capacity as shown in Figure 4.53. This relative toughness follows the same trend as that of absolute value. This trend analysis depicts that the loss of energy absorbing capacity decreases with a sudden drop in case of NSC after 400°C till 600°C, after that, it is stabilized till 800°C. This trend was not followed by CACC in which the loss in energy absorbing capacity was very gradual and steady from 400°C till 800°C with minor difference between the two test

program results. However, the total loss in toughness at 800°C as compared to that at room temperature, in case of CACC was around 22-24% more as compared to NSC.

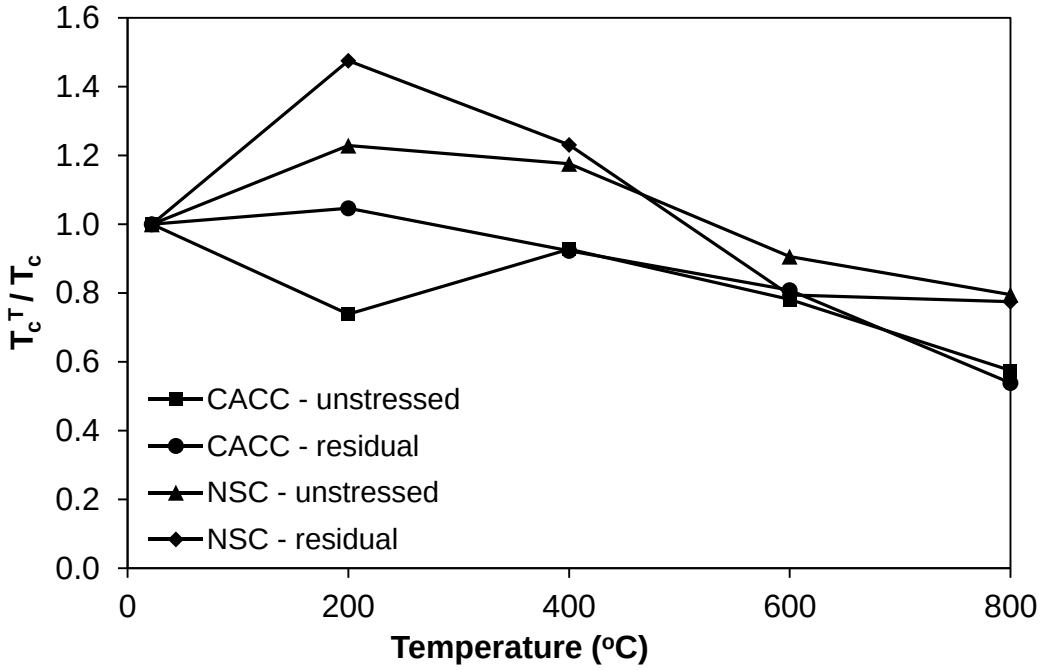

Figure 4.53– Comparison of relative unstressed and residual compressive toughness as a function of temperature

4.7.6 Comparison of Unstressed and Residual Mass Loss

In Figure 4.54, the mass loss of NSC and CACC is shown as a function of temperature for both types of test programs, namely unstressed and unstressed residual. The mass loss of both the concretes is very small, just 7-8% at 600°C irrespective of the test procedure adopted. However, after 600°C a considerable drop in mass was observed which is linked to the disintegration and dissociation of dolomite in carbonate aggregate of both types of concrete (Lie and Kodur, 1996). This results in a major loss of around 15-17% and 13-15% in NSC and CACC, respectively. This confirms the slight better performance of CACC in terms of mass loss with a lesser loss in density and higher strength, which can be attributed to the enhanced microstructure and stability of concrete. The difference between the unstressed and residual test results observed between NSC and CACC is very minor around 1-2% in both the cases till 800°C, which confirms that this material property majorly does not depends on the type of test program adopted.

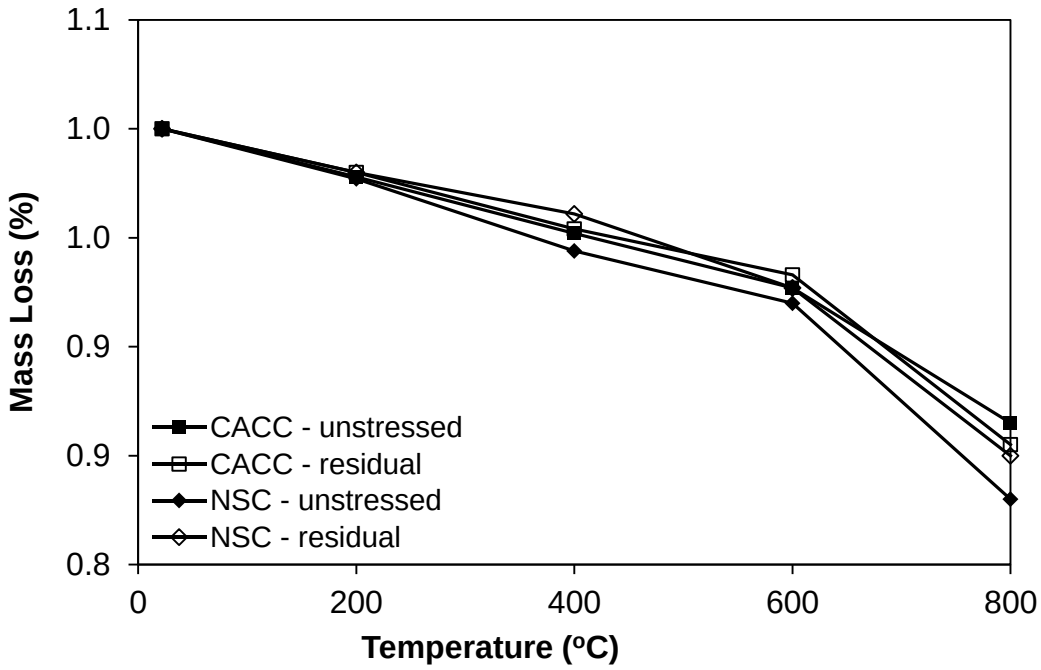

Figure 4.54– Comparison in the loss of mass for unstressed and residual test programs

4.8 Summary

Unstressed and residual tests were performed to determine the performance of CACC and to characterize high temperature material properties which includes, compressive strength, splitting tensile strength, elastic modulus, stress-strain response, toughness and mass loss. For all tested NSC and CACC, these high temperature material properties deteriorate with the increase in temperature. Microscopic and visual assessment of both NSC and CACC were also made to study the damages at macro and micro level due to elevated temperatures. Microstructure was identified using scanning electron microscopy (SEM) for both types of concrete at different levels of elevated temperatures. Major morphological changes and micro cracks due to extension of voids at elevated temperature were also observed at elevated temperatures which further confirm the disintegration and deterioration of concrete. Data from the tests was utilized to develop high temperature relations for compressive strength, splitting tensile strength, elastic modulus, toughness and mass loss of NSC and CACC. The proposed relations can be used as input data in computer programs for evaluating the fire response of NSC and CACC structures exposed to fire. Further, the performance of both types of concretes was analyzed in terms of the test program adopted to evaluate hot and residual behavior.

CHAPTER 5

CONCLUSIONS AND RECOMMENDATIONS

5.1 General

The present study compares the performance of CACC with NSC in terms of its material properties at elevated temperatures. These material properties include compressive strength, splitting tensile strength, elastic modulus, stress-strain response, toughness and mass loss. All the properties were measured at 23, 200, 400, 600 and 800°C temperatures. In addition, the performance of CACC is also compared in terms of different test scenarios i.e. unstressed and residual test conditions. Scanning electron microscope (SEM) analysis along with visual observations was also carried out to study the microstructural changes in CACC and NSC. The data acquired from these experimental studies is used to develop an insight for material properties of CACC at elevated temperatures. The data is further used to propose simplified mathematical relationships for expressing different structural properties of CACC as a function of temperature. These relationships can be used as input parameters in computer programs for evaluating the fire resistance performance of concrete structural members made of CACC.

5.2 Conclusions

Based on the results obtained from the above study, following conclusions are drawn:

- The loss of unstressed and residual compressive strength of CACC with the increase in temperature is lesser as compared to conventional NSC. However, beyond 600°C both types of concrete experience similar major loss in strength.
- CACC exhibits 20% higher initial tensile strength as compared to NSC. However, with the increase in temperature loss in tensile strength is observed which is higher in NSC to that of CACC. The performance of residual tensile strength of CACC is lesser as compared to high temperature tensile strength, particularly at 400°C.
- The initial absolute elastic modulus of CACC observed was 18% lesser as compared to conventional NSC. However, with the increase in temperature up to 400°C, no major loss in unstressed elastic modulus of CACC was observed. Beyond 400°C, the elastic modulus was 32% and 44% higher as compared to NSC at 600°C and 800°C, respectively.
- The stress-strain response depicts a reduced loss in the strength and an increased peak strain at both elevated and room temperature for CACC. The residual peak strains were higher as

compared to unstressed peak strain however; the difference between unstressed and residual response keeps decreasing with increase in temperature.

- The energy absorbed by CACC throughout the 23 to 800°C temperature range is 2.31 to 1.60 times higher than NSC. However, the gain in this energy is minor up to 400°C.
- The loss in mass exhibited by CACC was lower up to 600°C, however sudden reduction of 6% was observed at 800°C, unlike NSC where 9% mass loss was observed.
- Visual and microscopic assessments of CACC showed that its physical deterioration and microstructural damage was lesser as compared to NSC especially towards higher temperatures.
- The elevated temperature material property relationships proposed for CACC can be used as input data in computer programs for evaluating the fire response of CACC structures.

5.3 Recommendations

While this research advanced the state-of-the-art with respect to fire response of CACC and NSC, further studies are required to fully characterize the complex behavior of material properties of HPC. The results demonstrate that there is a need to carry out more in-depth study on the subject. The following are some of the key recommendations for future research works in this area:

- The material properties of CACC can be further refined by taking into account the significant factors such as change in permeability (pore structure), and moisture content as a function of temperature. Effect of cooling phase of fire on the properties should also be established so that model predictions can be enhanced for accuracy under design fire scenarios.
- There is a lack of data on the performance evaluation of fiber reinforced calcium aluminate cement concrete. Further, fire resistance test should be carried out to evaluate its performance against elevated temperatures.
- Further experimentation on evaluating the thermal properties of CACC like thermal conductivity, specific heat and thermal expansion should be carried out at elevated temperatures.
- Material properties of CACC should also be evaluated with addition of secondary raw materials like silica fume and fly ash at elevated temperatures.

REFERNCES

Abramowicz, M., and Kowalski, R. (2005). "The Influence of Short Time Water Cooling on the Mechanical Properties of Concrete Heated up to High Temperature." *Journal of Civil Engineering and Management, Lithuania*, XI(2), 85-90.

Abramowicz, M., and Kowalski, R. (2007). "Residual Mechanical Material Properties For The Reassessment Of Reinforced Concrete Structures After Fire " *Modern building materials, structures and techniques*, M. J. Skibniewski, ed.Vilnius, Lithuania., 1147-1151.

Abrams, M. S. (1971). "Compressive Strength of Concrete at Temperatures to 1600°F." *Temperature and Concrete, American Concrete Institute*, SP-25, 33–58.

ACI 211.1-91 (2002). "Standard Practice for Selecting Proportions for Normal, Heavyweight, and Mass Concrete." *ACI 211.1-91*, ACI Manual of Concrete Practice 2005, Mich, USA.

ACI 216.1 (2007). "Code requirements for determining fire resistance of concrete and masonry construction assemblies." *ACI-216.1-07/TMS-0216-07*, American Concrete Institute, Mich, USA.

ACI 216R-89 (2001). "Guide for Determining the Fire Endurance of Concrete Elements." *ACI 216R-89*, ACI Manual of Concrete Practice 2005, Mich, USA.

ACI 318-11 (2008). "Building code requirements for reinforced concrete and commentary." American Concrete Institute, Mich, USA.

Ali, F. (2002). "Is high strength concrete more susceptible to explosive spalling than normal strength concrete in fire?" *Fire and Materials*, 26, 127-130.

ASTM C33 (2003). "Standard Specification for Concrete Aggregates." ASTM International, West Conshohocken, PA.

ASTM C39 (2009). "Standard Test Method for Compressive Strength of Cylindrical Concrete Specimens." ASTM International, West Conshohocken, PA.

ASTM C78 (2009). "Standard Test Method for Flexural Strength of Concrete." ASTM International, West Conshohocken, PA.

ASTM C192 (2002). "Standard Test Method for Making and Curing Concrete Test Specimens in the Laboratory." ASTM International, West Conshohocken, PA.

ASTM C469 (2002). "Standard Test Method for Static Modulus of Elasticity and Poisson's Ratio of Concrete in Compression." ASTM International, West Conshohocken, PA.

ASTM C496 (2004). "Standard Test Method for Splitting Tensile Strength of Cylindrical Concrete Specimens." ASTM International, West Conshohocken, PA.

ASTM C1583 (2004). "Standard Test Method for Tensile Strength of Concrete Surfaces and the Bond Strength or Tensile Strength of Concrete Repair and Overlay Materials by Direct Tension (Pull-off Method)." ASTM International, West Conshohocken, PA.

ASTM C1723 (2010). "Standard guide for examination of hardened concrete using scanning electron microscopy." ASTM International, West Conshohocken, PA.

ASTM C1868 (2010). "Standard Test Method for Loss-On-Drying by Thermogravimetry.", ASTM International, West Conshohocken, PA.

Baldwin, R., and North, M. A. (1973). "A stress-strain relationship for concrete at elevated temperature." *Magazine of Concrete Research*, 25(28).

Bamonte, P., and Gambarova, P. (2009). "Thermal and mechanical properties at high temperature of a very high-strength durable concrete." *Journal of Materials in Civil Engineering*, 22(6), 545-555.

Bamonte, P., and Gambarova, P. G. (2012). "A study on the mechanical properties of self-compacting concrete at high temperature and after cooling." *Materials and structures*, 45(9), 1375-1387.

Bažant, Z. P., and Kaplan, M. F. (1996). *Concrete at high temperatures: material properties and mathematical model*, Longman Group Limited, Essex, England.

Campbell-Allen, D. A. (1965). "An Investigation of the Effect of Elevated Temperatures on Concrete for Reactor Vessels." *Nucl. Struct. Eng.*, 2, 3823-3888.

Campione, G., and Mindess, S. (1999). "Compressive Toughness Characterization of Normal and High-Strength Fiber Concrete Reinforced With Steel Spirals." *ACI, Special Publication*, 182, 141-162.

Campione, G., Mindess, S., and Zingone, G. (1999). "Compressive stress-strain behavior of normal and high-strength carbon fiber concrete reinforced with steel spirals." *ACI Materials Journal*, 96(1), 27-34.

Carette, G. G., Painter, K. E., and Malhotra, V. M. (1982). "Sustained High Temperature Effect on Concrete made with normal portland cement, normal portland cement and slag, or normal portland cement and fly ash." *Concrete International*, 4(7), 41-51.

Castillo, C., and Duranni, A. J. (1990). "Effect of transient high temperature on high-strength concrete." *ACI Materials Journal*, 87(1), 47-53.

Chan, Y. N., Peng, G. F., and Anson, M. (1999). "Residual strength and pore structure of high-strength concrete and normal strength concrete after exposure to high temperature." *Cement and Concrete Composites*, 21(1), 23-27.

Eglinton, M. (1998). "Resistance of Concrete to Destructive Agencies." *Lea's Chemistry of Cement and Concrete*, P. C. Hewlett, ed., Elsevier Science & Technology Books, New York, 299-342.

Eurocode 2 (2004). "EN 1992-1-2: Design of concrete structures. Part 1-2: General rules - Structural fire design.", European Committee for Standardization, Brussels, Belgium.

Furumura, T., Abe, T., and Shinohara, Y. (1995). "Mechanical Properties of High Strength Concrete at High Temperatures." *Proc. of 4th Weimar Workshop on High Performance Concrete: Material Properties and Design*Hochschule für Architektur und Bauwesen (HAB), Weimar, Germany, 237–254.

Georgali, B., and Tsakiridis, P. E. (2005). "Microstructure of fire-damaged concrete. A case study." *Cement and Concrete Composites*, 27(2), 255-259.

Gibbels, S. (1970). "Variation of Porosity in refractory concretes with temperature of Pre heat." *Concrete for High temperatures*, A. Petzold, and M. Rohrs, eds., Elsevier Science Ltd., 135.

Harada, T., Takeda, J., Yamane, S., and Furumura, F. (1972). "Strength, Elasticity and Thermal Properties of Concrete Subjected to Elevated Temperatures." *International Seminar on Concrete for Nuclear Reactor, ACI Special Publication, SP 31-21*, 34(1), 377-406.

Hu, X. F., Lie, T. T., Polomark, G. M., and MacLaurin, J. W. (1993). "Thermal properties of building materials at elevated temperatures." *Internal Report - 643*, Institute for Research in Construction, National Research Council Canada, 1-54.

Ideker, J. H., Gosselin, C., and Barborak, R. (2013). "An Alternative Repair Material. Basics and practical testing of calcium aluminate cement concrete." *ACI Committee 236*, 33-37.

JSCE SF-5 (1984). "Method of tests for compressive strength and compressive toughness of steel fiber reinforced concrete." *Concrete Library of JSCE No.3*, Standard SF-5, 63-66.

Karadeniz, E., Gurcan, C., Ozgen, S., and Aydin, S. (2007). "Properties of alumina based low-cement self flowing castable refractories." *European Ceramic Society*, 27(2), 1849–1853.

Karokoc, M. B. (2013). "Effect of cooling regimes on compressive strength of concrete with lightweight aggregate exposed to high temperature." *Construction and Building Materials*, 41, 21-25.

Katsavou, I. D., Krokida, M. K., and Ziomas, I. C. (2012). "Determination of mechanical properties and thermal treatment behavior of alumina-based refractories." *Ceramics International*, 38(7), 5747–5756.

Khaliq, W. (2012). "Performance characterization of high performance concretes under fire conditions." Doctor of Philosophy, PhD Dissertation, Michigan State University, Michigan, U.S.A.

Khaliq, W., and Kodur, V. (2011). "Thermal and mechanical properties of fiber reinforced high performance self-consolidating concrete at elevated temperatures." *Cement and Concrete Research*, 41(11), 1112-1122.

Khaliq, W., and Kodur, V. K. R. (2011). "Effect of high temperature on tensile strength of different types of high-strength concrete." *ACI Materials Journal*, 108(4), 394-402.

Kodur, V. (2014). "Properties of Concrete at Elevated Temperatures." *ISRN Civil Engineering*, 2014, 15.

Kodur, V. K. R. "Spalling in high strength concrete exposed to fire - concerns, causes, critical parameters and cures." *Proc., ASCE Structures Congress*, 1-9.

Kodur, V. R., and Sultan, M. A. (2003). "Effect of temperature on the thermal properties of high strength concrete." *Journal of Materials in Civil Engineering*, 15(2), 101-107.

Kowalski, R. (2010). "Mechanical Properties Of Concrete Subjected To High Temperature." *Architecture civil engineering and environment*, 3(2), 61-70.

Lankard, D. T. (1971). "Effects of Moisture Content on the Structural Properties of Portland Cement Concrete Exposed to Temperatures Up to 500°F." *Temperature and Concrete, American Concrete Institute*, SP-25, 59–102.

Li, M., Qain, C., and Sun, W. (2004). "Mechanical Properties of high-strength concrete after fire." *Cement and Concrete Research*, 34(6), 1001-1005.

Lie, T. T. (1992). "Structural fire protection." *ASCE Committee on Fire Protection, Structural Division*, New York, NY, 225-229.

Lie, T. T., and Kodur, V. R. (1996). "Thermal and mechanical properties of steel-fibre-reinforced concrete at elevated temperatures." *Canadian Journal of Civil Engineering*, 23(2), 511-517.

Malhotra, H. L. (1956). "The Effect of Temperature on the Compressive Strength of Concrete." *Magazine Concrete Research*, 8(23), 85–94.

Marar, K., Eren, Ö., and Celik, T. (2001). "Relationship between impact energy and compression toughness energy of high-strength fiber-reinforced concrete." *Materials letters*, 47(4), 297-304.

Marar, K., Erenb, Ö., and Yitmena, İ. (2011). "Compression Specific Toughness of Normal Strength Steel Fiber Reinforced Concrete (NSSFRC) and High Strength Steel Fiber Reinforced Concrete (HSSFRC)." *Materials Research*, 14(2), 239-247.

Marechal, J. C. (1972). "Variations in the modulus of elasticity and Poisson's ratio with temperature." *Int. Seminar on Concrete for Nuclear reactors, ACI SP-34*Detroit, Michigan, USA., 495-503.

Martinović, S., Vlahović, M., Majstorović, J., Matović, B., and Volkov-Husović, T. (2012). "Thermal And Mechanical Properties Of High Alumina Low Cement Castable." *Association of Metallurgical Engineers of Serbia, AMES.*, 18(1), 53-65.

Maslennikova (1970). "Relationship between cold compressive strength of cermsite refractory concretes and its density and temperature of Pre heat." *Concrete for High temperatures*, A. Petzold, and M. Rohrs, eds., Elsevier Science Ltd., 167.

Mehta, P. K., and Monteiro, P. J. M. (2006). *Concrete: Microstructure, Properties, and Materials*, The McGraw-Hill Companies, Inc., New York, USA.

Mindess, S., Young, J. F., and Darwin, D. (2003). *Concrete, second edition*, Prentice Hall, Pearson Education, Inc. Upper Saddle River, NJ, USA.

Mintab (2015). "http://www.minitab.com/en-us/." (2015).
Mitusch (1970). "Intermediate maxima of the cold compressive strength of Pre heated aluminous cement concretes." *Concrete for High temperatures*, A. Petzold, and M. Rohrs, eds., Elsevier Science Ltd., 129.
Mitusch., Hansen., and Livovich. (1970). "Hot compressive strength of aluminous cement concretes." *Concrete for High temperatures*, A. Petzold, and M. Rohrs, eds., Elsevier Science Ltd., 132.
Morita, T. "Residual Mechanical Properties of High Strength Concrete Members Exposed to High Temperature—Part 1. Test on Material Properties." *Proc., Summaries of Technical Papers of Annual Meeting, Architectural Institute of Japan*.
Mostafa, N. Y., Zaki, Z. I., and Abd Elkader, O. H. (2012). "Chemical activation of calcium aluminate cement composites cured at elevated temperature." *Cement and Concrete Composites*, 34(10), 1187-1193.
Navy, E. G. (2004). *Concrete Construction Engineering Handbook*, CRC Press Taylor and Francis Group.
Neville, A. M. (2004). *Properties of Concrete*, Pearson Education Limited, Essex, England, UK.
Noumowe, A. N., Clastres, P., Debicki, G., and Costaz, J.-L. (1996). "Thermal Stresses and Water Vapor Pressure of High Performance Concrete at High Temperature." *Proc. 4th International Symposium on Utilization of High-Strength/High-Performance Concrete*,Paris.
Onodera, M. (2002). "Refractory Concrete." The Fu Foundation of Engineering and Applied Science, Columbia University, New York.
Phan, L. T., and Carino, N. J. (2002). "Effects of Test Conditions and Mixture Proportions on Behavior of High-Strength Concrete Exposed to High Temperatures." *ACI Materials Journal*, 99(1), 54-66.
Phan, L. T., Lawson, J. R., and Davis, F. L. (2001). "Effects of elevated temperature exposure on heating characteristics, spalling, and residual properties of high performance concrete." *Materials and Structures*, 34(2), 83-91.
Prabha, S. L., Dattatreya, J. K., Neelamegam, M., and RAO, M. V. S. (2010). "Study on stress-strain properties of reactive powder concrete under uniaxial compression." *International Journal of Engineering Science and Technology*, 2(11), 6408-6416.
RILEM TC 129-MHT (1995). "Test methods for mechanical properties of concrete at high temperatures - Compressive strength for service and accident conditions." *Materials and Structures*, 28(3), 410-414.
RILEM TC 129-MHT (2000). "Test methods for mechanical properties of concrete at high temperatures, Part 4 - Tensile strength for service and accident conditions." *Materials and Structures*, 33, 219-223.
Roux, F. J. (1974). "Concrete at Elevated Temperatures." Doctoral Thesis, University of Capetown, Capetown, South Africa.
Scrivener, K. L., Cabiron, J.-L., and Letourneux, R. (1999). "High-Performance concretes from calcium aluminate cements." *Cement and Concrete Research*, 29(8), 1215-1223.
Scrivener, K. L., and Capmas, A. (1998). "Calcium Aluminate Cements." *Lea's Chemistry of Cement and Concrete*, P. C. Hewlett, ed., Elsevier Science & Technology Books, New York, 713-782.
Wackerly, D. D., Mendenhall III, W., and Scheaffer, R. L. (2008). *Mathematical statistics with applications*, Thomson Higher Education, Belmont, CA, USA.
Xiao, J., and König, G. (2004). "Study of Concrete at High Temperature in China—An Overview." *Fire Safety Journal*, 39, 89-103.

Zoldners, N. G. (1960). "Effect of High Temperatures on Concrete Incorporating Different Aggregates." *ASTM Proc.*, 60, 1087–1108.

Zoldners, N. G., Malhotra, V. M., and Wilson, H. S. (1963). "High-temperature behaviour of aluminous cement concretes containing different aggregates." *66th Annual Meeting, Amererican Society for Testing and Materials*.